

# Environmental impact of tidal power in the Eastern Scheldt Storm Surge Barrier

Appendix B: Analysis ADCP data Eastern Scheldt Barrier with and without turbine deployment

**Prepared for:**

OTP PROJ-00275, Stimulus: UP-16-01097  
Deltares project: 11200444

**Analysis ADCP data Eastern  
Scheldt Barrier with and without  
turbine deployment**

Wilbert Verbruggen

11200444-000

**Title**  
Analysis ADCP data Eastern Scheldt Barrier with and without turbine deployment

<b>Client</b>	<b>Project</b>	<b>Reference</b>	<b>Pages</b>
OTP	11200444-000	11200444-000-0008	48

**Keywords**  
Tidal energy, Eastern Scheldt, ADCP data, tidal turbines




**Summary**  
In 2015 an array of five tidal turbines has been installed in Gate #08 of the Roompot Section of the Eastern Scheldt Barrier in the framework of a tidal power pilot project. As this power plant is an obstruction in the barrier, Rijkswaterstaat would like to know the environmental effects of the barrier. Deltares has worked on a number of study tasks, which have been summarized in the main report (reference: 11200119-000-HYE-0006). The present report describes the analysis of ADCP measurements to investigate the effect of the turbines on the flow through the barrier.

In 2011, horizontal and vertical measurements were carried out in the gate of the barrier. From 2015 onwards, horizontal measurements have been carried out in the flow direction through the barrier. As these measurements do not overlap, a direct comparison between these measurements was difficult to make. However from the available measurements the following conclusions are drawn:

- Due to inertia, flow velocities at the end of a tidal phase are higher than at the start of the tidal phase for similar head differences over the Eastern Scheldt Barrier.
- The measurement locations for the situation without turbines and with turbines do not overlap, which complicates the assessment on the effect of the velocity profiles and discharge coefficient
- During flood, the velocity above the sill (upstream of the turbines) is not significantly influenced. During ebb, the velocity above the sill (downstream of the turbines, thus in the wake zone) for the situation with turbines is approximately 25% lower than without turbines.
- A comparison between stall mode and normal mode showed that the velocity profile is upstream almost unaffected, while downstream (in the wake of the turbines) large differences are measured
- The uncertainty in discharge coefficient is too large to make an assessment on the change in discharge coefficient due to the presence of the turbines.

The analysed data provide a good source of reference for the detailed CFD model that has been setup for the tidal power plant in the Eastern Scheldt.

**References**  
Oosterschelde Tidal Power PROJ-00275, Stimulus ref: UP-16-01097  
Deltare, Environmental impact of tidal energy plan in Eastern Scheldt Storm Surge Barrier, 11200119-000-HYE-0006

Version	Date	Author	Initials	Review	Initials	Approval	Initials
1	Aug. 2018	W. Verbruggen		A. de Fockert		B. van Vossen	

**State**  
final

## Contents

<b>1</b>	<b>Introduction</b>	<b>1</b>
1.1	Background	1
1.2	Objective	1
1.3	Research framework	1
1.4	Reading guide	1
<b>2</b>	<b>Available data</b>	<b>3</b>
<b>3</b>	<b>ADCP measurements without turbines</b>	<b>4</b>
3.1	Description of data	4
3.2	Analysis of velocity profiles	5
3.2.1	Approach	5
3.2.2	General observations	6
3.2.3	Velocity profiles during ebb	7
3.2.4	Velocity profiles during flood	12
<b>4</b>	<b>ADCP measurements during turbine deployment</b>	<b>18</b>
4.1	Description of data	18
4.2	Analysis of 1-beam measurements during normal turbine operation	20
4.2.1	Approach	20
4.2.2	Velocity profiles during ebb	20
4.2.3	Velocity profiles during flood	21
4.3	Analysis of 5-beam measurements during normal turbine operation	22
4.3.1	Determining flow angle and overall flow magnitude	22
4.3.2	Velocity profiles during ebb	25
4.3.3	Velocity profiles during flood	25
4.4	Analysis of 1-beam measurements during stall-mode turbine operation	26
4.4.1	Velocity profiles during ebb	26
4.4.2	Velocity profiles during flood	27
4.5	Analysis of 5-beam measurements during stall-mode turbine operation	28
4.5.1	Velocity profiles during ebb	28
4.5.2	Velocity profiles during flood	29
4.6	Analysis of RPM, power and thrust	30
<b>5</b>	<b>Effect of turbines based on ADCP data</b>	<b>34</b>
5.1	Introduction	34
5.2	Comparison of ADCP measurement before and during turbine deployment	34
5.2.1	Approach	34
5.2.2	Results	36
5.3	Comparison of the ADCP measurement during normal turbine deployment with ADCP measurements during stall mode deployment	39
5.3.1	Approach	39
5.3.2	Results	41
<b>6</b>	<b>Estimated influence of the turbines on the discharge coefficients</b>	<b>43</b>
6.1	Introduction	43
6.2	Discharge coefficient for situation without turbines	43
6.2.1	Example for -0.2 m head difference	43



6.2.2	Results for all four cases	45
6.3	Discharge coefficients for situation with turbines	45
6.4	Comparison of discharge coefficients with and without turbines	46
<b>7</b>	<b>Summary and conclusions</b>	<b>47</b>
<b>8</b>	<b>References</b>	<b>48</b>
<b>Appendices</b>		
<b>A</b>	<b>Photographs of ADCP brackets</b>	<b>A-1</b>
<b>B</b>	<b>Quality checks on ADCP measurements without turbine deployment</b>	<b>B-1</b>
B.1	Quality checks performed by Partrac	B-1
B.2	Quality checks performed by Deltares	B-1
B.3	Brief overview of quality checked data	B-3
<b>C</b>	<b>Velocity profiles without turbine deployment</b>	<b>C-4</b>
C.1	Case 1 (head difference = -0.2 m)	C-4
C.2	Case 2 (head difference = -0.32 m)	C-6
C.3	Case 3 (head difference = +0.2 m)	C-8
C.4	Case 4 (head difference = +0.55 m)	C-10
<b>D</b>	<b>Quality checks for ADCP data during turbine deployment</b>	<b>D-1</b>
D.1	Quality checks on ADCP data during normal turbine operation	D-1
D.2	Quality checks on ADCP data during stall mode turbine operation	D-3
D.3	Results of quality checks for the 1-beam measurements (normal turbine operation)	D-4
D.3.1	Southern turbine	D-5
D.3.2	Middle turbine	D-7
D.3.3	Northern turbine	D-10
<b>E</b>	<b>Velocity profiles during turbine deployment</b>	<b>E-1</b>
E.1	Case 1 (head difference = -0.2 m)	E-1
E.2	Case 2 (head difference = -0.32 m)	E-5
E.3	Case 3 (head difference = +0.2 m)	E-8
E.4	Case 4 (head difference = +0.55 m)	E-11
<b>F</b>	<b>Relation between RPM, Power, thrust and head difference</b>	<b>F-1</b>
F.1	Turbine T0012	F-2
F.2	Turbine T0014	F-3
F.3	Turbine T0011	F-4
F.4	Turbine T0015	F-6
F.5	Turbine T0009	F-7

# 1 Introduction

## 1.1 Background

The Eastern Scheldt Storm Surge Barrier (OSK) was completed in 1986. The barrier counts 62 individual gates, and is constructed of concrete pillars, top beams and sill beams connecting to a rockfill sill construction and about 600 m of bed protection on both sides, see Rijkswaterstaat (ref [3]). In normal conditions the ebb and flood flow through the barrier is characterized by a maximum head loss of about 1 m with maximum velocities of 4 m/s and higher. The outflow of the barrier is extremely turbulent. In 2015 an array of five tidal turbines was deployed in Gate #08 of the Roompot Section of the barrier in the framework of the tidal power pilot project.

As this power plant is an obstruction in the barrier, Rijkswaterstaat would like to know the environmental effects of the barrier. The main concerns for RWS are the flow patterns around the tidal turbines and the potential effect of the tidal turbines on the bed protection. Deltares has worked on a number of study tasks, which have been summarized in the main report (reference: 11200119-000-HYE-0006).

This report focusses on the ADCP measurements that have been carried out to assess the impact of the turbines on the discharge through the gate. For both the situation with and without turbines, ADCP (Acoustic Doppler Current Profiler) measurements have been carried out in gate #08 of the OSK.

The results of this analysis are also used as input to the validation of the CFD modelling work, which are described in the CFD modelling report (reference: 11200119-003-HYE-0004).

## 1.2 Objective

The objective of this study was:

- to check the quality of the ADCP measurements in gate 8 of the Eastern Scheldt Barrier and to analyse the observed current profiles.
- to get an indication of the effect of the turbines on the discharge through the gate based on the measurements.

## 1.3 Research framework

The Eastern Scheldt Tidal Power project (OTP) consists of a consortium of 6 partners researching the effect of the tidal turbines on the environment. This research is part of the OTP project - Task 1, which is led by Deltares. Research Task 1 aims to investigate the environmental effects of the tidal turbines. Part of this task is to investigate the effect of the tidal turbines on the flow through the barrier.

## 1.4 Reading guide

The ADCP measurements before turbine deployment will be described in Chapter 3. The ADCP measurements during turbine deployment will be described in Chapter 4. Both chapters will start with a description of the received data and an overview of the locations and directions of the measurements. Subsequently, the measured current profiles will be analysed for both a typical ebb and flood case (objective 1).

Chapter 5 covers the second part of the objective. The influence of the turbine operation on the flow profiles is analysed by comparing measurement during and before turbine operations. In addition, a comparison is made of the flow profiles and spatial flow distributions

for situations when the turbine operation was in normal mode and stall mode (i.e. reduced resistance on the flow).

In Chapter 6 an assessment is made on the change in discharge coefficient based on the available measurements. And Chapter 7 summarizes the findings and contains the main conclusions from this study.

## 2 Available data

To assess the influence of the turbine operation on the hydrodynamics around gate #08 of the Eastern Scheldt, multiple measurement campaigns have been carried out. The difference between the measurement campaigns were the presence of turbines, type of turbine deployment and the orientation of the ADCP beams. The table below gives an overview of the available data for the different periods.

Period (UTC)	Type of turbine deployment <sup>1</sup>	Available data	Data source
15-08-2011– 21-08-2011	No turbines	Vertical ADCP measurements Gate #08 Horizontal ADCP measurements in Gate #08 Water levels at Roompot Binnen and Roompot Buiten	Tocardo Tocardo RWS
10-10-2016 – 26-10-2016	Normal	1-beam ADCP measurements for 3 backward-looking and 2 forward-looking ADCP devices RPM records for all turbines Power records for all turbines Thrust measurements for the middle and northern turbine Water levels at Roompot Binnen and Roompot Buiten	Tocardo Tocardo Tocardo RWS
22-06-2017 14:00 – 24-06-2017 9:50	Normal	5-beam ADCP measurements for 3 backward-looking and 2 forward-looking ADCP devices Water levels at Roompot Binnen and Roompot Buiten	Tocardo RWS
28-08-2017 7:25 – 29-08-2017 7:10	Stall mode	1-beam ADCP measurements for 3 backward-looking and 1 forward-looking ADCP device RPM records for the middle turbine Water levels at Roompot Binnen and Roompot Buiten	Tocardo Tocardo RWS
14-09-2017 8:00 – 15-09-2017 23:50	Stall mode	5-beam ADCP measurements for 3 backward-looking and 2 forward-looking ADCP devices RPM records for all turbines Power records for all turbines Water levels at Roompot Binnen and Roompot Buiten	Tocardo Tocardo RWS

<sup>1</sup> During stall mode, the turbine has a lower rotation speed compared to normal operation, resulting in less resistance to the flow



### 3 ADCP measurements without turbines

#### 3.1 Description of data

In August 2011 a 7-day measurement campaign was carried out at one of the gates of the Eastern Scheldt storm surge barrier. During this period, both a vertically (deployed from 15 August 2011 12:15 till 21 August 2011 21:15) and horizontally (deployed from 16 August 2011 12:45 till 22 August 2011 13:50) oriented ADCP were mounted on the inland side of the gate, see Figure 3.2. Tocardo contracted Partrac to carry out the measurement campaign and perform a first quality control analysis (ref [2]). Tocardo subsequently provided Deltares with two binary MATLAB files containing the quality checked data for both the vertical and horizontal ADCP (Partrac OSK - CurrentVER.mat and Partrac OSK - CurrentHOR.mat).

The ADCP's were deployed in Gate #08 of the Roompot Section of the barrier, see Figure 3.1. The vertical ADCP (measuring upwards) was attached directly at the lagoon side of the sill beam (ADCP axis at 13 cm from the edge of the sill beam) at 9.2 m from pillar R9 at a vertical depth of -9.5 m NAP, see Figure 3.2. The horizontal ADCP was located at -4.8 m NAP on pillar R9 at 3.33 m from the edge of the sill beam (at the lagoon side of the sill beam) and was measuring towards pillar R8. Photographs of the brackets which were used to mount the ADCP devices on the barrier can be found in Appendix A.

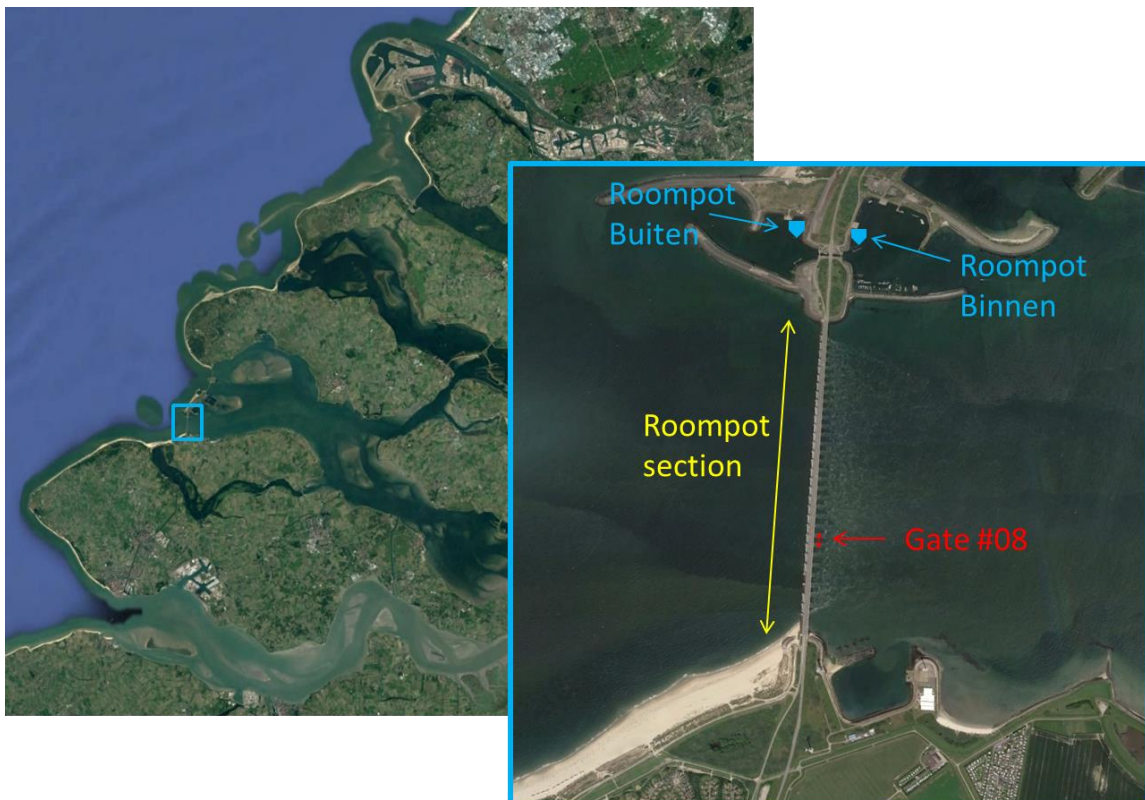


Figure 3.1 Location of Gate #08 of the Roompot section of the Eastern Scheldt Barrier, shown on a satellite image (source: Google Earth)

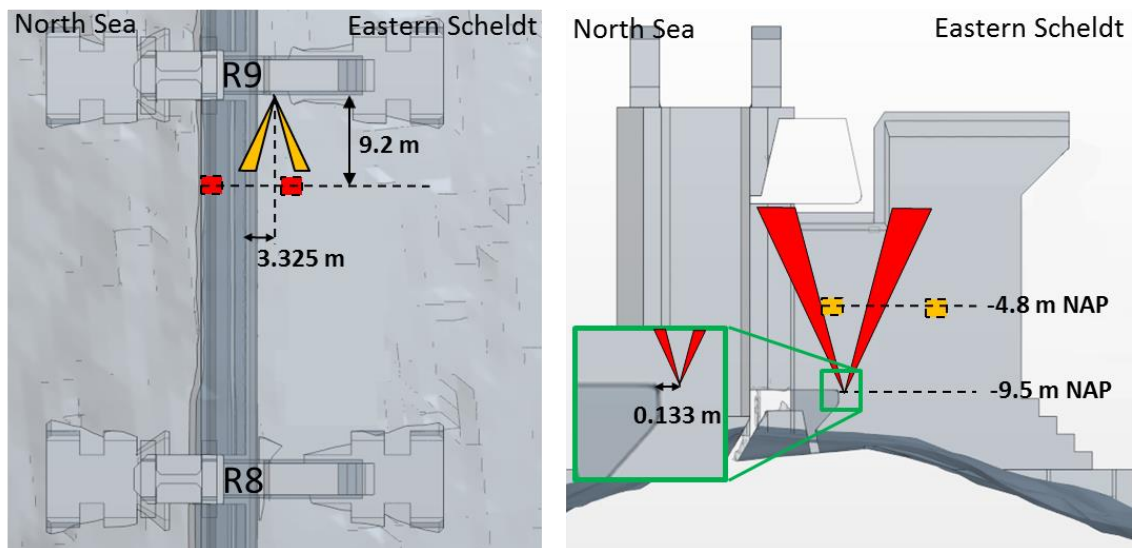


Figure 3.2 Overview of the 2011 ADCP measurements. Left: Top view, right: Side view.

The ADCP measurements were carried out with 1200 kHz RDI ADCP devices (ref [2]). Based on the provided photographs of the devices and the provided characteristics in the Partrac report (ref [2]), it was determined that the Workhorse Sentinel 1200 kHz was selected. The main characteristics of the ADCP setup are given in the table below. The ADCP data was provided by Partrac with a 75 s interval.

<b>Bin size</b>	0.25 m
<b>Blanking distance</b>	0.44 m
<b>Beam angle</b>	20°
<b>Beam width</b>	3.7°

The ADCP measurements have been checked against a number of quality criteria. An overview of the criteria and the quality checked data is included in Appendix B.

As shown in Figure 3.2, the ADCP's measure the current velocity by means of two angled beams. The ADCP's therefore do not directly measure the velocity in above or in front of the ADCP. Since the velocity gradients at the locations of the measurements (i.e. close to the edge of the sill beam) are relatively large, the average of two beams may differ from the current velocity in between the two beams. The averaging of the 2 beams was already performed by Partrac before the data was provided to Deltares.

## 3.2 Analysis of velocity profiles

### 3.2.1 Approach

To increase the understanding of the flow profiles through the Eastern Scheldt Barrier, the average flow profiles were analysed for different head differences. In this report two ebb and two flood cases are discussed in detail, see Table 3.1 for the characteristics of these cases. The four cases are selected such that they cover the whole range of head differences for which quality checked (vertical and horizontal) ADCP data was available.

Table 3.1 Overview of cases that are discussed in detail

	Case number	water level North Sea side	water level Eastern Scheldt side	Head difference
		[m; NAP]	[m; NAP]	[m]
Ebb	1	0.93	1.13	-0.20
	2	0.68	1.00	-0.32
Flood	3	-0.57	-0.77	0.20
	4	1.12	0.57	0.55

The velocity profiles corresponding to the above cases have been determined using the following routine:

1. Based on the Roompot Buiten and Roompot Binnen water level timeseries, the periods are selected with a corresponding head difference.
2. Subsequently all ADCP data within 5 minutes before and after these selected moments are selected.
3. The selected ADCP data are split into velocity measurements during increasing and decreasing absolute head<sup>2</sup>. This is done because the present analysis showed that the flow inertia plays a significant effect on the current profile (current velocities are generally higher during decreasing head), which will be more elaborated upon in the section below. In this section data corresponding to increasing head is always visualised in black, whereas the data corresponding to decreasing absolute head is always visualised in blue.
4. Based on the selected ADCP data, the following parameters are determined for each individual bin (for increasing and decreasing head separately):
  - Median u-velocity<sup>3</sup>
  - 15.9-percentile u-velocity (which is equal to the median velocity minus one standard deviation if a normal distribution is assumed)
  - 84.1-percentile u-velocity (which is equal to the median velocity plus one standard deviation if a normal distribution is assumed)

### 3.2.2 General observations

As already mentioned in the previous section, inertia has a significant effect on the current profile, which is illustrated by Figure 3.3. The upper plot of this figure shows the head difference over the barrier during the measurement period. The black and red dots show during which periods quality checked data is available. The black dots represent period of increasing absolute head, whereas the blue dots represent periods of decreasing absolute head. The period corresponding to decreasing absolute head always occurs after the peak flood/ebb flow. The lower plot shows the relation between the head difference over the barrier and the average velocity in the vertical ADCP data. The colours again show whether the corresponding measurements were taken during increasing or decreasing absolute head.

The figure shows that especially in the range of -0.2 m to +0.2 m head difference, the average velocity through the gate during increasing and decreasing absolute head is very different. For a head difference of +0.1 m, for example, the average velocity is about 1.1 m/s during increasing absolute head and about 1.6 m/s during decreasing absolute head. The difference in flow velocity for a similar head difference can be explained by the inertia of the

<sup>2</sup> The word "absolute" is added here to stress that increasing head refers to conditions that the absolute difference between the water level at Sea and the Eastern Scheldt is increasing. The period corresponding to decreasing absolute head always occurs after the peak flood/ebb flow.

<sup>3</sup> The median velocity is less sensitive to outliers in the data compared to the mean velocity.

flow. At the start of the flood/ebb phase (i.e. during increasing absolute head) the flow still needs to be accelerated and therefore lags behind the head difference variation. The opposite is valid at the end of the flood/ebb phase (i.e. during decreasing absolute head). Due to inertia the flow direction can even be opposite to the head difference. The data shows that, for example, during a head difference of  $-0.03$  m (the water level at the North Sea is  $0.03$  m lower than at the Eastern Scheldt), the average velocity is still about  $+0.5$  m/s at the start of the ebb phase, whereas at the end of the ebb phase the average velocity is about  $-1$  m/s.

It is noted that all ADCP data for head differences smaller than about  $-0.33$  m were removed by Partrac (ref [2]) because the data didn't meet the quality criteria (for example due to vibrations of the vertical ADCP device).

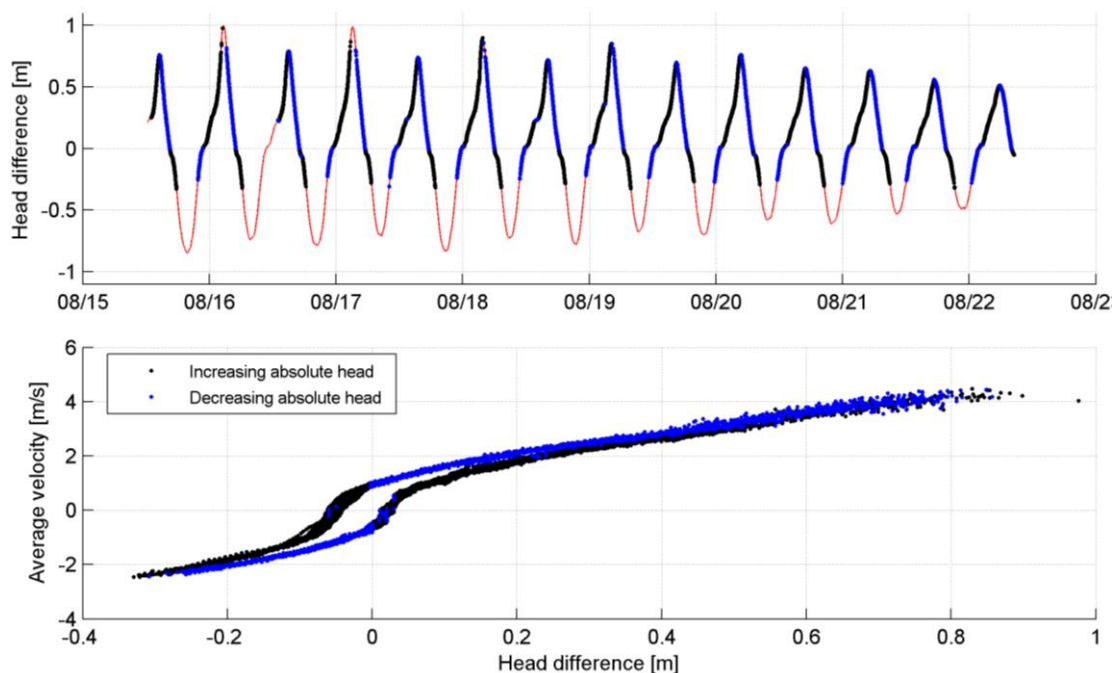


Figure 3.3 Upper plot: timeseries of the head difference over the barrier. The black dots indicate periods during increasing absolute head in which quality checked ADCP data is available. The blue dots indicate periods of decrease absolute head. Lower plot: Relation between the head difference over the barrier and the average velocity in the vertical ADCP data. The black dots again correspond to increasing absolute increasing head, whereas the blue dots correspond to decreasing absolute head.

### 3.2.3 Velocity profiles during ebb

This section describes the measured velocity profile corresponding to a head difference of  $-0.2$  m (case 1). The results for the other ebb case are included in Appendix C.

#### Vertical ADCP

Figure 3.4 shows the water level at sea and the head difference over the barrier, in which the dots show the periods which correspond to Case 1. The black and blue lines and dots show the periods when quality checked data is available for the vertical ADCP. The vertical ADCP datasets contains 25 periods corresponding to Case 1, of which 13 are during increasing absolute head and 12 during decreasing absolute head.



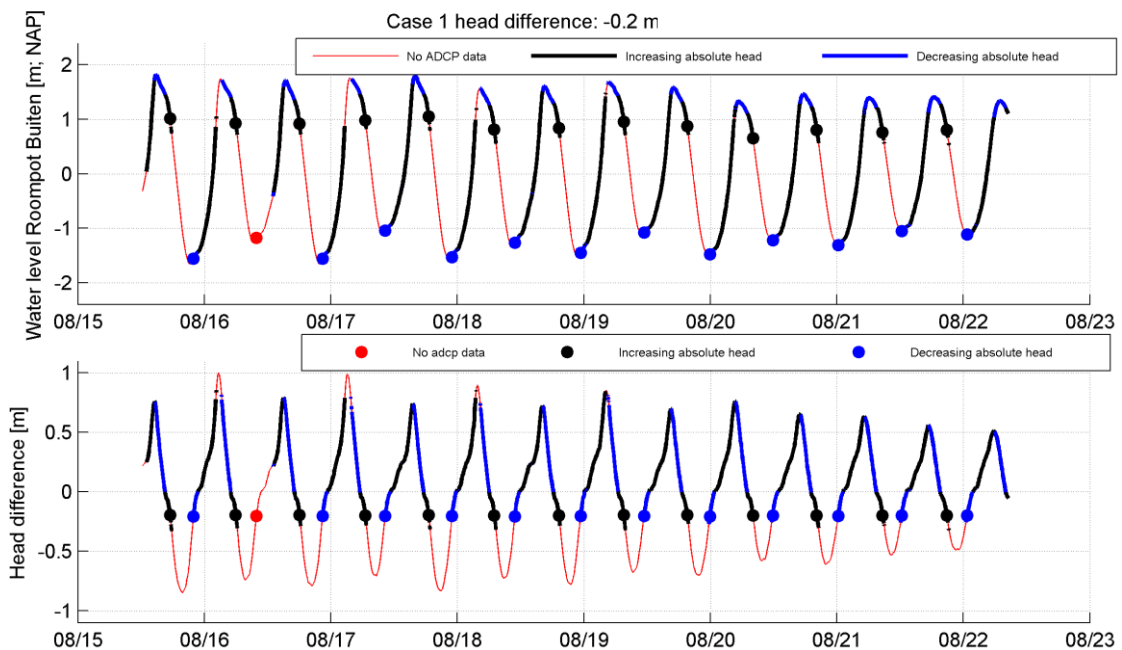


Figure 3.4 Periods corresponding to a head difference of  $-0.2$  m (Case 1) for the vertical ADCP. Upper plot: Timeseries of the water level at Roompot Buiten. The colours represent periods without quality checked ADCP data (red), quality checked ADCP data during increasing head (black) and during decreasing head (blue). The dots show the periods corresponding to a head difference of  $-0.2$  m. Lower plot: Timeseries of the head difference over the barrier.

Figure 3.5 shows the velocity profile for Case 1 based on the vertical ADCP measurements (left) and the number of observations used for each bin (right). The figure shows that during ebb, the velocity profiles are relatively flat for a large part of the water column. During periods of increasing absolute head, the average velocity in the main part of the water column is about  $-1.8 \pm 0.1$  m/s. For decreasing absolute head, the average velocity is slightly higher:  $-2.1 \pm 0.1$  m/s. The difference between the increasing and decreasing absolute head profiles can be explained by inertia, see Section 3.2.2.

The vertical ADCP couldn't measure the current velocity in the first 0.44 m above the sill beam, due to blanking. However, the influence of the sill beam can still be seen in the reduction of the flow velocity in the lower 1.5 m.

The velocity profile for decreasing absolute head shows a large spread around  $-2$  m NAP. This is related to the fact that during some of the selected measurements, the water level is close to  $-2$  m NAP, which results in inaccurate measurements. For some periods these bins have already been removed from the dataset by the Partrac quality procedures (ref [2]), as can be seen in the decreasing amount of observations (see Figure 3.5, right). Although Partrac removed most of the in-air measurements, some of these in-air measurements, which are on the limit of the quality criteria, are still present in this dataset.

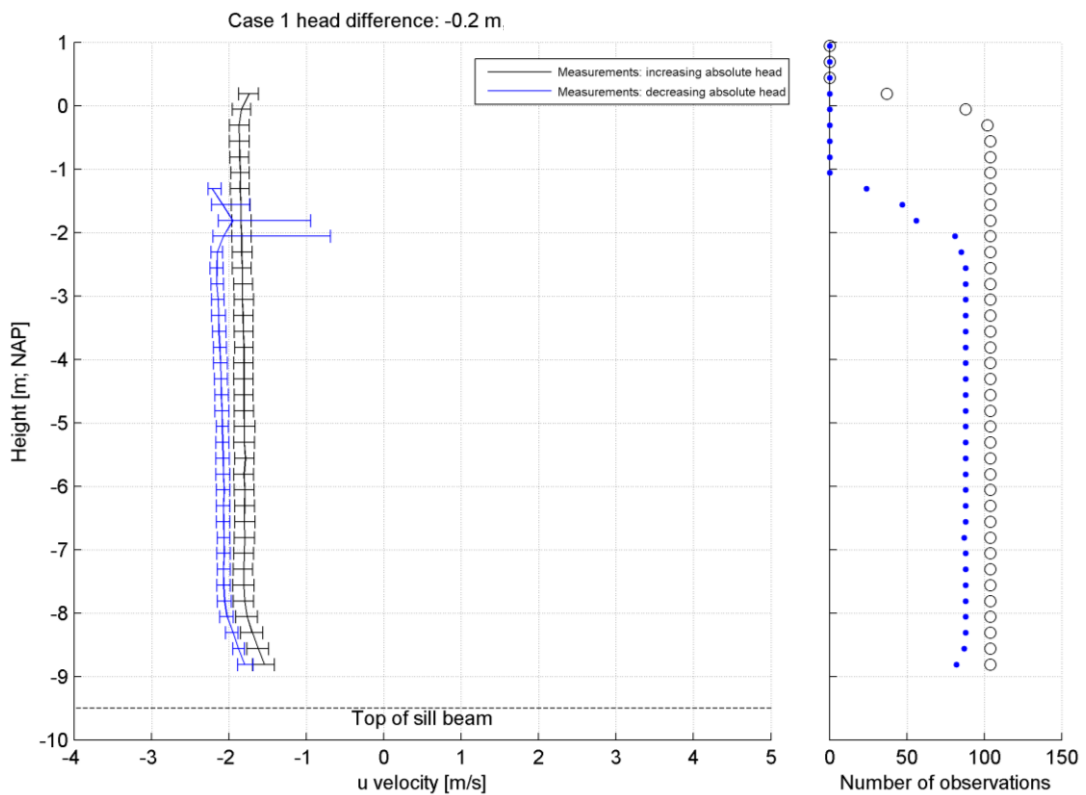


Figure 3.5 Left: Velocity profile for Case 1 (head difference of  $-0.2$  m) as measured by the vertical ADCP. Distinction is made between periods of increasing and decreasing absolute head. Right: Number of observations used per bin.

#### Horizontal ADCP

Figure 3.6 shows the water level at sea and the head difference over the barrier, in which the dots show the periods which correspond to Case 1. The horizontal ADCP datasets contains 24 periods corresponding to Case 2, of which 12 are during increasing absolute head and also 12 during decreasing absolute head.

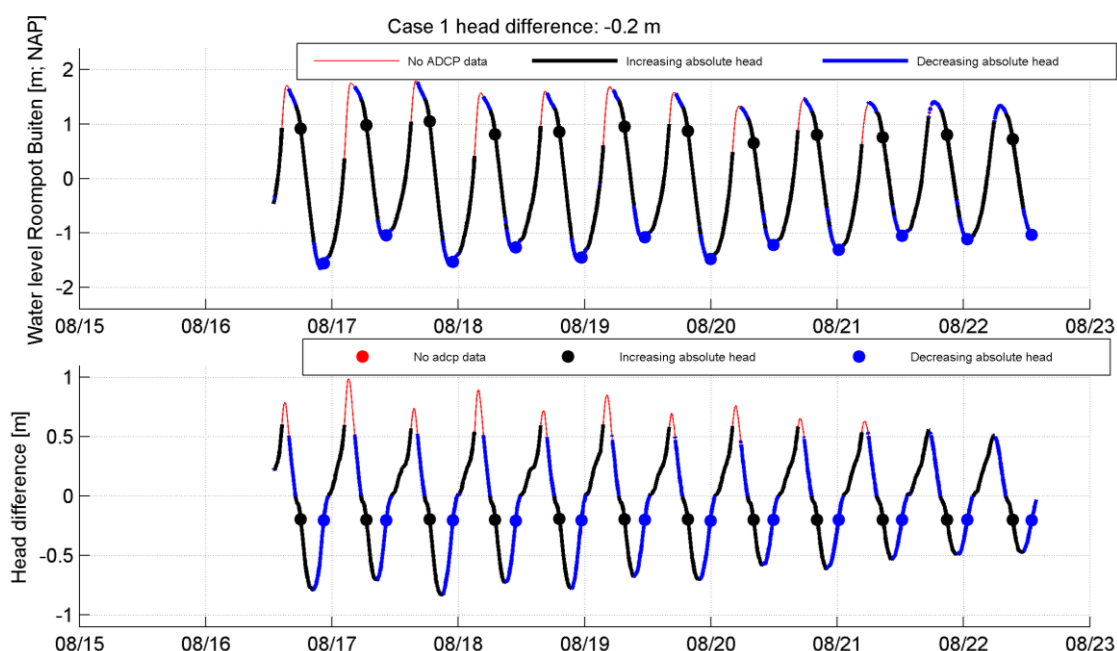


Figure 3.6 Periods corresponding to a head difference of  $-0.2$  m (Case 1) for the horizontal ADCP. Upper plot: Timeseries of the water level at Roompot Buiten. The colours represent periods without quality checked ADCP data (red), quality checked ADCP data during increasing head (black) and during decreasing head (blue). The dots show the periods corresponding to a head difference of  $-0.2$  m. Lower plot: Timeseries of the head difference over the barrier.

Figure 3.7 shows the velocity profile for Case 1 based on the horizontal ADCP measurements (left) and the number of observations used for each bin (right). The figure also shows the location of the vertical ADCP, which is at  $9.2$  m from pillar R9. The horizontal ADCP is located at  $-4.8$  m NAP. Unfortunately, the horizontal ADCP couldn't obtain reliable velocity measurements at the location of the vertical ADCP. Given the fact that the horizontal velocity profile at  $-4.8$  m NAP is relatively constant, still a comparison between the horizontal and vertical ADCP can be made. Please note the vertical ADCP is located about  $3.2$  m closer to the sill beam, see Figure 3.2. At the bin closest to the vertical ADCP location, the flow velocity is about  $-1.8 \pm 0.1$  m/s for increasing absolute head and about  $-2.0 \pm 0.1$  m/s for decreasing absolute head. This is in close agreement with the velocity profile at  $-4.8$  m NAP as measured by the vertical ADCP.

The horizontal velocity profiles show a slight increase from the pillar towards the middle of the gate. At about  $8$  m from pillar R9, the current velocity is about  $0.1 - 0.3$  m/s higher than at  $0.6$  m from pillar R9.

It is noted that all horizontal ADCP data for head differences larger than about  $+0.6$  m were removed by Partrac because the data didn't meet the quality criteria (for example due to vibrations of the horizontal ADCP device).

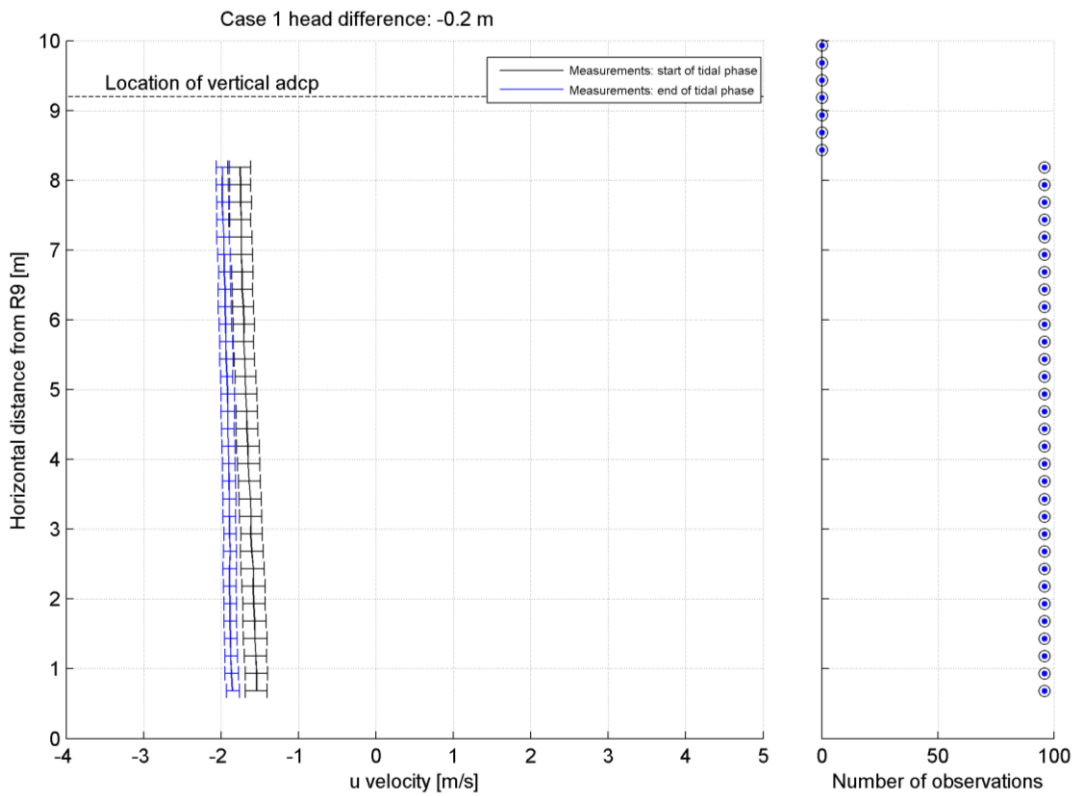


Figure 3.7 Left: Velocity profile for Case 1 (head difference of -0.2 m) as measured by the horizontal ADCP. Distinction is made between periods of increasing and decreasing absolute head. Right: Number of observations used per bin.

*Combined horizontal and vertical ADCP*

Figure 3.8 shows an impression of the measured velocity profiles for Case 1 during decreasing absolute head.



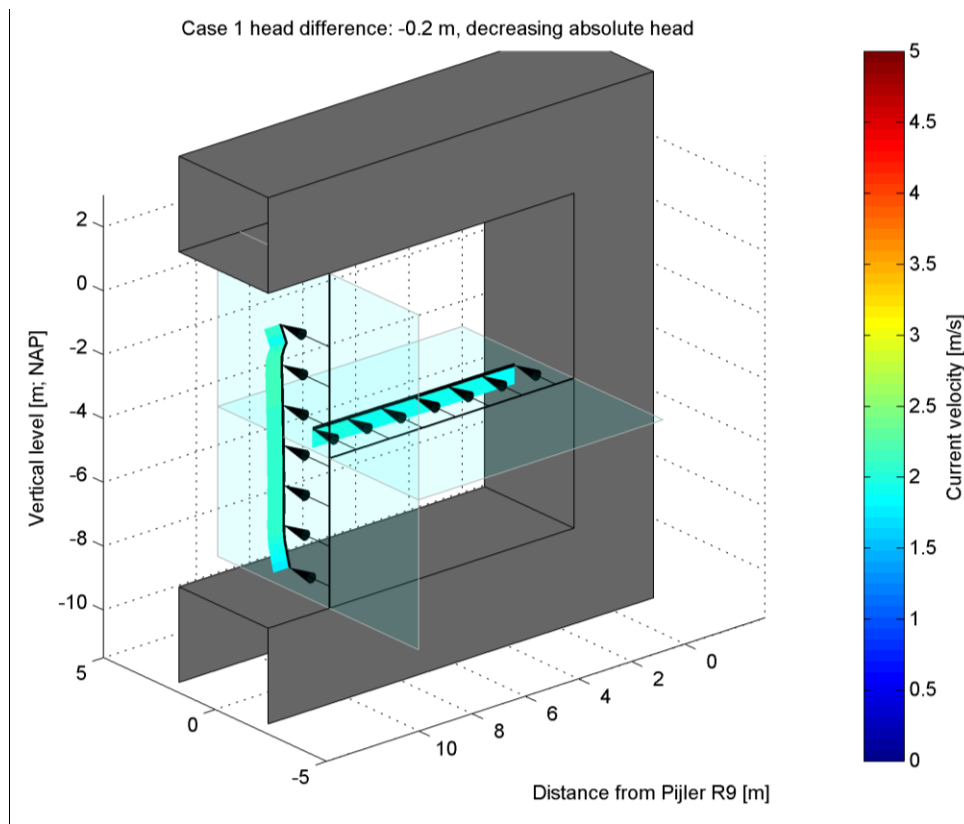


Figure 3.8 Impression of the measured current profiles for Case 1 during decreasing absolute head.

### 3.2.4 Velocity profiles during flood

This section describes the measured velocity profile corresponding to a head difference of +0.55 m (case 4). The results for the other flood case (case 3, head difference of +0.2 m) are included in Appendix C.

#### *Vertical ADCP*

Figure 3.9 shows the water level at sea and the head difference over the barrier, in which the dots show the periods which correspond to Case 4 (head difference of +0.55 m). The black and blue lines and dots show the periods when quality checked data is available for the vertical ADCP. The vertical ADCP datasets contains 26 periods corresponding to Case 4, of which 13 are during increasing absolute head and also 13 during decreasing absolute head.

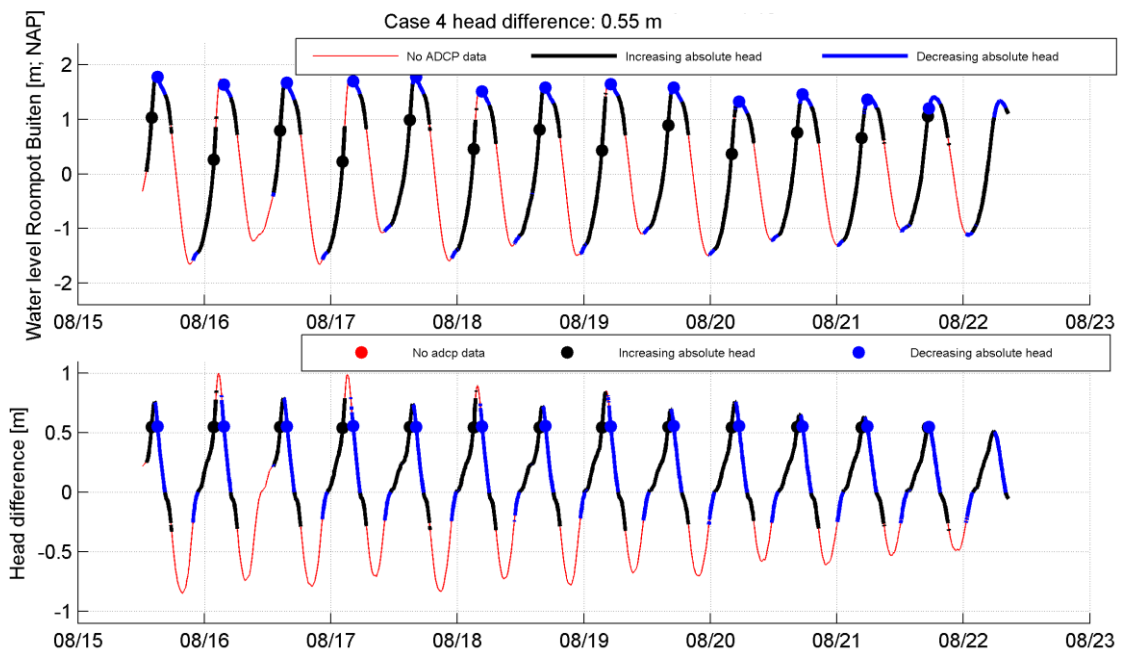


Figure 3.9 Periods corresponding to a head difference of +0.55 m (Case 4) for the vertical ADCP. Upper plot: Timeseries of the water level at Roompot Buitten. The colours represent periods without quality checked ADCP data (red), quality checked ADCP data during increasing head (black) and during decreasing head (blue). The dots show the periods corresponding to a head difference of +0.55 m. Lower plot: Timeseries of the head difference over the barrier.

Figure 3.10 shows the velocity profile for Case 4 based on the vertical ADCP measurements (left) and the number of observations used for each bin (right). The figure shows that during flood, the velocity profiles are relatively flat for a large part of the water column. During periods of decreasing absolute head, the average velocity in the main part of the water column is about  $+3.6 \pm 0.1$  m/s. For increasing absolute head, the average velocity is slightly higher:  $+3.8 \pm 0.1$  m/s. The difference between the increasing and decreasing absolute head profiles can be explained by inertia, see Section 3.2.2.

The influence of the sill beam extends up to about 3 m above the sill beam, which is further upwards than during the ebb case (only 1.5 m) as described in Section 3.2.3. Below -8.5 m NAP negative flow velocities are recorded, which indicates a recirculation zone in the first 1 m above the sill beam. The fact that the influence of the sill beam is more pronounced during flood is mainly related to the fact that the vertical ADCP is located on the Eastern Scheldt side of the sill beam.

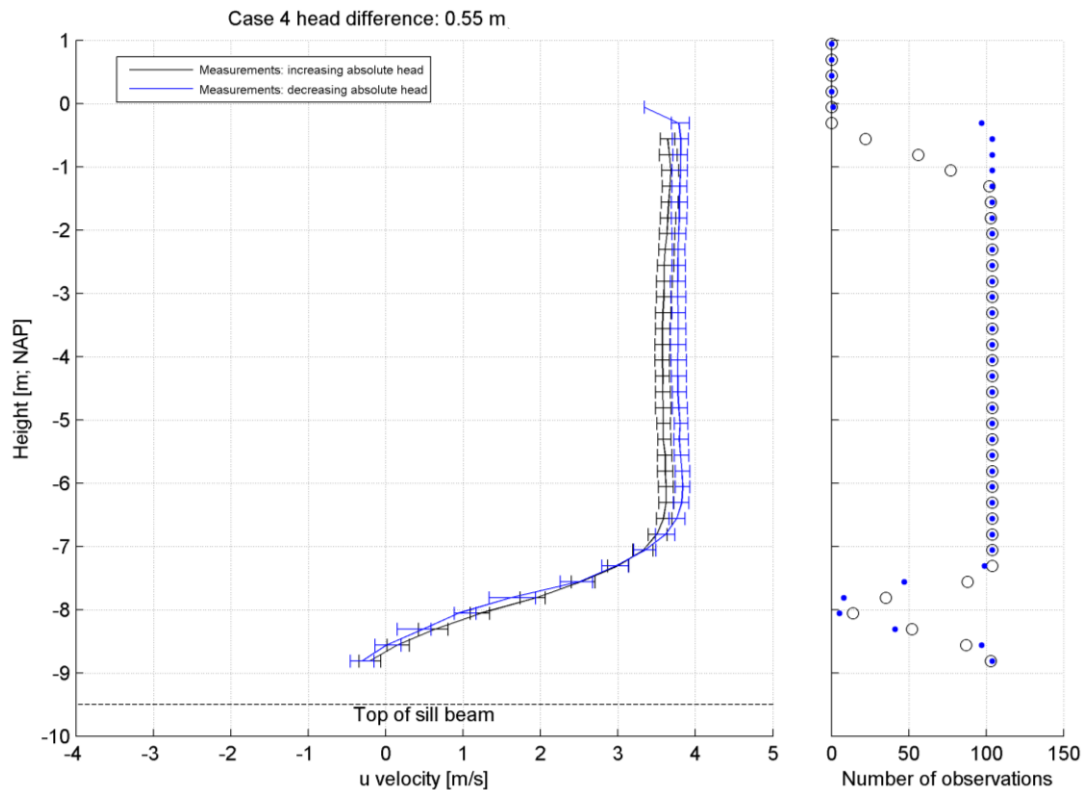


Figure 3.10 Left: Velocity profile for Case 4 (head difference of +0.55 m) as measured by the vertical ADCP. Distinction is made between periods of increasing and decreasing absolute head. Right: Number of observations used per bin.

#### Horizontal ADCP

Figure 3.11 shows the water level at sea and the head difference over the barrier, in which the dots show the periods which correspond to Case 4 (head difference of +0.55 m). The black and blue lines and dots show the periods when quality checked data is available for the horizontal ADCP. The horizontal ADCP datasets contains 16 periods corresponding to Case 4, of which 11 are during increasing absolute head and only 5 during decreasing absolute head. Due to inertia, the flow velocity during decreasing absolute head is higher, which resulted in larger forces on the ADCP causing unreliable measurements. This is the reason why fewer observations could be obtained for decreasing absolute head.

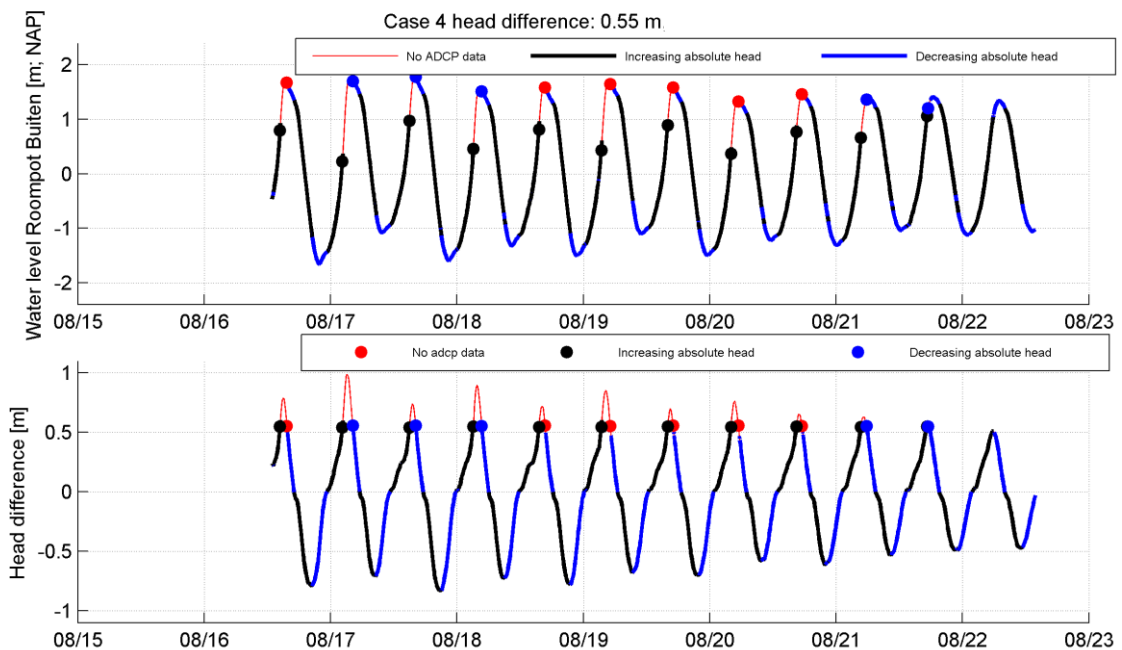


Figure 3.11 Periods corresponding to a head difference of +0.55 m (Case 4) for the horizontal ADCP. Upper plot: Timeseries of the water level at Roompot Buitten. The colours represent periods without quality checked ADCP data (red), quality checked ADCP data during increasing head (black) and during decreasing head (blue). The dots show the periods corresponding to a head difference of +0.55 m. Lower plot: Timeseries of the head difference over the barrier.

Figure 3.12 shows the velocity profile for Case 4 based on the horizontal ADCP measurements (left) and the number of observations used for each bin (right). The figure also shows the location of the vertical ADCP, which is at 9.2 m from pillar R9. Since only 1 to 8 observations could be obtained per bin for decreasing absolute head, the corresponding flow profile is slightly unstable (for a better statistical representation of the flow profile more measurements would be required).

At the bin closest to the vertical ADCP location, the flow velocity is about  $-3.7 \pm 0.1$  m/s for increasing absolute head and about  $-3.8 \pm 0.1$  m/s for decreasing absolute head. This is in close agreement with the velocity profile at -4.8 m NAP as measured by the vertical ADCP.

The horizontal velocity profiles show a slight increase up to 2 m from pillar R9. Further away from the pillar, the velocity decreases again with about 0.2 m/s at 8 m from pillar R9.



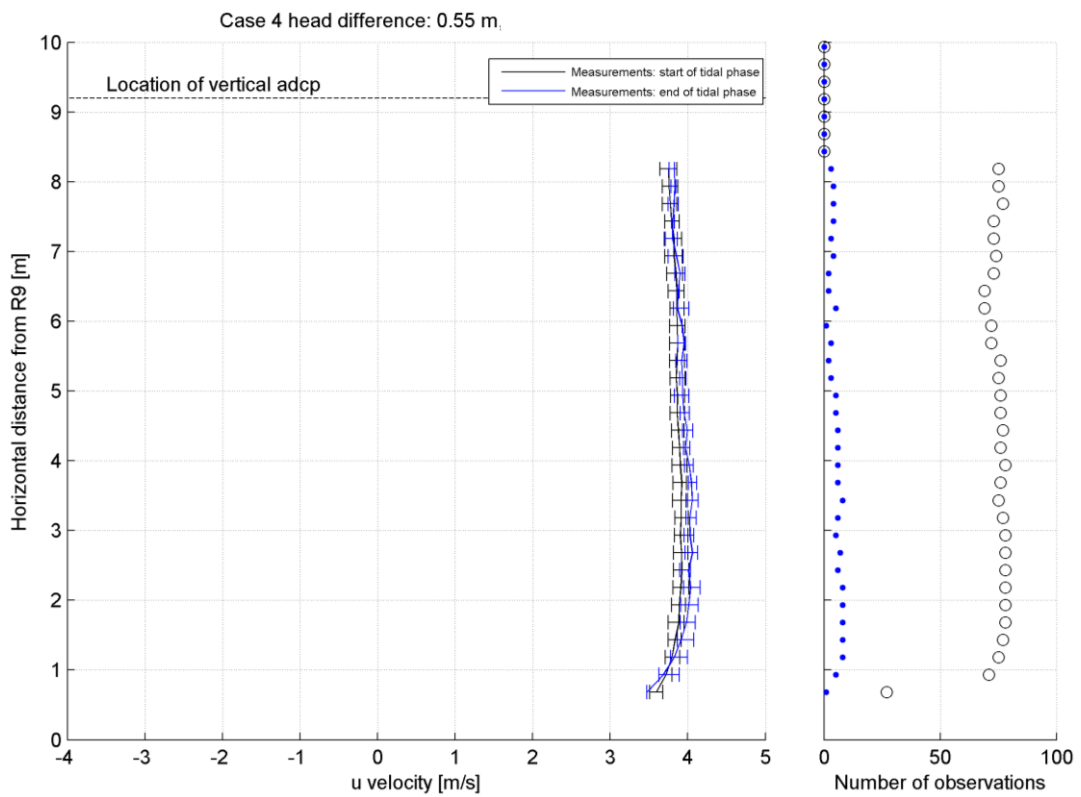


Figure 3.12 Left: Velocity profile for Case 4 (head difference of +0.55 m) as measured by the horizontal ADCP. Distinction is made between periods of increasing and decreasing absolute head. Right: Number of observations used per bin.

#### Combined horizontal and vertical ADCP

Figure 3.13 shows an impression of the measured velocity profiles for Case 4 during decreasing absolute head.

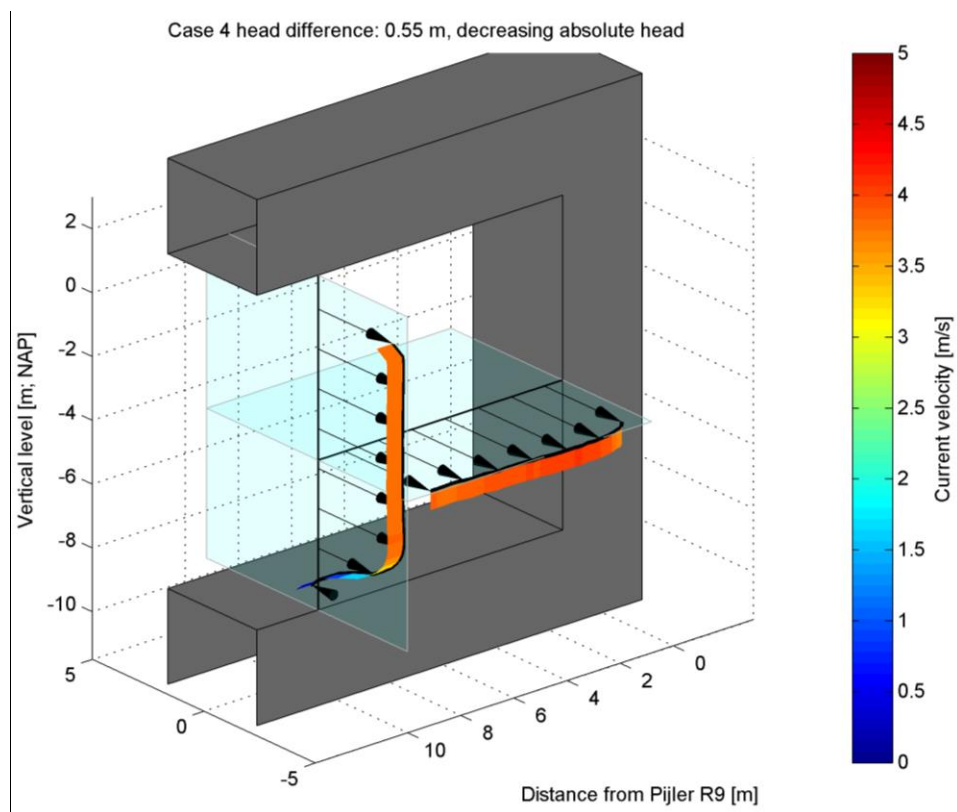


Figure 3.13 Impression of the measured current profiles for Case 4 during decreasing absolute head.

## 4 ADCP measurements during turbine deployment

### 4.1 Description of data

In 2015, 5 turbines have been installed on the Eastern Scheldt side of Gate #08 of the Eastern Scheldt Barrier Roompot section. The middle and outer turbines have been equipped with two ADCP's, one pointed forwards (towards the North Sea) and one pointed backwards (towards the Eastern Scheldt), see Figure 4.1. The turbines are placed with a distance of 6.7 m in between. The outer turbines are located at 6.35 m from the edge of the nearest pillar. The names of the forward-looking and backward-looking ADCP's are included in Figure 4.1 in green. The axis of the turbine is located at -4.83 m NAP. The distance between the rotor blades of the turbine and the edge of the sill beam is 6.76 m. The backward-looking ADCP is located at the same height as the axis of the turbine (at -4.83 m NAP) at 4.33 m east of the rotor blades. The forward-looking ADCP is located at a higher elevation, at -3.70 m NAP at 1.48 m east of the rotor blades.

The ADCP devices were installed in a "+" configuration, see Figure 4.2. Beam 1 and 3 were measuring in the horizontal plane, Beam 2 and 4 in the vertical plane and Beam 5 in front of the ADCP. As shown in Figure 4.1, the downward beam (Beam 2) measurements cannot be used for the forward-looking ADCP's, since it hits the turbine nacelle.

Tocado provided Deltares with ADCP data for 4 different periods. In between these different periods the type of turbine deployment was varied (normal mode – vs – stall mode) and the ADCP measurements were carried out for 1 or 5 beams. An overview of the different periods is given below:

Period (UTC)	Type of turbine deployment	Number of beams	Comments
10-10-2016 – 26-10-2016	Normal	1 (only beam 5)	ADCP-348 was missing
22-06-2017 14:00 – 24-06-2017 9:50	Normal	5	ADCP-348 was missing
28-08-2017 7:25 – 29-08-2017 7:10	Stall mode	1 (only beam 5)	ADCP-348 and ADCP-367 were missing. The blades of the northern turbine were removed.
14-09-2017 8:00 – 15-09-2017 23:50	Stall mode	5	ADCP-348 and ADCP-367 were missing. During part of the period, some turbines were not in stall mode. The blades of the northern turbine were removed

In addition to the ADCP data also records of the RPM and Power per turbine were provided. These records also specified if the turbines were "operational" or "parked".

The ADCP measurements were carried out with the Nortek Signature 1000. The main characteristics of the ADCP setup are given in the table below.

The ADCP measurements were provided in .ad2cp format and were read using MATLAB scripts. The ADCP data contained on average about 16 records per second. The ADCP data was referenced to the GMT time zone.

The ADCP measurements have been checked against a number of quality criteria. An overview of the criteria and the quality checked data is included in Appendix D.

<b>Bin size</b>	0.5 m
<b>Blanking distance</b>	0.5 m
<b>Beam width</b>	2.9°
<b>Beam angle</b>	25 °

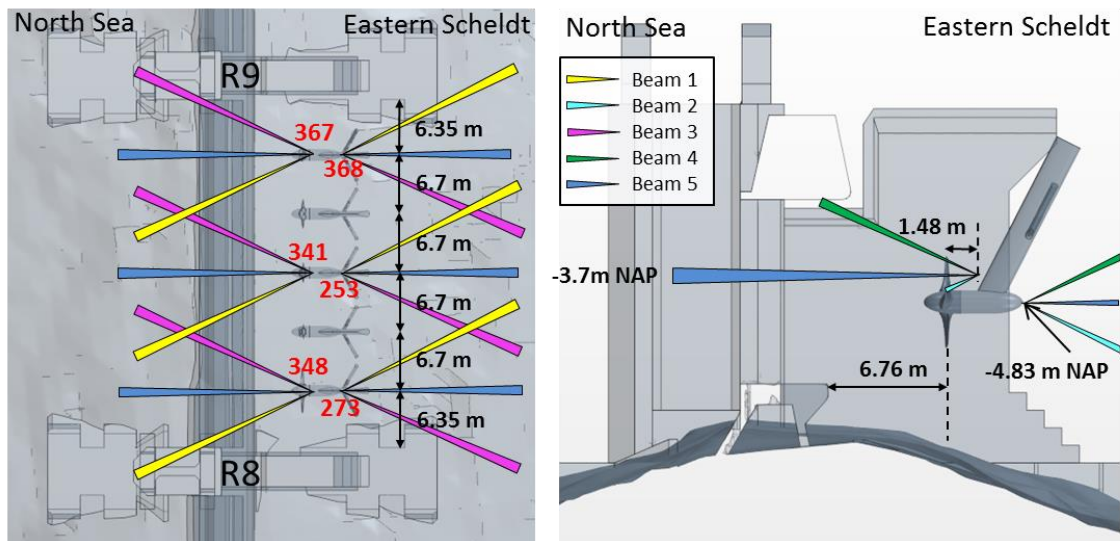


Figure 4.1 Top view (left) and side view (right) of the turbine configuration at Gate #08 of the Eastern Scheldt Roompot Section. The red numbers show the names of the forward-looking and backward-looking ADCP devices.

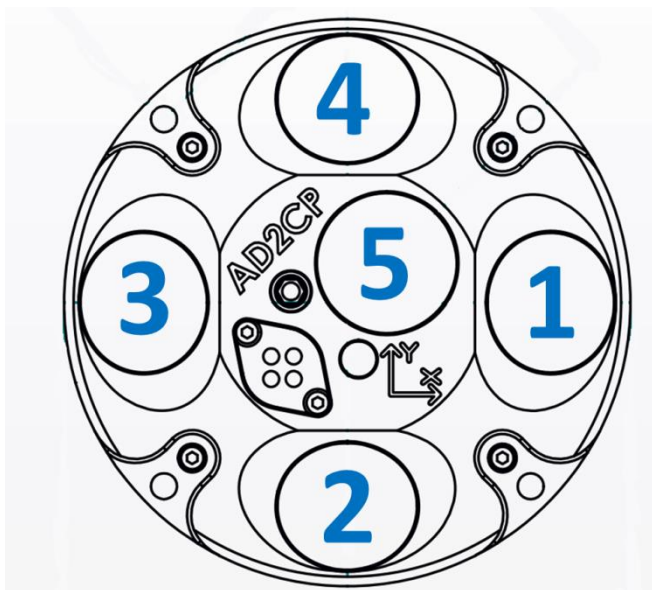


Figure 4.2 Orientation of the Nortek Signature 1000 ADCP. Beam 1 and 3 are measuring in the horizontal plane, Beam 2 and 4 in the vertical plane, Beam 5 is measuring in front of the ADCP.

## 4.2 Analysis of 1-beam measurements during normal turbine operation

### 4.2.1 Approach

The approach for analysing the velocity profiles for different head differences is exactly similar to the approach applied on the 2011 ADCP measurements, see Section 3.2.1. See Table 3.1 for the characteristics of the cases that have been analysed and are discussed in this Chapter and Appendix E.

### 4.2.2 Velocity profiles during ebb

This section describes the measured velocity profile corresponding to a head difference of -0.2 m (case 1). The results for the other ebb case are included in Appendix E.

Figure 4.3 shows the velocity profile for Case 1 based on the forward-looking and backward-looking ADCP devices on the middle turbine. The black (blue) lines show the velocity profile (median including the  $\pm$  one standard deviation) during increasing (decreasing) absolute head. A negative velocity corresponds to a velocity towards the North Sea. The blue arrow indicates the flow direction during this ebb case, which is from the Eastern Scheldt (top) to the North Sea (down). The vertical axis shows the distance from the rotor axis (positive towards the Eastern Scheldt). For interpretation, the location of the sill beam is indicated with the grey patch. The right plot shows the number of 1-minute averaged observations used per bin.

The figure shows that the flow accelerates from far upstream to about 6 m upstream of the rotor, after which the velocity decreases due to the turbine. At the rotor blade, the ADCP measurements show a large spreading. Downstream of the rotor, the flow accelerates again due to the presence of the gates and sill beam. The spreading in the ADCP shows that upstream of the turbine, the variation in the current velocity is relatively low (standard deviation of about 0.15 m/s). Downstream of the turbine, the turbulence induced by the turbine operation results in relatively large velocity variations (standard deviation of about 0.35 m/s). The largest standard deviation can be found in the bin just downstream of the rotor, which is expected and confirms that the bin locations are correctly interpreted.

The effect of inertia can also be seen in Figure 3.10. The flow velocities during decreasing absolute head (later in the tidal phase) are generally about 0.05 m/s to 0.3 m/s higher.

The velocity profile for the other turbines are very similar to the middle turbine, see Appendix E.

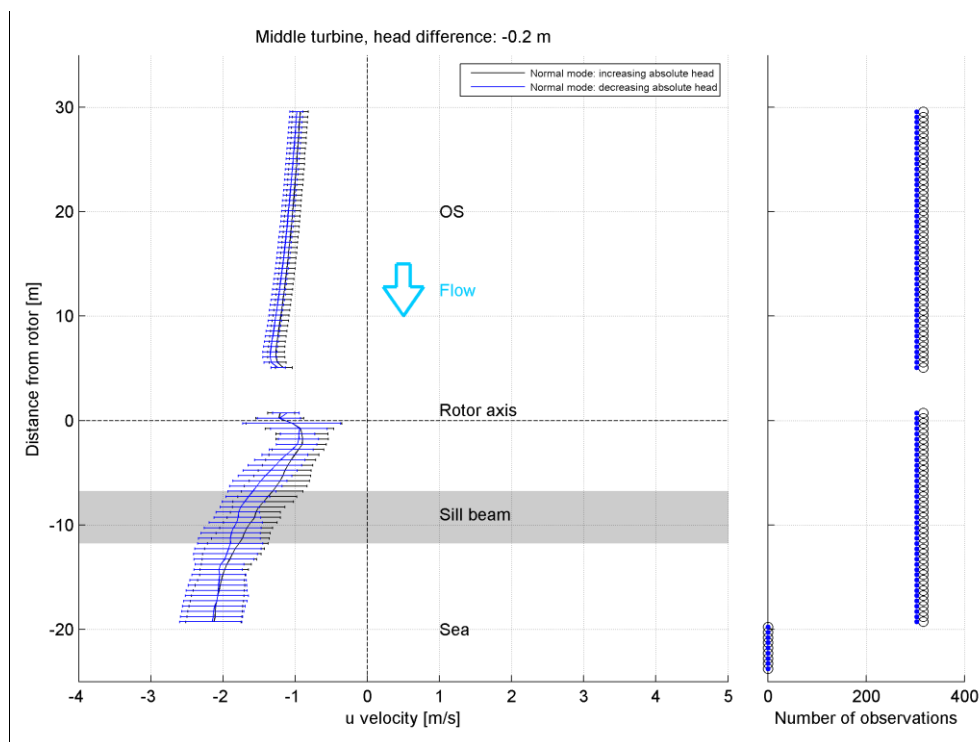


Figure 4.3 Left: Velocity profile for Case 1 (head difference of -0.2 m) as measured by the forward-looking and backward-looking ADCP devices on the middle turbine. Distinction is made between periods of increasing and decreasing absolute head. Right: Number of observations used per bin.

#### 4.2.3 Velocity profiles during flood

This section describes the measured velocity profile corresponding to a head difference of +0.55 m (case 4). The results for the other flood case are included in Appendix E.

Figure 4.4 shows the velocity profile for Case 4 based on the forward-looking and backward-looking ADCP devices on the middle turbine. The black (blue) lines show the velocity profile (median including the  $\pm$  one standard deviation) during increasing (decreasing) absolute head. A positive velocity corresponds to a velocity towards the Eastern Scheldt. The blue arrow indicates the flow direction during this flood case, which is from the North Sea (down) to the Eastern Scheldt (up). The vertical axis shows the distance from the rotor axis (positive towards the Eastern Scheldt). For interpretation, the location of the sill beam is indicated with the grey patch. The right plot shows the number of 1-minute averaged observations used per bin. During decreasing absolute head (later in the flood phase), the number of observations are significantly less than during increasing absolute head (earlier during the flood phase). This is related to the fact that the turbines are lifted out of the water at +0.8 m head difference and again lowered into the water when the head difference is lower than +0.8 m head. Subsequently, it takes time before the turbines are fully operational, which is why generally the turbines are not yet operational at a head difference of +0.55 during decreasing head.

The figure shows that the flow accelerates from far upstream to a few meters downstream of the sill beam, due to the presence of the gate and sill beam. At this location, the contraction of the flow has reached a maximum, resulting in the highest current velocities (up to about 4 m/s). Subsequently the flow velocity decreases and reaches the rotor blade. Downstream of the rotor blade, the flow becomes more turbulent indicated by the larger spreading in the flow



velocity results. Further downstream of the turbine, the flow velocity fluctuates after which a steady increase can be observed further downstream.

Around the location of the sill beam, the standard deviation of the recorded flow velocity is about 0.2 m/s to 0.5 m/s. Downstream of the turbine, the flow is highly turbulent, resulting in a standard deviation of about 0.6 – 0.8 m/s.

The ADCP results again show the effect of inertia. The flow velocities during decreasing absolute head (later in the tidal phase) are generally about 0.1 m/s to 0.15 m/s higher.

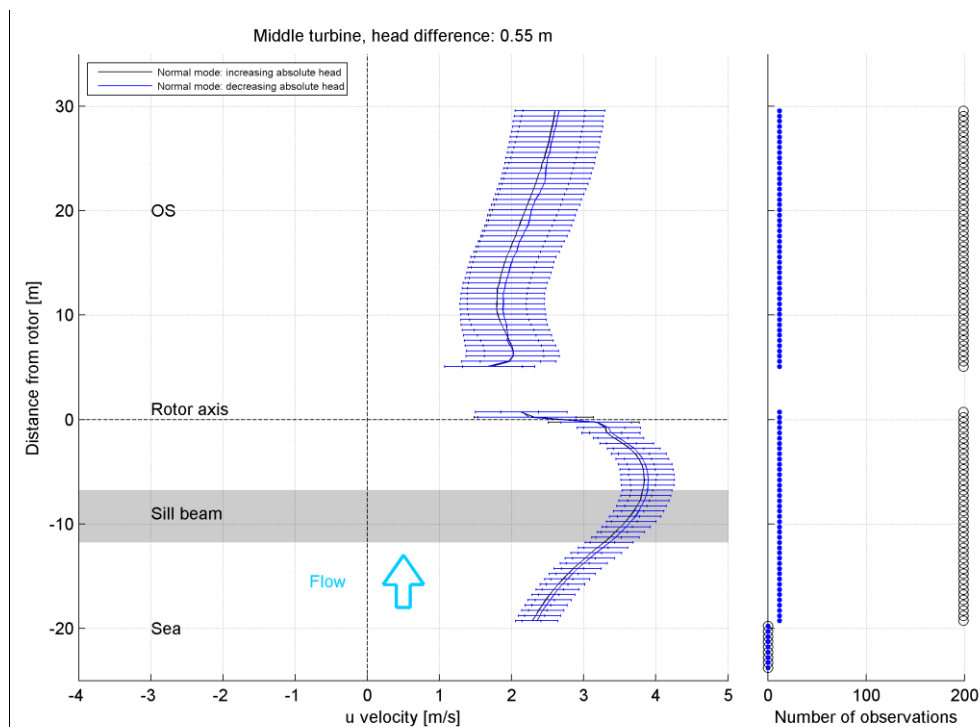


Figure 4.4 Left: Velocity profile for Case 4 (head difference of +0.55 m) as measured by the forward-looking and backward-looking ADCP devices on the middle turbine. Distinction is made between periods of increasing and decreasing absolute head. Right: Number of observations used per bin.

### 4.3 Analysis of 5-beam measurements during normal turbine operation

#### 4.3.1 Determining flow angle and overall flow magnitude

Each of the ADCP beams only measures the component of the flow velocity which is parallel to the beam. If the flow angle is not exactly parallel to the beam, the measured velocity is lower than the overall flow velocity. The exact flow velocity and flow angle can therefore only be determined at a location where two beams overlap. Figure 4.5 shows the locations where this is the case.

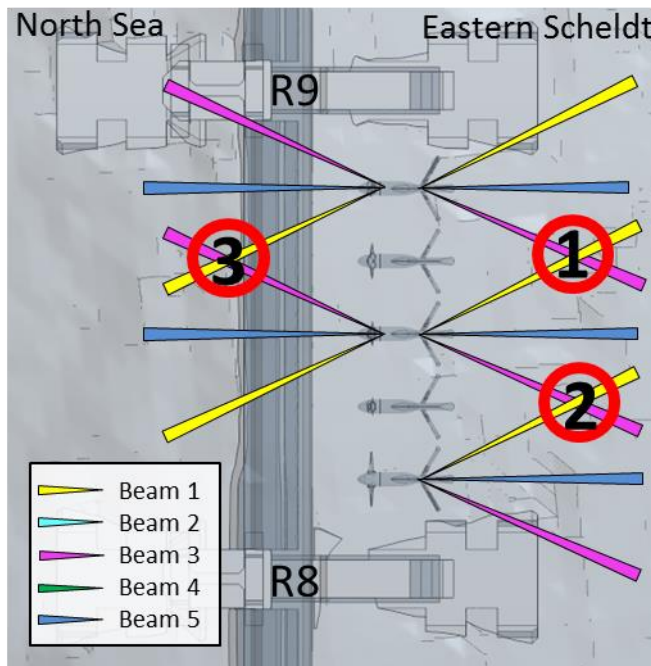


Figure 4.5 Available ADCP beams during normal operation. The circles show the available locations where beams overlap

Figure 4.6 shows the obtained overall flow velocity and direction after combining the velocity measurements at overlapping location 1. The blue (red) dots show the head difference over the barrier, flow velocity and flow direction during ebb (flood). One of the interesting observations from this analysis is that initially during ebb, the flow is approaching Gate #08 under an angle of about  $30^\circ$  to  $45^\circ$ . This angle decreases until the flow is about perpendicular to the barrier after about one hour.

During flood, the flow direction shows a bit more short-term variability than during ebb. The figure shows that during flood, the flow direction generally ranges from  $70^\circ\text{N}$  -  $100^\circ\text{N}$  (ENE to ESE).

Figure 4.7 shows the obtained overall flow velocity and direction at overlapping location 2. In general, the observed phenomena at location 2 are similar to the ones observed at location 1. One big difference however is the observed flow velocity during flood. At location 2, the peak flood velocities are about 0.5-0.8 m/s higher than at location 1. This indicates that the flood flow downstream of the turbines is not symmetrical, which can be explained by the fact that the blades of the northern turbine were not in place during the measurements. The northern turbine therefore has a lower resistance on the flow, which results in a higher discharge through the northern part of the gate. Subsequently the increased flow in the northern part will push the wakes of the other turbines a bit more towards the south, resulting in an asymmetrical flow pattern.

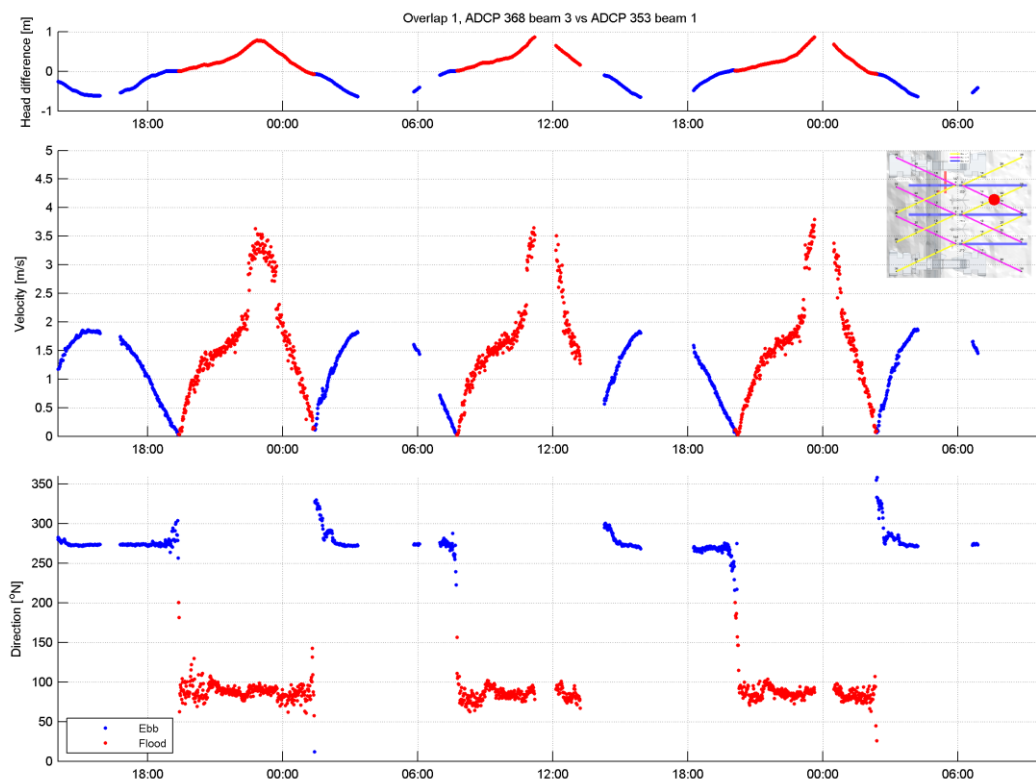


Figure 4.6 Overall current velocity and direction at overlapping location 1 (ADCP 368 beam 3 and ADCP 353 beam 1)

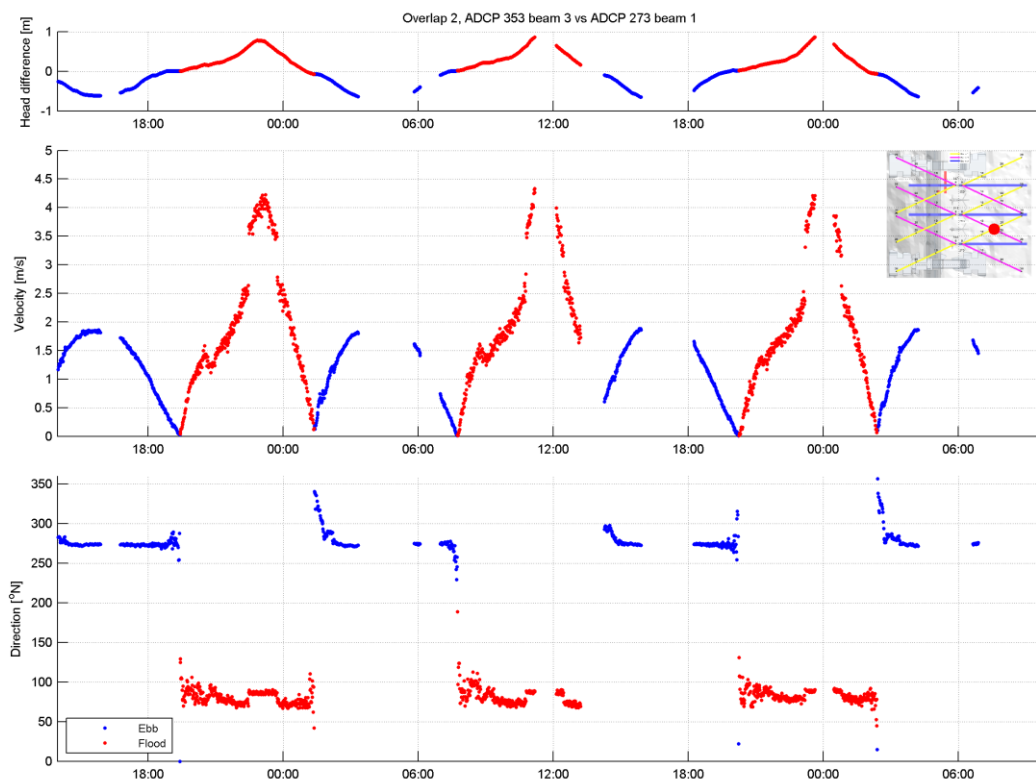


Figure 4.7 Overall current velocity and direction at overlapping location 2 (ADCP 353 beam 3 and ADCP 273 beam 1)

#### 4.3.2 Velocity profiles during ebb

This section describes the measured velocity profile corresponding to a head difference of -0.2 m (case 1). The results for the other ebb case are included in Appendix E.

Figure 4.8 shows the median velocities for Case 1 based on the beams located in the horizontal plane of the ADCP's. It is noted that each beam could only measure the velocity component in the measurement direction. In case the flow is perpendicular to the Eastern Scheldt Barrier, the angled beams (beam 1 and beam 3) will record only part of the total flow velocity. A quantitative interpretation of the spatial flow patterns is therefore difficult. This section therefore focusses on a qualitative interpretation.

The figure shows that the flow is accelerated while it approaches the Eastern Scheldt Barrier. Immediately downstream of the turbines, the low velocities indicate the wake of the turbines. The angled beams show the wake of the neighbouring turbines also further downstream. In between the turbines a flow acceleration can be observed. This phenomenon can be observed more clearly during flood.

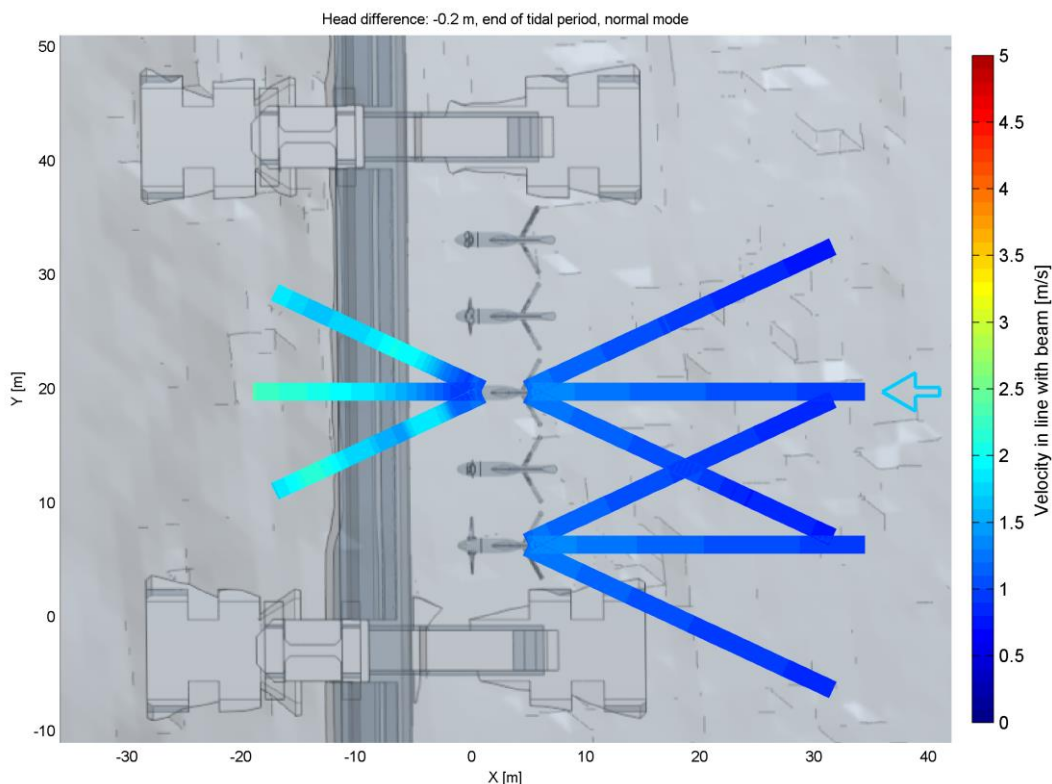


Figure 4.8 Left: Velocity profile for Case 1 (head difference of -0.2 m) as measured in the horizontal plane by the forward-looking and backward-looking ADCP devices.

#### 4.3.3 Velocity profiles during flood

This section describes the measured velocity profile corresponding to a head difference of +0.55 m (case 4). The results for the other flood case are included in Appendix E.

Figure 4.9 shows the median velocities for Case 4 based on the beams located in the horizontal plane of the ADCP's.

The figure shows again a relatively smooth acceleration towards the Eastern Scheldt Barrier. Downstream of the turbines an alternating pattern of high and low flow velocities can be observed. The wake of the middle turbine is angled towards the south, which may be related to the missing rotor blades on the northern turbine, which triggers an asymmetrical flow through the gate.

It is noted that these figures are based on a limited amount of data (3 occurrences).

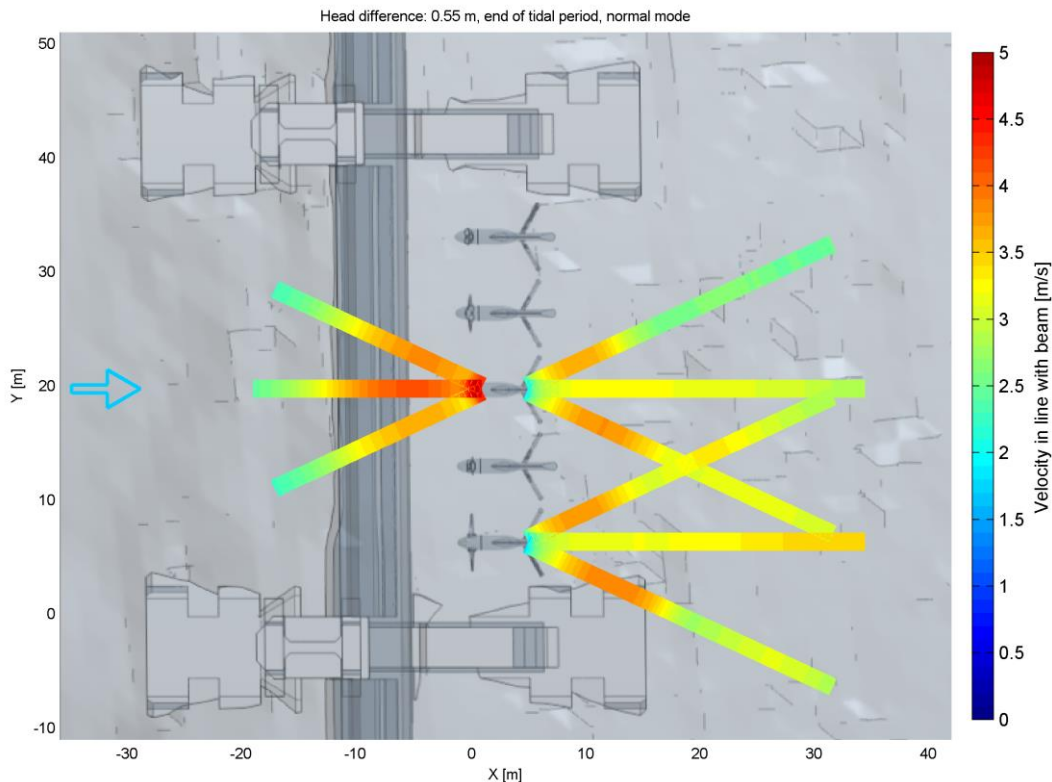


Figure 4.9 Left: Velocity profile for Case 4 (head difference of +0.55 m) as measured in the horizontal plane by the forward-looking and backward-looking ADCP devices.

#### 4.4 Analysis of 1-beam measurements during stall-mode turbine operation

##### 4.4.1 Velocity profiles during ebb

This section describes the measured velocity profile corresponding to a head difference of -0.2 m (case 1). The results for the other ebb case are included in Appendix E.

Figure 4.10 shows the velocity profile for Case 1 based on the forward-looking and backward-looking ADCP devices on the middle turbine. The red (magenta) lines show the velocity profile during increasing (decreasing) absolute head. A negative velocity corresponds to a velocity towards the North Sea. The blue arrow indicates the flow direction during this ebb case, which is from the Eastern Scheldt (top) to the North Sea (down). The vertical axis shows the distance from the rotor axis (positive towards the Eastern Scheldt). For interpretation, the location of the sill beam is indicated with the grey patch. The right plot shows the number of 1-minute averaged observations used per bin. It is noted that in these plots, the standard deviation of the velocity measurements is not included, since only a couple of flow profiles were available per head difference.

As the flow approaches the Eastern Scheldt Barrier, the flow velocity slightly increases until it feels the presence of the turbine at about 8 m upstream of the rotor blade. Downstream of the turbine, the velocity increases further until it reached the other side of the sill beam.

A comparison to the velocity results during normal mode is described in Section 5.3.

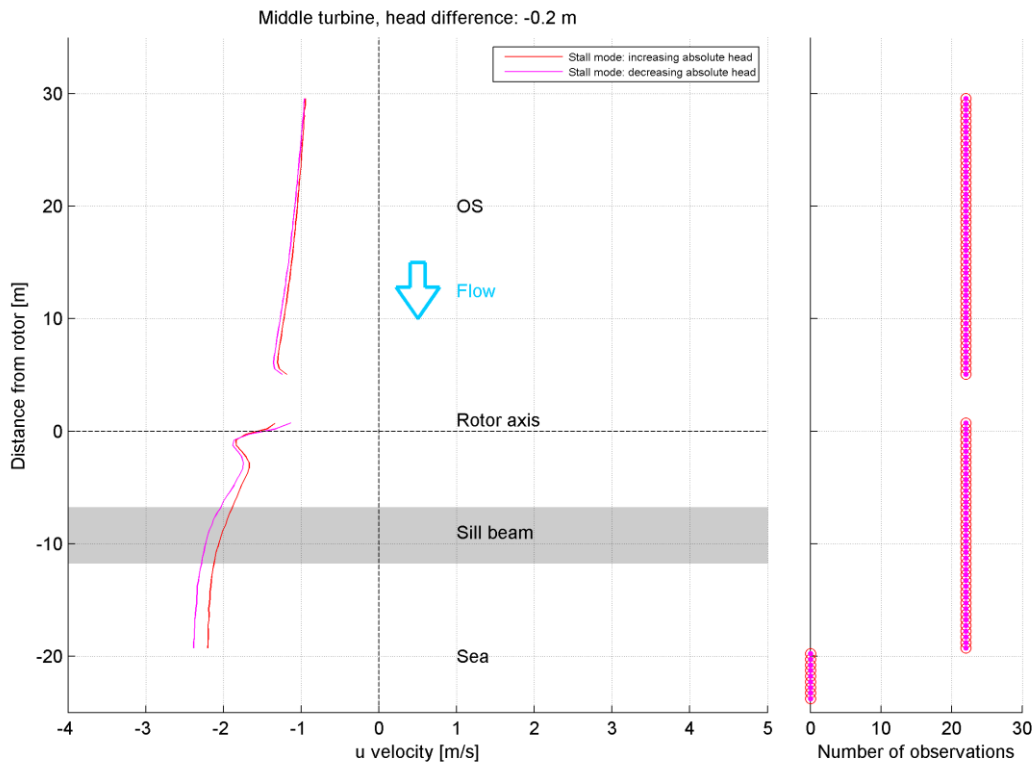


Figure 4.10 Left: Velocity profile for Case 1 (head difference of -0.2 m) as measured by the forward-looking and backward-looking ADCP devices on the middle turbine during stall mode operation. Distinction is made between periods of increasing and decreasing absolute head. Right: Number of observations used per bin.

#### 4.4.2 Velocity profiles during flood

This section describes the measured velocity profile corresponding to a head difference of +0.55 m (case 4). The results for the other flood case are included in Appendix E.

Figure 4.11 shows the velocity profile for Case 4 based on the forward-looking and backward-looking ADCP devices on the middle turbine. A description of the presentation format can be found in the previous section

The figure shows that the flow accelerates from far upstream to a few meters downstream of the sill beam, due to the presence of the gate and sill beam. At this location, the contraction of the flow has reached a maximum, resulting in the highest current velocities (up to about 4 m/s). Subsequently the flow velocity decreases and reaches the rotor blade. Downstream of the rotor blade, the flow quickly re-establishes to a flow velocity of about 3 m/s.

A comparison to the velocity results during normal mode is described in Section 5.3.



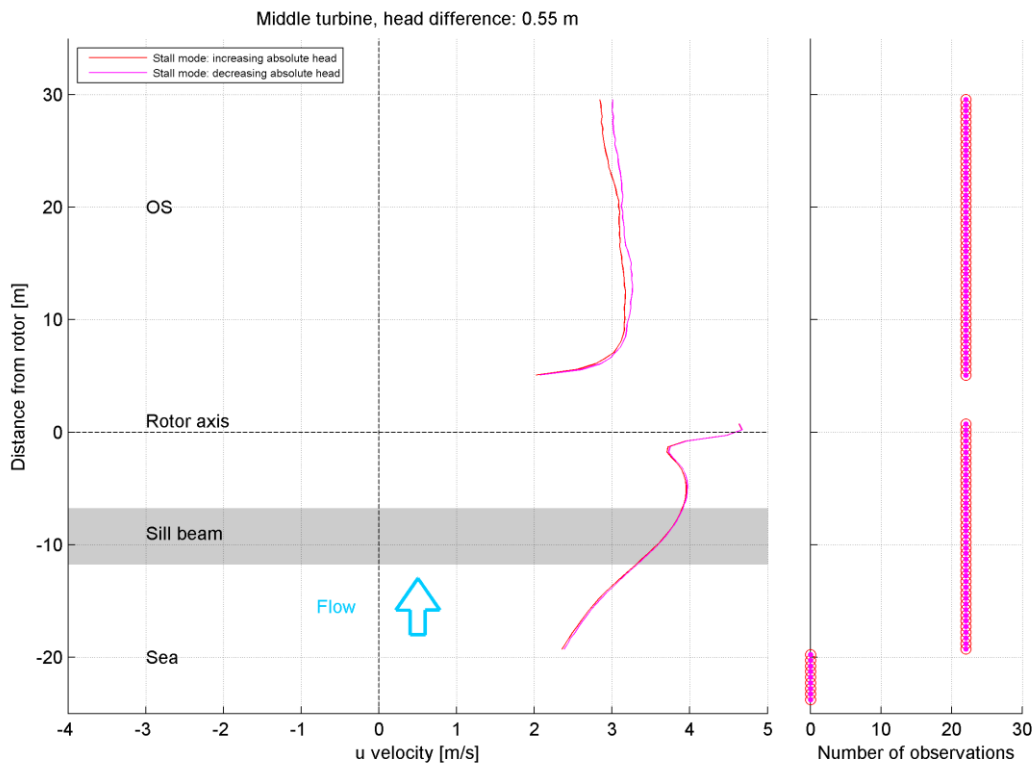


Figure 4.11 Left: Velocity profile for Case 4 (head difference of 0.55m) as measured by the forward-looking and backward-looking ADCP devices on the middle turbine during stall mode operation. Distinction is made between periods of increasing and decreasing absolute head. Right: Number of observations used per bin.

## 4.5 Analysis of 5-beam measurements during stall-mode turbine operation

### 4.5.1 Velocity profiles during ebb

This section describes the measured velocity profile corresponding to a head difference of -0.2 m (case 1). The results for the other ebb case are included in Appendix E.

Figure 4.12 shows the median velocities for Case 1 based on the beams located in the horizontal plane of the ADCP's. During stall mode, the resistance of the turbine on the flow is less than during normal operation, which is why the wake of the turbines is confined to the zone very close to the turbine. Further downstream, the wake of the turbines can hardly be recognized.

A comparison to the velocity results during normal mode is described in Section 5.3.



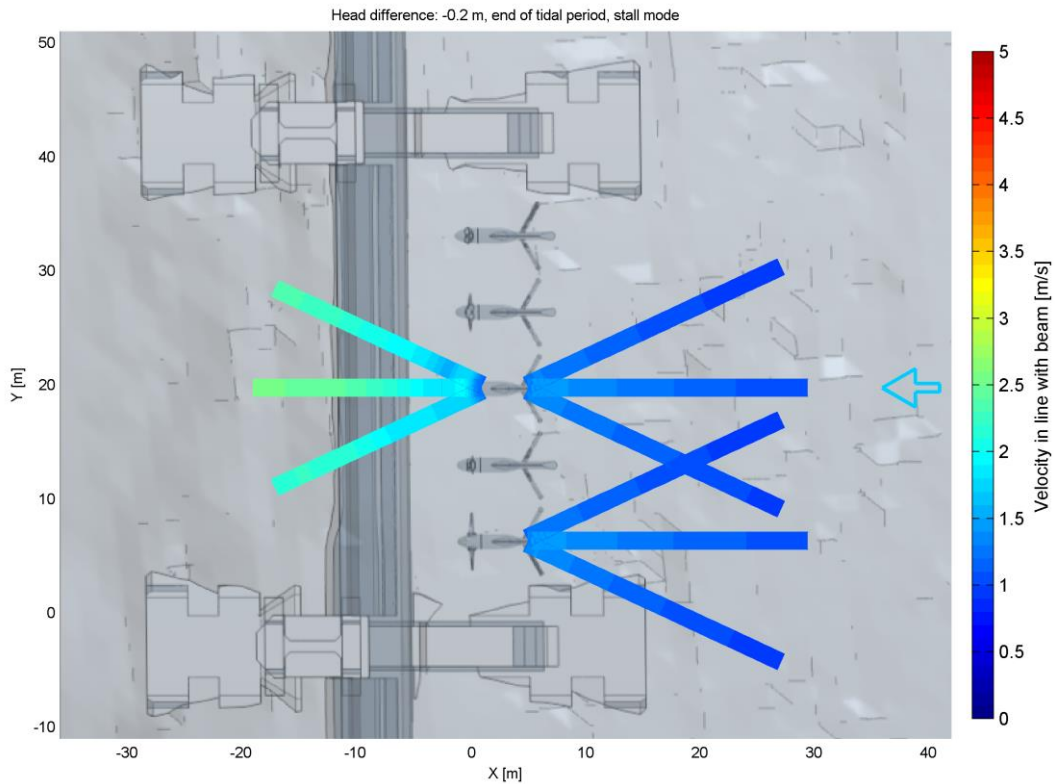


Figure 4.12 Left: Velocity profile for Case 1 (head difference of -0.2 m) as measured in the horizontal plane by the forward-looking and backward-looking ADCP devices during stall mode operation.

#### 4.5.2 Velocity profiles during flood

The 5-beam dataset only covered head differences of up to +0.3 m. Therefore, results for case 4 (head difference of +0.55m) are not available. Figure 4.13 shows the median velocities for Case 3 based on the beams located in the horizontal plane of the ADCP's. Downstream of the turbines, a very confined wake can be seen. The southern backward-looking beam clearly shows the wake of the pillar.

A comparison to the velocity results during normal mode is described in Section 5.3.

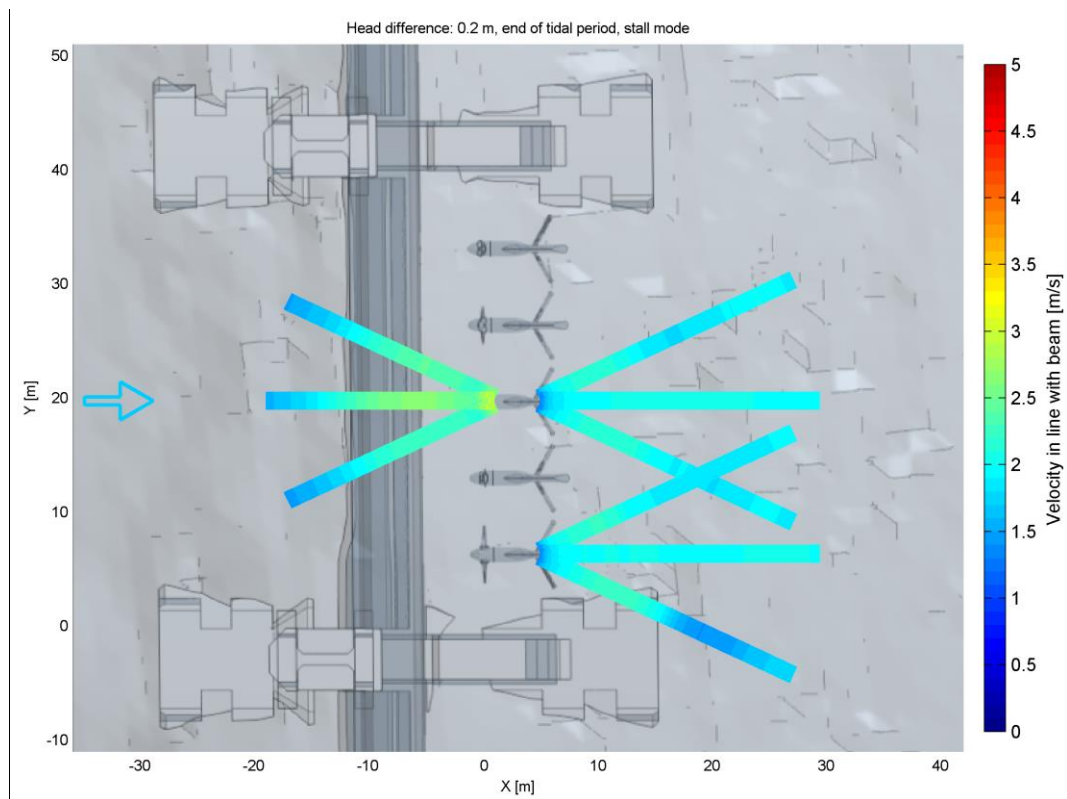


Figure 4.13 Left: Velocity profile for Case 3 (head difference of +0.2 m) as measured in the horizontal plane by the forward-looking and backward-looking ADCP devices during stall mode operation.

#### 4.6 Analysis of RPM, power and thrust

Tocado provided in addition to the ADCP data also records of the RPM and Power per turbine and the thrust for two turbines (T0011 and T0009). Figure 4.14 shows the names of the different turbines. This section describes the RPM, Power and thrust in relation to the head difference for the middle turbine (T0011). The results for the other turbines are included in Appendix F.

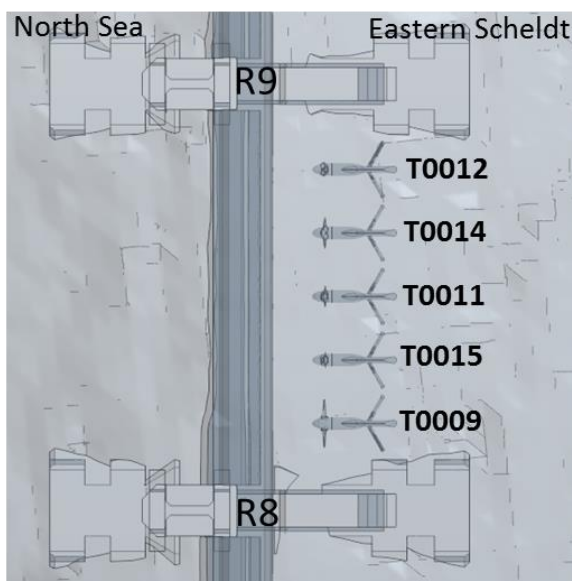


Figure 4.14 Overview of the 5 turbines

Figure 4.15 shows the relation between the registered RPM and head difference for the middle turbine. During the deployment, the turbines are regularly lifted out of the water (since it is not allowed for the turbines to be operational during large head differences) or put in stall mode (i.e. rotating with low RPM). Since these registered turbine characteristics are not corresponding to the “normal” operation of the turbines they have not been considered in this figure.

The figure shows that the relation between RPM and head difference is qualitatively similar to the relation between the current velocity and head difference. At the end of the tide (during decreasing absolute head), the RPM is higher than at the start of the tide (during increasing absolute head). The maximum recorded RPM is about  $45 \text{ min}^{-1}$ .

Figure 4.16 shows the relation between the registered power and head difference for the middle turbine. The power varies between 0 kW and about 200 kW (for a head difference of about +0.6 m).

Figure 4.17 shows the relation between the registered thrust and head difference for the middle turbine. The maximum recorded thrust is about 110 kN (for a head difference of about +0.6 m).

Table 4.1 gives an overview of the average RPM, Power and Thrust per turbine for the four cases that were defined in this study.

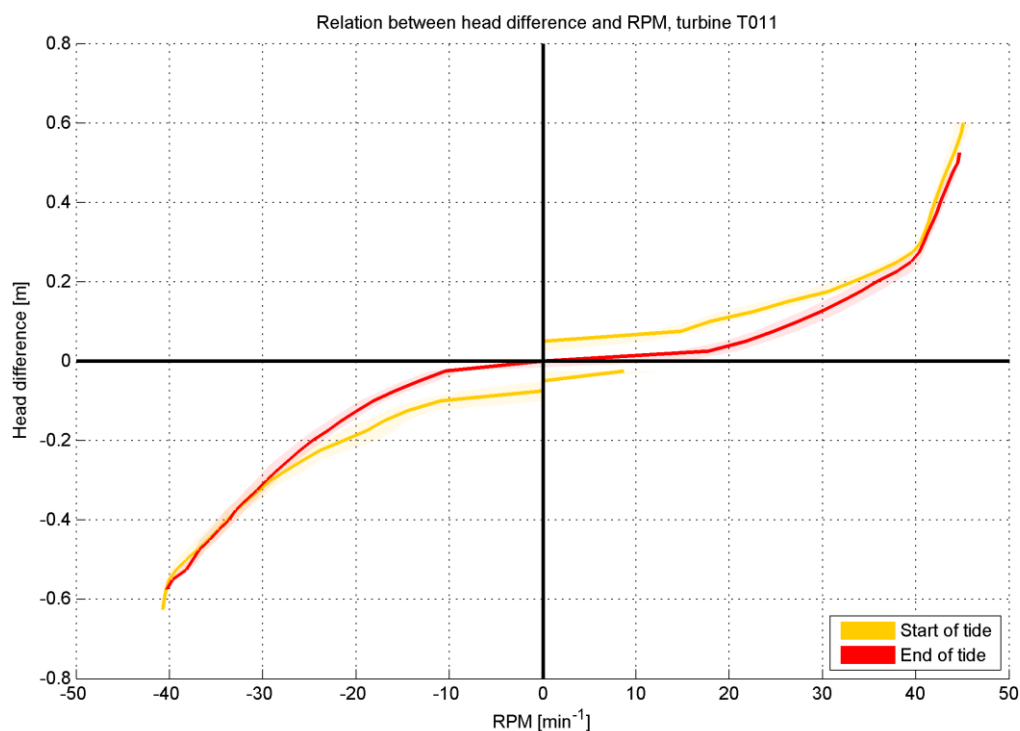


Figure 4.15 Relation between registered RPM and head difference for the middle turbine for the ADCP data period.

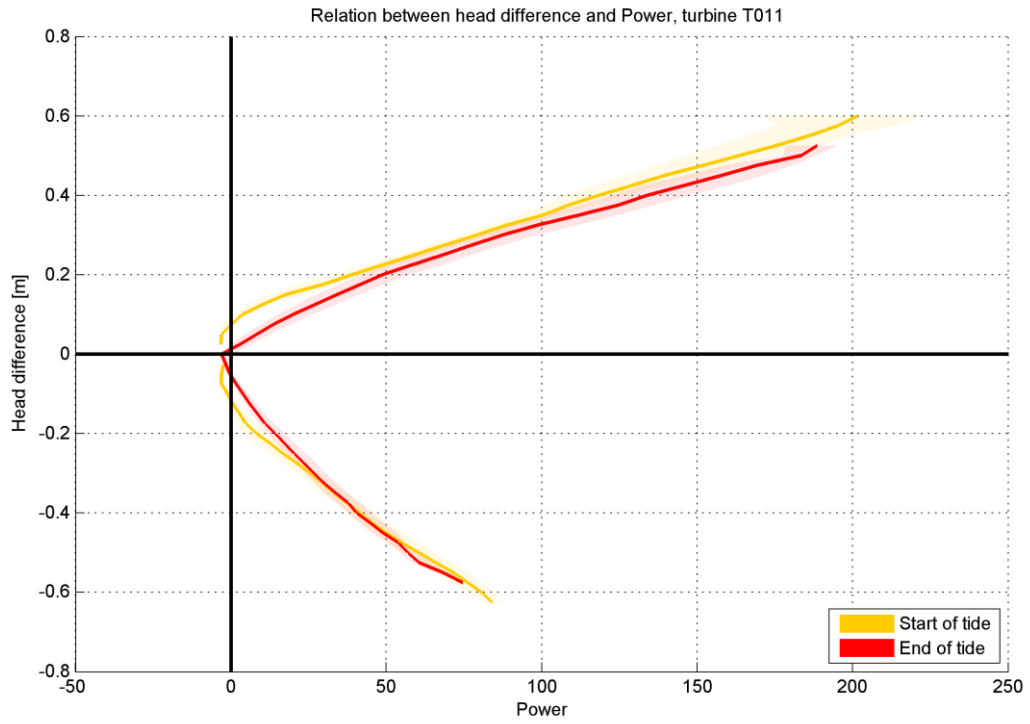


Figure 4.16 Relation between registered Power (kW) and head difference (m) for the middle turbine for the ADCP data period.

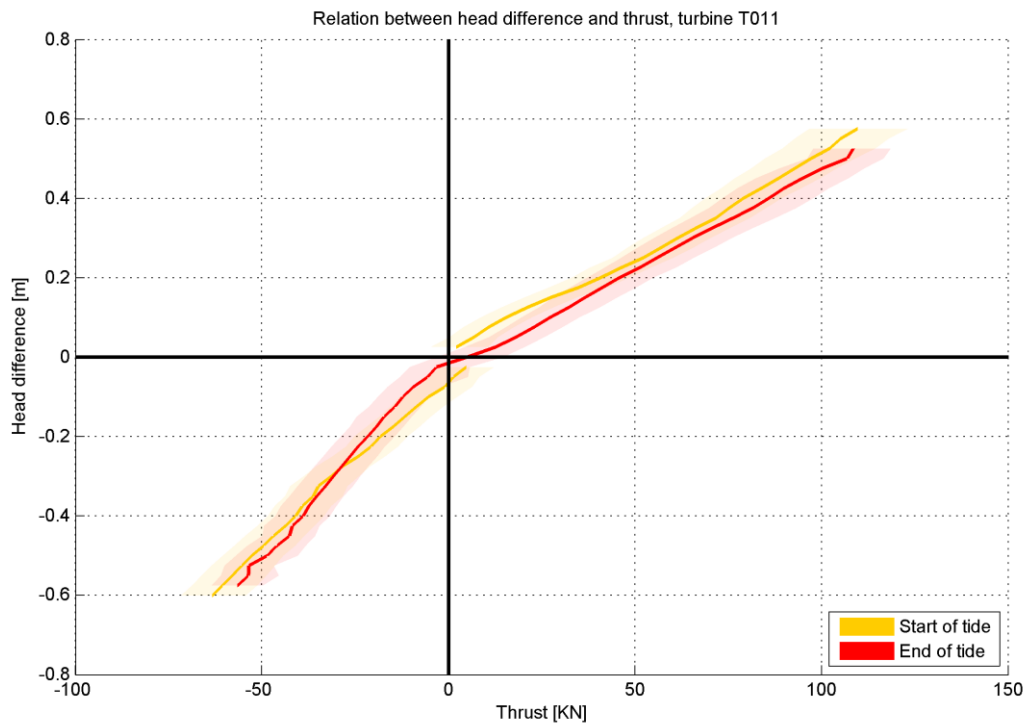


Figure 4.17 Relation between registered thrust and head difference for the middle turbine for the ADCP data period.

Table 4.1 Overview of the average RPM, Power and Thrust per turbine for the four cases that were defined in this study

			Case 1	Case 2	Case 3	Case 4
<b>Head difference</b>	<b>[m]</b>		-0.2	-0.32	0.20	0.55
		<b>T0012</b>	-24.3	-31.3	34.9	44.6
<b>RPM</b>	<b>[min<sup>-1</sup>]</b>	<b>T0014</b>	-24.0	-31.2	35.4	44.9
		<b>T0011</b>	-23.0	-30.5	34.5	44.5
		<b>T0015</b>	-23.7	-31.0	35.1	44.6
		<b>T0009</b>	-21.9	-30.4	35.1	44.7
		<b>T0012</b>	13.8	32.6	46.3	191.0
<b>Power</b>	<b>[kW]</b>	<b>T0014</b>	12.7	31.1	46.8	193.9
		<b>T0011</b>	11.3	29.7	43.9	186.0
		<b>T0015</b>	12.3	31.0	46.0	188.7
		<b>T0009</b>	9.9	29.3	46.8	192.8
		<b>T0011</b>	-20.0	-34.0	43.3	105.0
<b>Thrust</b>	<b>[KN]</b>	<b>T0009</b>	-25.4	-40.1	45.4	117.7

## 5 Effect of turbines based on ADCP data

### 5.1 Introduction

This chapter focusses on the second part of the objective, which was formulated as: To get an indication of the effect of the turbines on the current velocities through the gate based on the measurements.

This has been investigated by means of two comparisons:

- Comparing the ADCP measurements before turbine deployment (2011) to the ADCP measurements during turbine deployment (2016)
- Comparing the ADCP measurement during normal turbine deployment with ADCP measurements during stall mode deployment.

The advantage of the first comparison is that the 2011 measurement are representing the situation without any turbines in the gate. However, the ADCP measurements do not overlap completely, which requires some interpretations. The advantage of the second comparison is that the measurement locations are exactly identical. However, even though the resistance on the flow is less during stall mode, this situation will not completely represent the situation without turbines.

### 5.2 Comparison of ADCP measurement before and during turbine deployment

#### 5.2.1 Approach

The ADCP measurements before and during turbine deployment are at different locations and were located in different planes, see Figure 5.1. Therefore there is no real overlap between the data locations. However, since the horizontal ADCP measurements in 2011 ( $H_{2011}$ , indicated in orange) have shown that the velocity differences along the gate are small, it is assumed that a comparison can be made between the vertical ADCP measurements in 2011 ( $V_{2011}$ , indicated in red) and the forward-looking horizontal ADCP measurements during turbine deployment ( $H_{2016}$ , indicated in blue). The  $H_{2016}$  ADCP measurements were taken at -3.7 m NAP. At this height, the two bins of the  $V_{2011}$  measurements are a few meters apart. For a proper comparison, therefore, the average is taken from the corresponding bins in the  $H_{2016}$  measurements. It is noted that given the relatively large velocity gradients close to the sill beam, even a slight mismatch between the  $V_{2011}$  ADCP and the  $H_{2016}$  ADCP in terms of measurement location may influence this comparison.

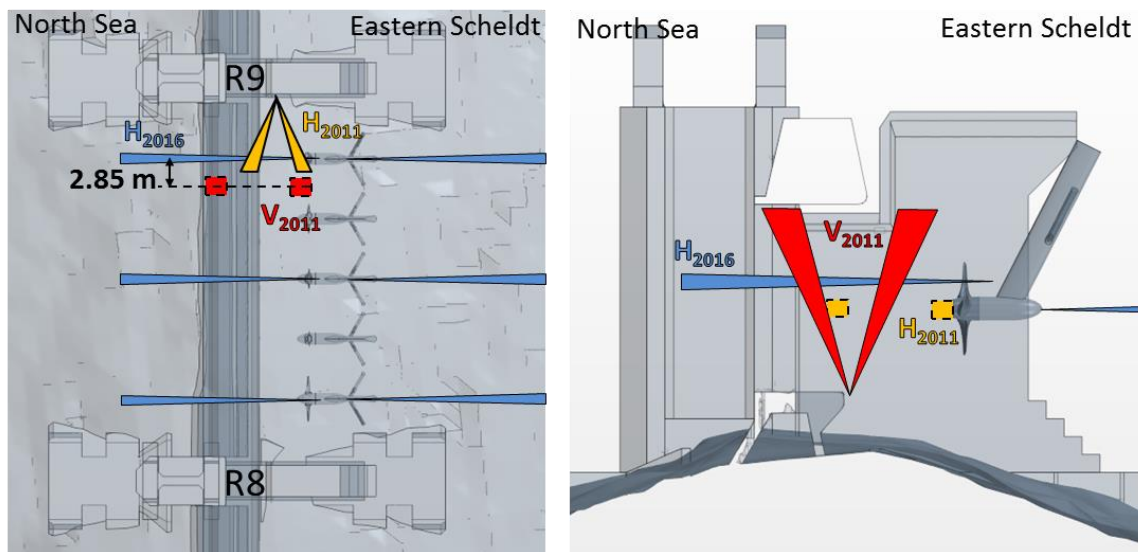


Figure 5.1 Turbine configuration at Gate #08 of the Eastern Scheldt Roompot Section including the location of the turbine-mounted ADCP measurements (blue) and the 2011 measurements (red and orange). Left: Top view, right: side view.

Such a comparison is illustrated for Case 1 (head difference of -0.2 m), see Figure 5.2. The left plot shows the velocity profile based on the  $V_{2011}$  ADCP and the right plot shows the velocity profile for the  $H_{2016}$  ADCP of the northern turbine for Case 1. The yellow patches indicate the locations where these ADCP's overlap. At -3.7 m NAP, the median velocity in the  $V_{2011}$  data was about -1.8 m/s (increasing absolute head) and -2.1 m/s (decreasing absolute head). For the  $H_{2016}$  ADCP, the average is calculated of the bins corresponding to the two beam locations of the  $V_{2011}$  ADCP: about -1.3 m/s (increasing absolute head) and -1.4 m/s (decreasing absolute head). These results show that for this specific ebb case, the current velocity at the overlapping location is about 25% – 35% lower during turbine deployment. This difference at the overlapping location cannot automatically be translated to a comparable reduction in the total discharge through the gate. During ebb, the overlapping location is downstream of the turbine and therefore in the wake of the turbine, especially since the ADCP mounted on the turbine is measuring close to the axis of the turbine. CFD modelling is required to assess the effects of the turbine on the total discharge through the gate during ebb. During flood, the overlapping location is upstream of the turbine and therefore only to a limited extent influenced by the presence of the turbine. It is therefore expected that the flood phase comparison gives a better indication of the turbine effects on the total discharge through the gate than during the ebb phase.

The comparison as illustrated in Figure 5.2 and described above is carried out for the available range of head differences with an interval of 0.025 m. The results of this analysis are described in Section 5.2.2.



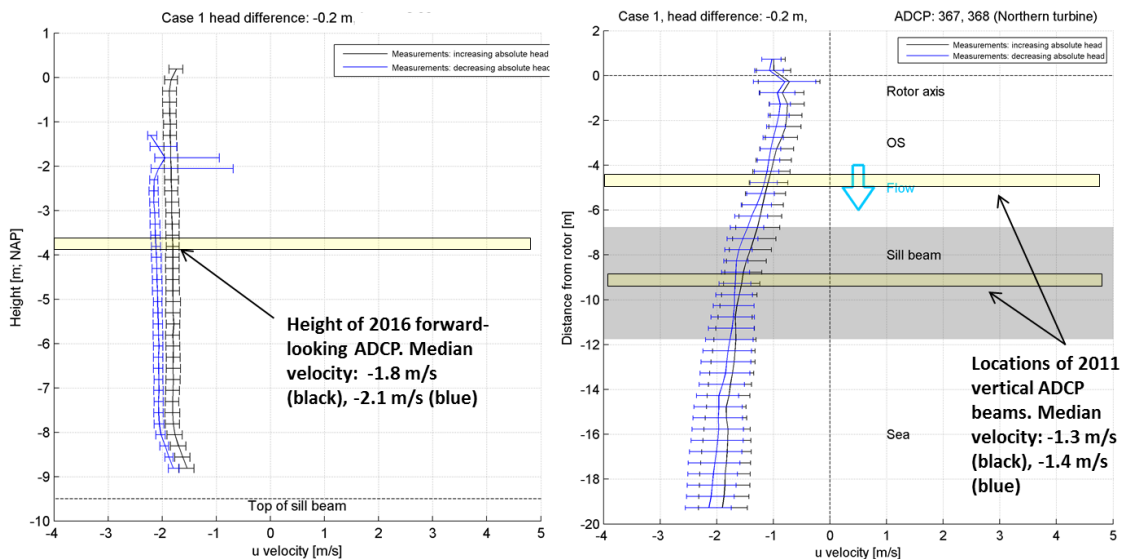


Figure 5.2 Comparison of the 2011 vertical ADCP data (left) and the 2016 forward-looking ADCP data (right) at overlapping locations for Case 1 (head difference = -0.2 m).

### 5.2.2 Results

This section describes the comparison of the ADCP data before and during turbine deployment. Figure 5.3 shows the comparison based on the forward-looking ADCP of the northern turbine (ADCP 367) at the locations as described in Section 5.2.1. The lightblue and darkblue lines show the median current velocity during increasing and decreasing absolute head respectively before turbine deployment. The orange and red lines show the median current velocity at the overlapping location for the ADCP measurements during turbine deployment. The patches with corresponding colours indicate the spreading of the data ( $\pm$  one standard deviation).

During ebb, the current velocity at the overlapping location is significantly reduced with about 25% to 35% due to the turbine deployment. As discussed in Section 5.2.1, this difference in velocity at the overlapping location cannot automatically be translated to a comparable reduction in the total discharge through the gate.

During flood, the current velocity at the overlapping location is slightly higher (up to 5%) during turbine deployment. One reason for this is that the  $V_{2011}$  measurements are located 2.85 m south (further from pillar R9) from the line of sight of the  $H_{2016}$  measurements. Based on the  $H_{2011}$  measurements it can be assumed that the current velocity at the  $H_{2016}$  ADCP is up to 0.2 m/s higher than at the  $V_{2011}$ . If this is taken into account, the flow velocity at the overlapping location is very similar for both before and during turbine deployment. Based on this ADCP comparison, the effect of the turbines on the discharge through the gate during flood is expected to be relatively small.

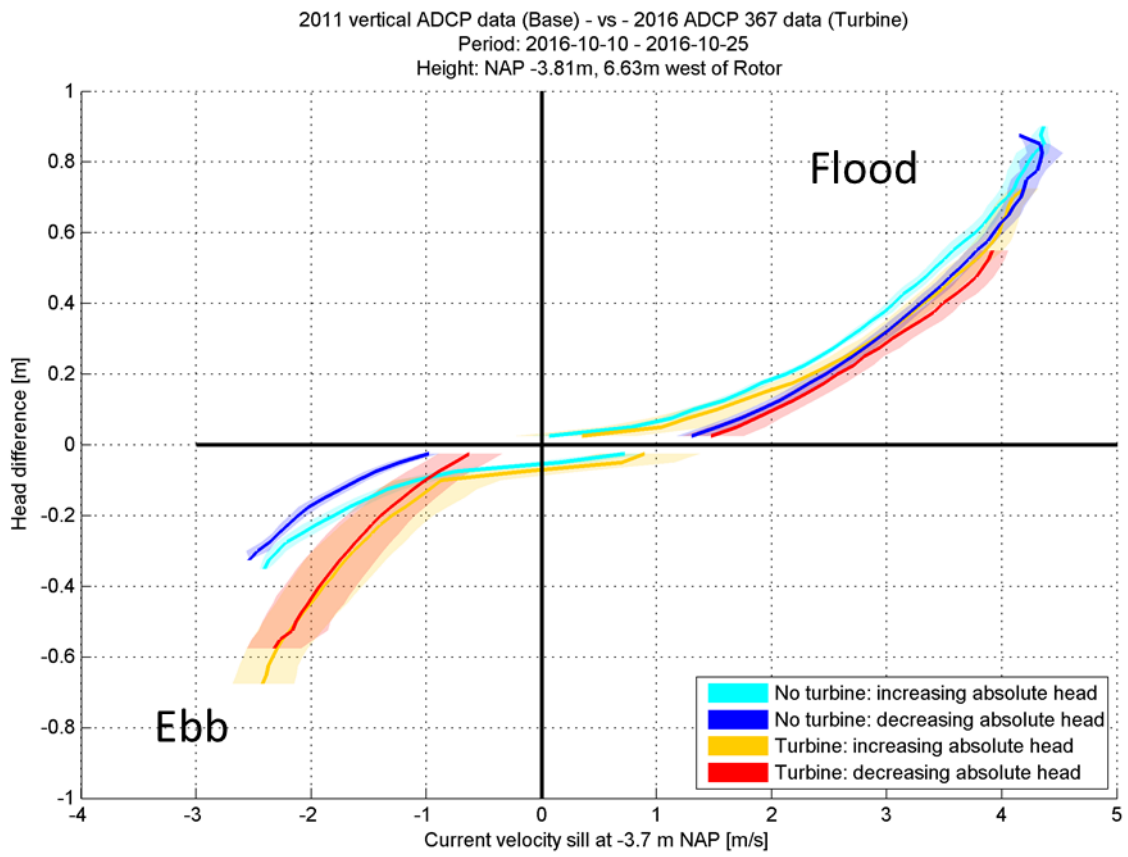


Figure 5.3 Comparison of the 2011 vertical ADCP data (No Turbine) and the 2016 forward-looking ADCP data (Turbine) at the overlapping location versus the head difference. The lines show the median values and the patches show the bandwidth of the data ( $\pm$  one standard deviation). For the period during turbine deployment, the forward-looking ADCP of the northern turbine is used (ADCP 367).

Figure 5.4 shows a similar comparison based on the forward-looking ADCP of the middle turbine (ADCP 341). The differences between the situation with and without turbine are in this figure slightly smaller, but overall the same observations can be made as described above.

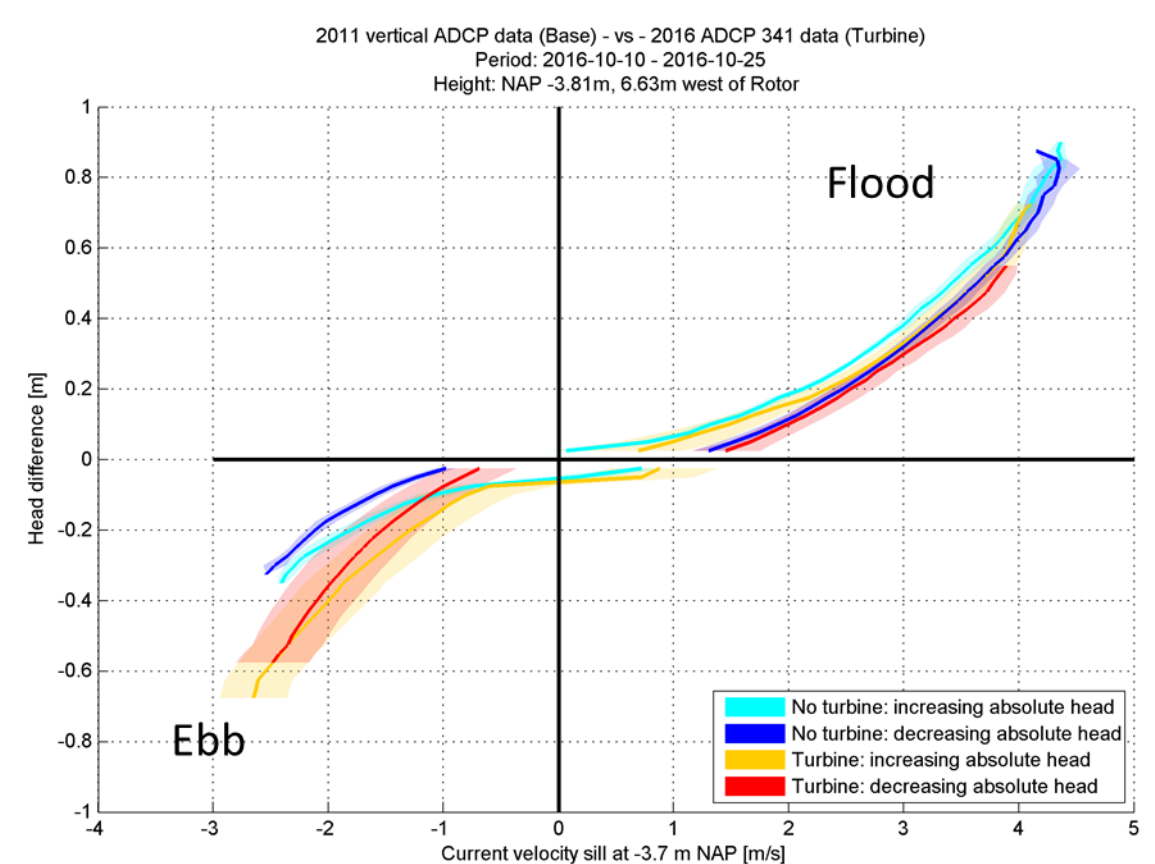


Figure 5.4 Comparison of the 2011 vertical ADCP data (No Turbine) and the 2016 forward-looking ADCP data (Turbine) at the overlapping location versus the head difference. The lines show the median values and the patches show the bandwidth of the data ( $\pm$  one standard deviation). For the period during turbine deployment, the forward-looking ADCP of the middle turbine is used (ADCP 341).

Figure 5.5 shows a comparison between the 2011 measurement data and the forward-looking ADCP of the middle turbine (ADCP 341) during stall mode. During stall mode, the rotation speed of the turbine is much lower, which results in a much smaller wake zone behind the turbine compared to a turbine that is operated in normal mode. This can be observed due to the fact that the follows better the 2011 data for ebb compared to Figure 5.4. For flood, the velocity during stall mode is about 5-10% higher than for the situation without turbines. This is similar to the comparison between the cases with turbines and without turbines (Figure 5.3 and Figure 5.4). From Figure 5.5, it can be concluded that a comparison between the results of the turbine in stall mode and normal model gives a good indication on the effect of the tidal turbines on the flow through the barrier. This is further discussed in Section 5.3.

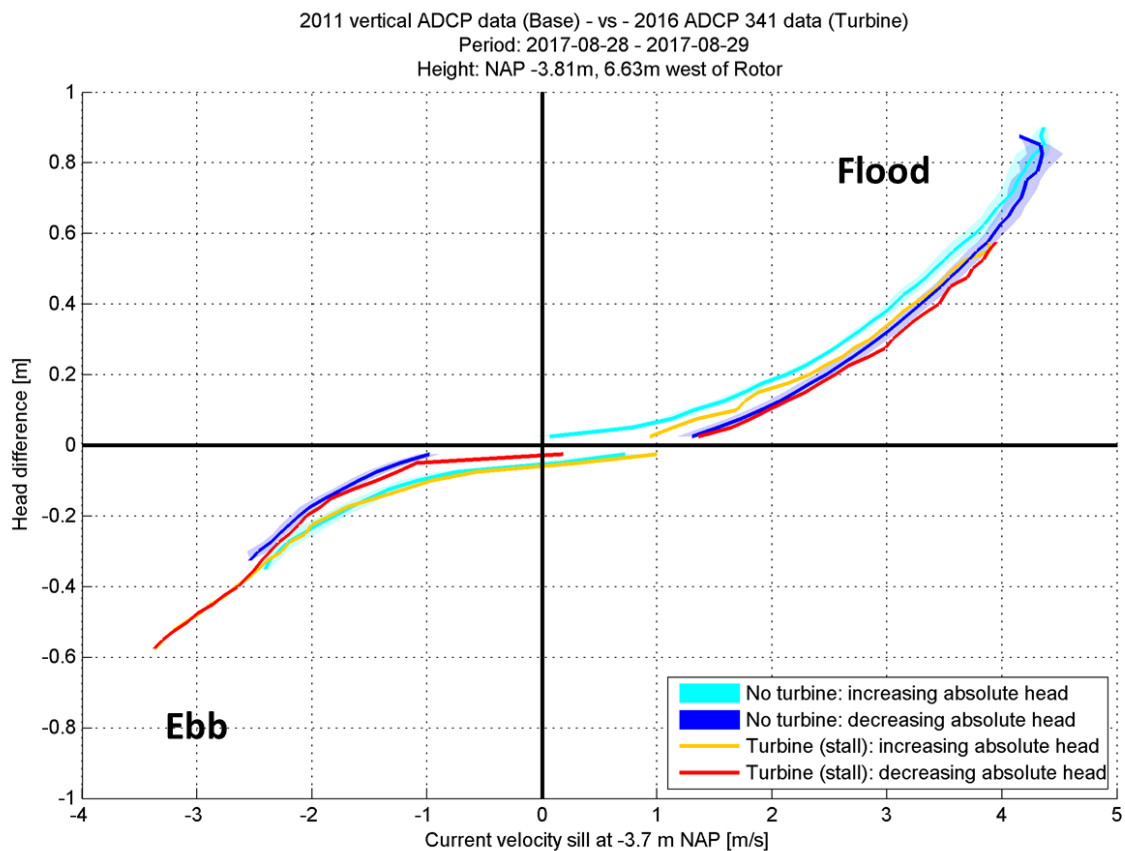


Figure 5.5 Comparison of the 2011 vertical ADCP data (No Turbine) and the 2016 forward-looking ADCP data (Turbine, during stall mode) at the overlapping location versus the head difference. The lines show the median values and the patches show the bandwidth of the data ( $\pm$  one standard deviation). For the period during turbine deployment, the forward-looking ADCP of the middle turbine is used (ADCP 341).

### 5.3 Comparison of the ADCP measurement during normal turbine deployment with ADCP measurements during stall mode deployment

#### 5.3.1 Approach

In addition to the comparison as discussed in Section 5.2, also a comparison can be made of the velocity measurement during normal mode and stall mode operation. This comparison gives an indication of the influence of the turbine operation on the flow velocities. Note that also during stall mode the turbine has some resistance effects on the flow and is therefore not completely similar to background conditions (i.e. without turbine deployment). In the following section the normal and stall mode measurements will be compared in two different ways. First, the average velocity above the sill beam is compared. This comparison is quite similar as the one with the 2011 measurements (before turbine deployment) as discussed in the previous section. The disadvantage of this comparison is that during ebb, the velocity above the sill beam is in the wake of the turbine, which results in large velocity fluctuations (see Figure 5.6). During flood, however, the sill beam is located upstream of the turbine (see Figure 5.7). The second comparison analyses the measured flow velocities directly upstream of the turbine. During the flood phase, the comparison is made at the seaward side of the turbine, whereas during the ebb phase, the velocities on the Eastern Scheldt side are compared.

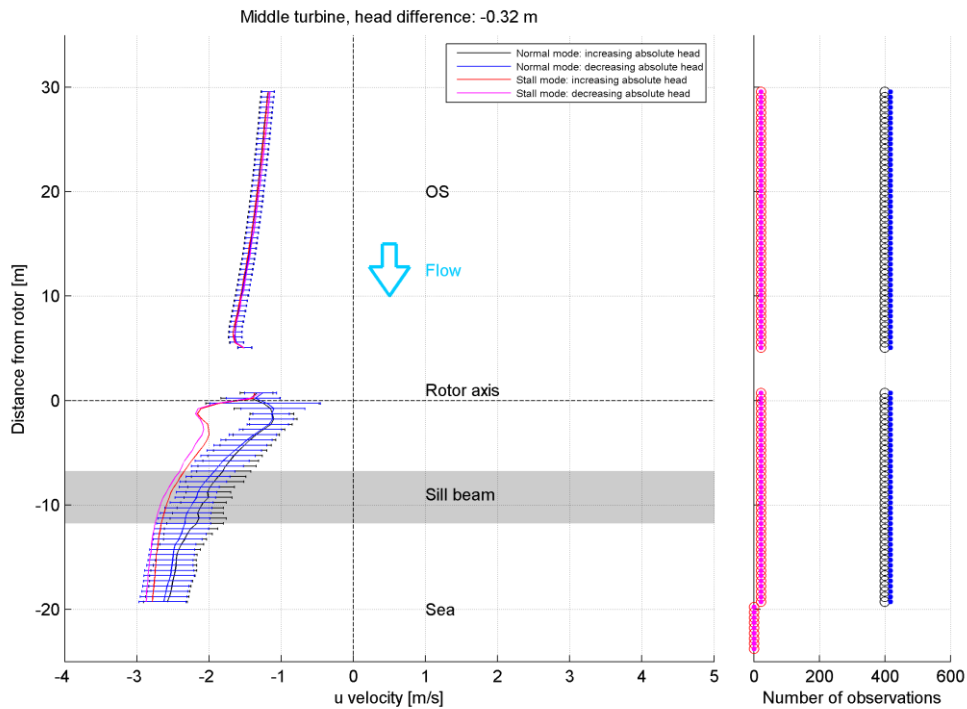


Figure 5.6 Velocity profile for Case 2 (head difference of  $-0.32$  m) as measured by the forward-looking and backward-looking ADCP devices on the middle turbine. Distinction is made between periods of increasing and decreasing absolute head. Right: Number of observations used per bin.

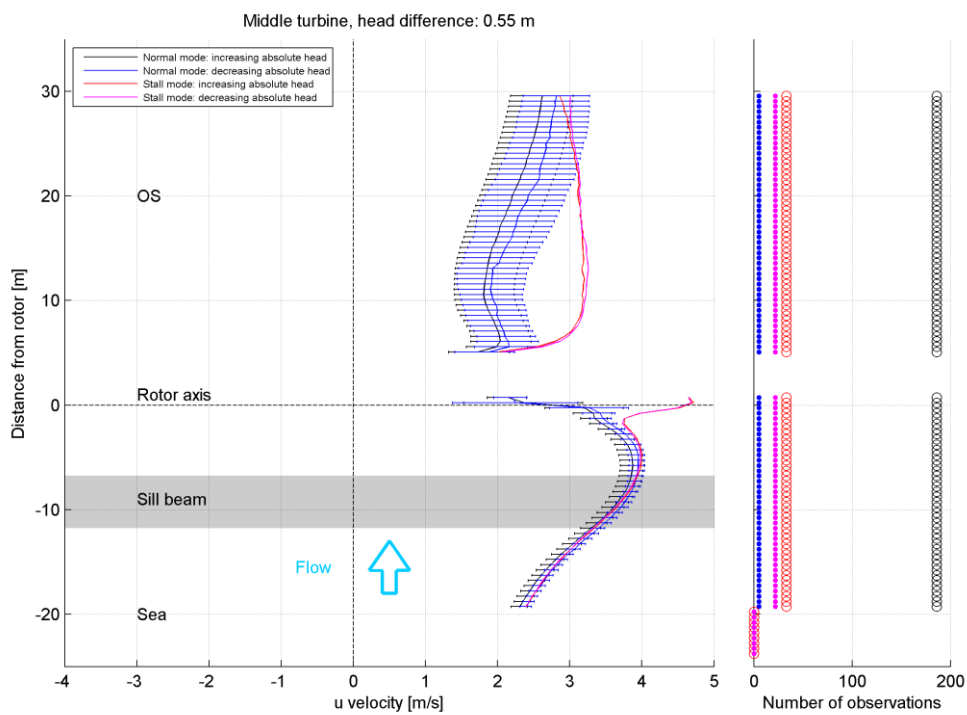


Figure 5.7 Left: Velocity profile for Case 4 (head difference of  $+0.55$  m) as measured by the forward-looking and backward-looking ADCP devices on the middle turbine. Distinction is made between periods of increasing and decreasing absolute head. Right: Number of observations used per bin.

5.3.2 Results

Figure 5.8 shows the average velocity above the sill beam for both during stall mode and normal mode measurements. During flood, the average velocity above the sill is very similar for both turbine operations, which is consistent with the observations in Section 5.2. During the ebb the velocity above the sill beam is generally about 20%-25% lower during normal operation compared to stall mode operation. This is also very consistent to the comparison against the pre-turbine measurements. This lower velocity is related to the wake of the turbine which is much weaker during stall mode operation.

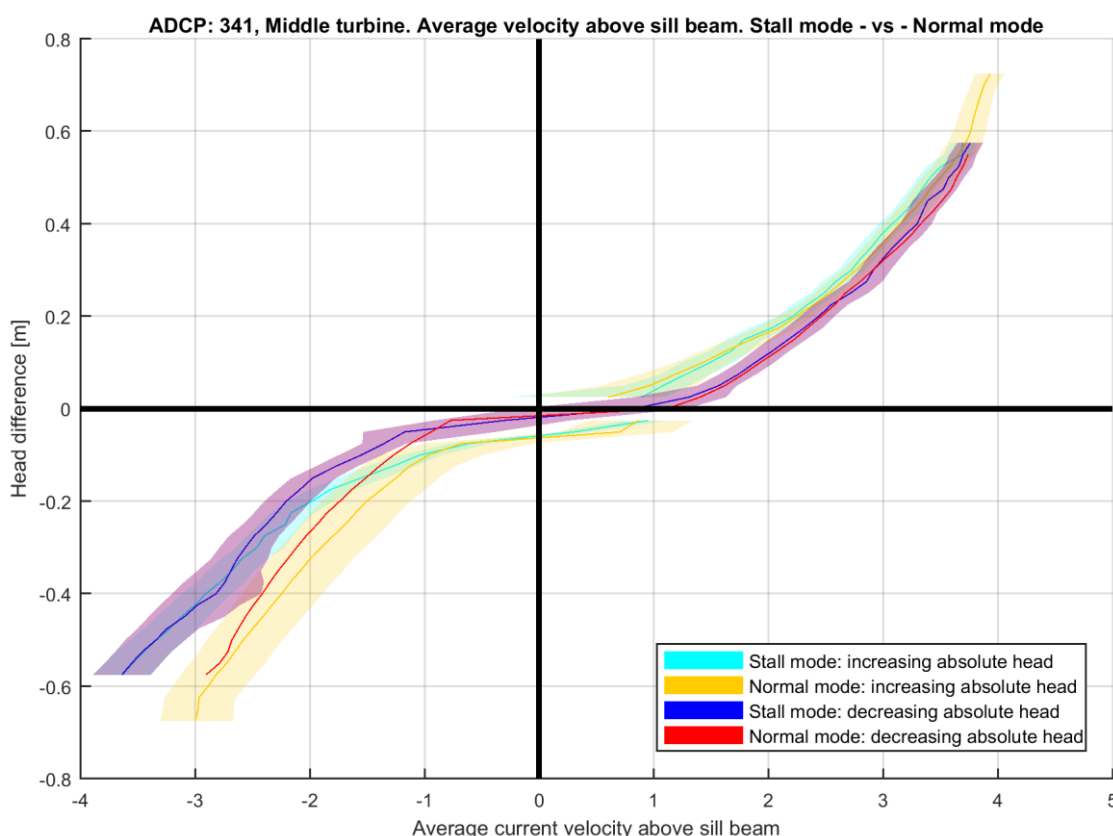


Figure 5.8 Comparison of the average velocity above the sill beam during stall mode and normal mode versus the head difference. The lines show the median values and the patches show the bandwidth of the data ( $\pm$  one standard deviation). The forward-looking ADCP of the middle turbine is used (ADCP 341).

Figure 5.9 shows the velocity 6m upstream of the turbine during stall mode and normal mode operation. The velocity differences are generally very small ( $<0.1$  m/s) during both the flood and ebb phase and fall within the observed spreading of the results.

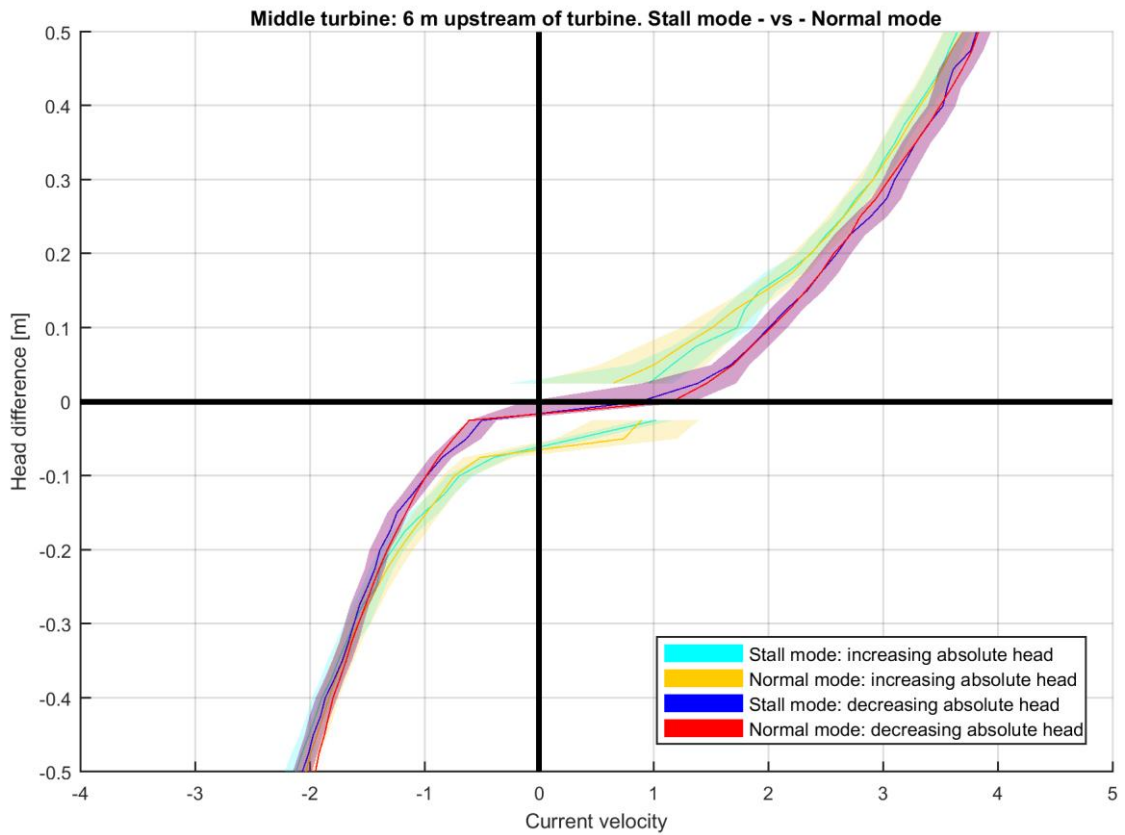


Figure 5.9 Comparison of the velocity 6 m upstream of the turbine during stall mode and normal mode versus the head difference. The lines show the median values and the patches show the bandwidth of the data ( $\pm$  one standard deviation). The forward-looking ADCP of the middle turbine is used (ADCP 341).



## 6 Estimated influence of the turbines on the discharge coefficients

In this Chapter an attempt is made to determine the effect of the turbines on the discharge coefficient based on the velocity measurements as described in the previous chapters.

### 6.1 Introduction

The discharge through a gate in the Eastern Scheldt can be expressed with the following formula:

$$Q = A \cdot \mu \sqrt{2 \cdot g \cdot \Delta H}$$

In which  $\mu$  is the discharge coefficient. One of the main objectives of this study is to assess the influence of the turbines on the discharge coefficient. The ADCP measurements that have been carried out during turbine deployment can be used to assess the current velocity in the axis of the turbine (see Section 5), but need an interpretation to assess the discharge through the gate. For this reason, CFD computations as described in ref [1] have been used to assess the spatial distribution of the velocity in the gate. The approach that has been applied in this chapter is described in the below:

- Step 1: The discharge coefficient of the CFD model (with and without turbines) is computed:  $\mu_{CFD} = \frac{Q}{A \sqrt{2 \cdot g \cdot \Delta H}}$
- Step 2: The ratio between the measured and modelled velocity is calculated:  $c_{scaling} = \frac{u_{mean,meas}}{u_{mean,CFD}}$ 
  - In the situation without turbines, the scaling coefficient is based on the difference between the CFD computation (ref [1]) and the vertical 2011 ADCP measurements
  - In the situation with turbines, the scaling coefficient is calculated for the location above the sill beam.
- Step 3: The 'final' discharge coefficient is calculated:  $\mu = \mu_{CFD} \cdot c_{scaling}$

This approach assumes that the relative spatial distribution of the velocity in the gate is correctly computed by CFD. Unlike the measurements, the CFD computations have been carried out for the four cases as defined before (see Table 3.1). Inertia effects are not considered in the CFD simulations and one quasi-steady state simulation is carried out per head difference (unlike the measurements that show two situations for one head case: at the start of the tidal phase and at the end of the tidal phase).

The present analysis also includes accuracy bands for the discharge coefficients, which are based on:

- Spreading of the measured velocity
- Accuracy of the head difference in the measurements  $\approx 1$ cm
- Accuracy of the head difference in the CFD model  $\approx 1$ cm

### 6.2 Discharge coefficient for situation without turbines

#### 6.2.1 Example for -0.2 m head difference

The methodology, as described in Section 6.1, is illustrated for Case 1 (head difference of -0.2)

### Step 1: Discharge coefficient CFD model

The discharge, area and head difference in the CFD computation for Case 1 is shown in the table below. Based on this information, the discharge coefficient in the CFD model is about 0.96 (see ref [1]).

### Step 2: Ratio between measured and modelled velocity

Figure 6.1 shows a comparison of the current profile as measured by the vertical ADCP in 2011 (blue and black data) and modelled in the CFD computation (red line) for a head difference of -0.2 m. The blue dots represent the median velocity in the measurements at the end of the tide (during decreasing absolute head). The black dots represent the start of tide (during increasing absolute head). Near the water surface, unreliable measurements can be observed, which have been ignored for this analysis. The measured current profile has been extrapolated towards to water surface, to be able to estimate the average velocity above the sill beam. For this case, the scaling coefficients are calculated as follows:

$$\text{Start of tide: } C_{scaling,start} = \frac{1.77}{1.8} = 0.98$$

$$\text{End of tide: } C_{scaling,end} = \frac{2.02}{1.8} = 1.12$$

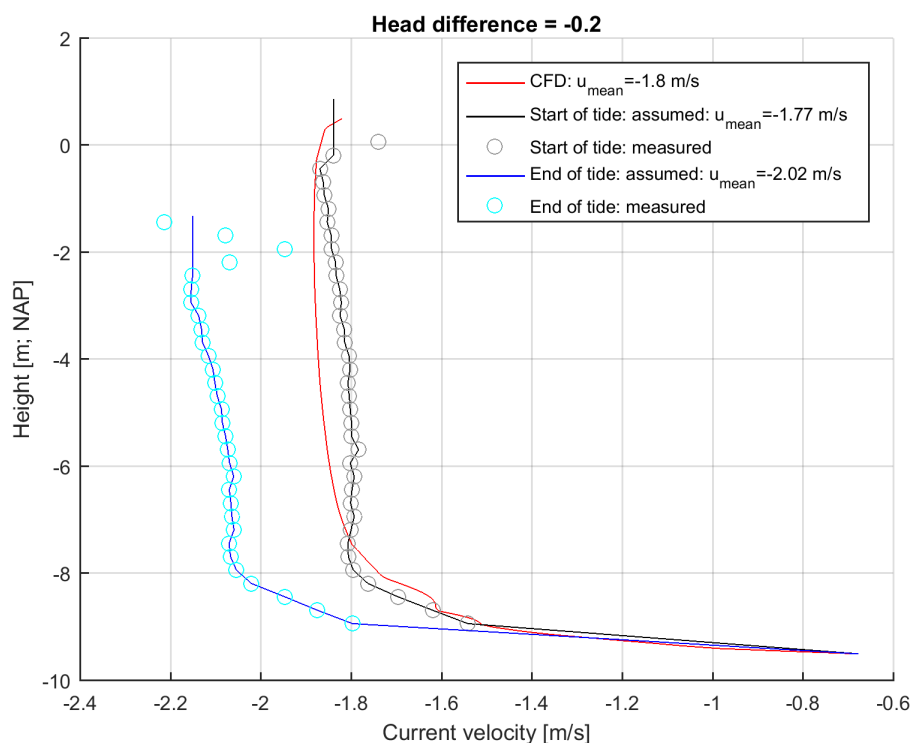


Figure 6.1 Comparison of velocity profile as measured by the vertical ADCP in 2011 (blue and black data) and the CFD computation (red line) for a head difference of -0.2 m.

### Step 3: Calculate final discharge coefficient

As explained in Section 6.1, the ‘final’ discharge coefficient is calculated by multiplying the discharge coefficient from the CFD computation by the correction coefficient based on a comparison of the CFD model to the measurements:

$$\mu_{start} = \mu_{CFD} \cdot C_{scaling,start} = 0.94$$

$$\mu_{end} = \mu_{CFD} \cdot C_{scaling,end} = 1.08$$

This approach results in different discharge coefficients for the start and end of the tide. The average from these discharge coefficients is 1.01.

### 6.2.2 Results for all four cases

Figure 6.2 shows the calculated discharge coefficients for the situation without turbines for the four head difference cases that have been considered in this study. The figure shows for each head difference the calculated discharge coefficient for the start of the tide, end of the tide and the average thereof. The spreading in discharge coefficients is based on the spreading of the measured velocity and the accuracy of the head difference in the measurements and CFD model. The green dots show the head difference in the CFD computations.

The figure shows that the uncertainty of the discharge coefficients is about 5-10%. The uncertainty bands increase for smaller head differences, which is related to the assumed accuracy of the head difference of about 1 cm.

During ebb, the average discharge coefficient is about 1.00-1.02. During flood the average discharge coefficient is about 0.93 – 0.99. It has to be noted that all cases as used in the CFD consider the water levels corresponding to the start of the tide (increasing head).

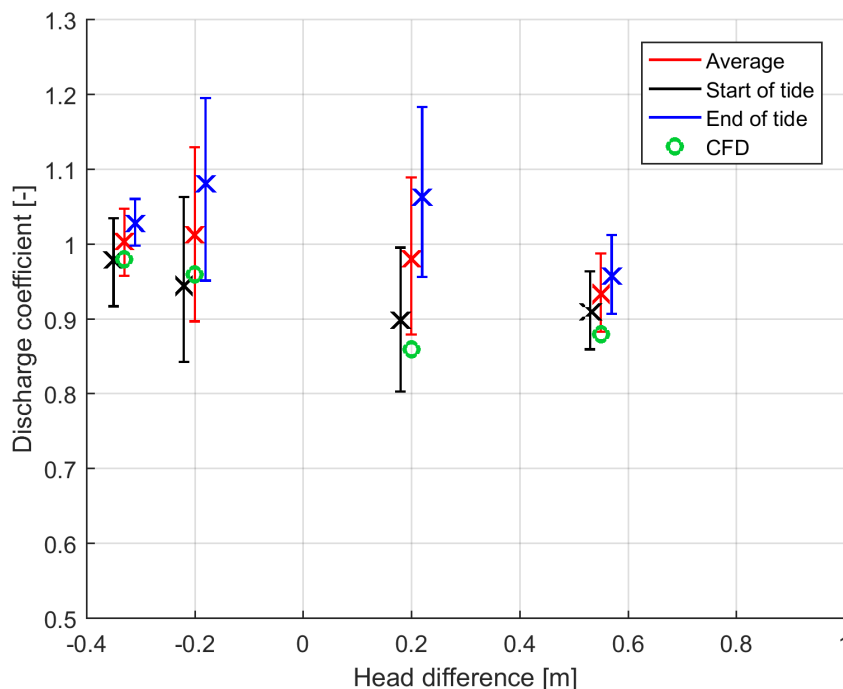


Figure 6.2 Calculated discharge coefficients for the situation without turbines. The discharge coefficient is calculated for four different head differences. The figure also shows the discharge coefficient calculated from the CFD computations.

### 6.3 Discharge coefficients for situation with turbines

Figure 6.3 shows the calculated discharge coefficients for the situation with turbines for the four head difference cases that have been considered in this study. The CFD discharge coefficients have been scaled by comparing the modelled and measured current velocity above the sill beam.

The calculated average discharge coefficient for ebb is about 0.75-0.82. For flood the average calculated discharge coefficient is about 0.99-1.00.

The ebb discharge coefficients are much lower than computed using Option A. Since the sill beam is located in the wake of the turbine during ebb, the scaling coefficient largely depends on the accuracy of the flow velocity in the wake in the CFD computation. The comparison for the discharge coefficient for this method is judged to be unreliable for the ebb cases.

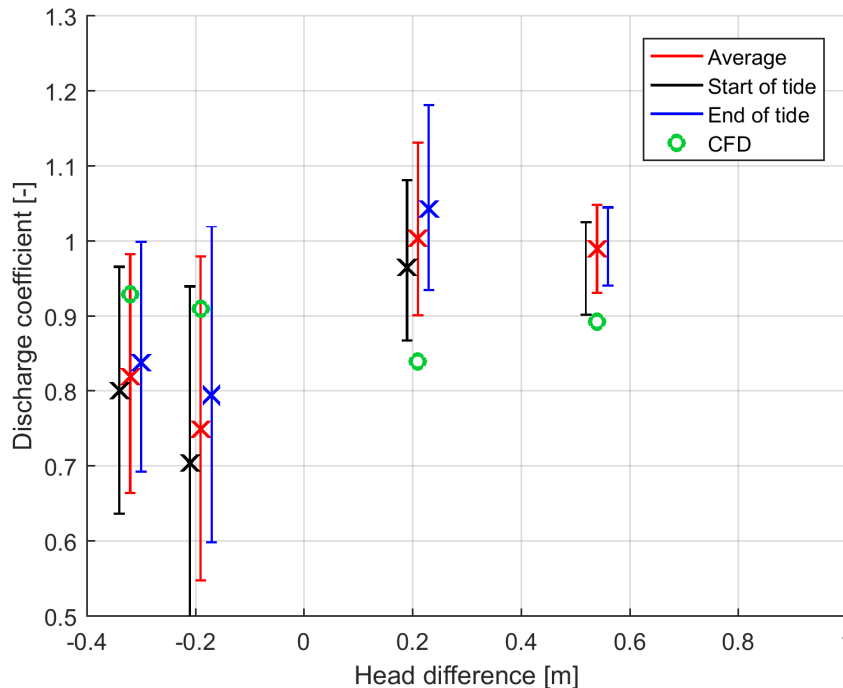


Figure 6.3 Calculated discharge coefficients for the situation with turbines, option B. The discharge coefficient is calculated for four different head differences. The figure also shows the discharge coefficient calculated from the CFD computations.

#### 6.4 Comparison of discharge coefficients with and without turbines

Because the computation of the discharge coefficient for the situation with turbines during ebb is unreliable, only a comparison has been made on the change in discharge coefficient for the flood cases. As observed in Figure 6.2 and Figure 6.3, the average discharge coefficient during flood is for the situation without turbines between 0.93 and 0.99 and for flood between 0.99 and 1.00. Given the large spreading of the calculated discharge coefficients, the differences between the situation with and without turbines are assessed to be statistically insignificant for flood.

## 7 Summary and conclusions

In 2015 an array of five tidal turbines was deployed in Gate #08 of the Roompot Section of the barrier in the framework a tidal power pilot project. For both the situation with and without turbines, ADCP measurements have been carried out in gate #08 of the Eastern Scheldt Barrier (OSK). Based on these measurements the following conclusions have been drawn:

### *Effect of inertia:*

- Due to inertia, flow velocities at the end of a tidal phase are higher than at the start of the tidal phase for similar head differences over the Eastern Scheldt Barrier.
- Due to inertia, the flow direction through the barrier can even be opposite to the head difference over the barrier.

### *Characteristics of the horizontal and vertical flow profile:*

- The time-averaged horizontal and vertical flow profiles in Gate #08 of the Eastern Scheldt Barrier are generally very flat, except for the region close to the sill beam and pillar.
- During flood, the 2011 vertical ADCP measurements show a shearing layer with a thickness of about 3 m above the sill beam. Close to the sill beam (within 1 m above the sill beam), the flow direction is opposite to the average flow direction.
- During ebb the observed shearing layer is less pronounced, which can be explained by the fact that the vertical ADCP is located on the Eastern Scheldt side of the sill beam (upstream during the ebb tidal phase).

### *Inflow angle:*

- At the start of the ebb phase, the tidal flow initially approaches Gate #08 under an angle of about 30° to 45°.

### *Effect of turbine operation on flow profiles*

- Downstream of the turbine, the observed variation in flow velocity is larger than upstream of the turbine, which can be explained by the increased turbulence.
- During normal turbine operation, the wakes of the turbines are more pronounced than during stall mode operation
- Upstream of the turbine, the flow profile is very similar for both stall mode and normal mode operation. Only in the zone very close to the turbine (about 6-7m from the rotor) differences in flow velocity can be observed.
- Downstream of the turbine, the flow velocity during stall mode operation is significantly larger than during normal mode operation.

### *Effect of turbine operation on discharge through the gate*

- An attempt is made to assess the change in discharge coefficients based on the available ADCP measurements. In this assessment, the CFD model (ref [1]) is used to assess the velocity profile in the gate. During ebb, the ADCP's are measuring in the wake of the turbines. This gives large fluctuations in the velocity profile and leads to unreliable results in the discharge coefficient. During flood, the effect of the turbine on the discharge through the gate is assessed to be statistically insignificant (i.e. smaller than the observed spreading in the velocity results).

## 8 References

- [1] O'Mahoney, 2018, CFD simulations of the Eastern Scheldt Barrier with and without tidal turbines – validation study and determination of the discharge coefficients, Deltares report, reference: 11200119-003-HYE-0004, dated July 2018
- [2] Partrac, 2011. Monitoring Turbulence Oosterscheldekering, Tocardo Tidal Energy. P1199.05.D01v01. August 2011.
- [3] Rijkswaterstaat (1994). *Design plan Oosterschelde Storm-surge barrier; Overall design and design philosophy*. Rotterdam, Balkema.

## A Photographs of ADCP brackets

The photographs below show how the brackets which were used to mount the ADCP on the Eastern Scheldt Barrier.

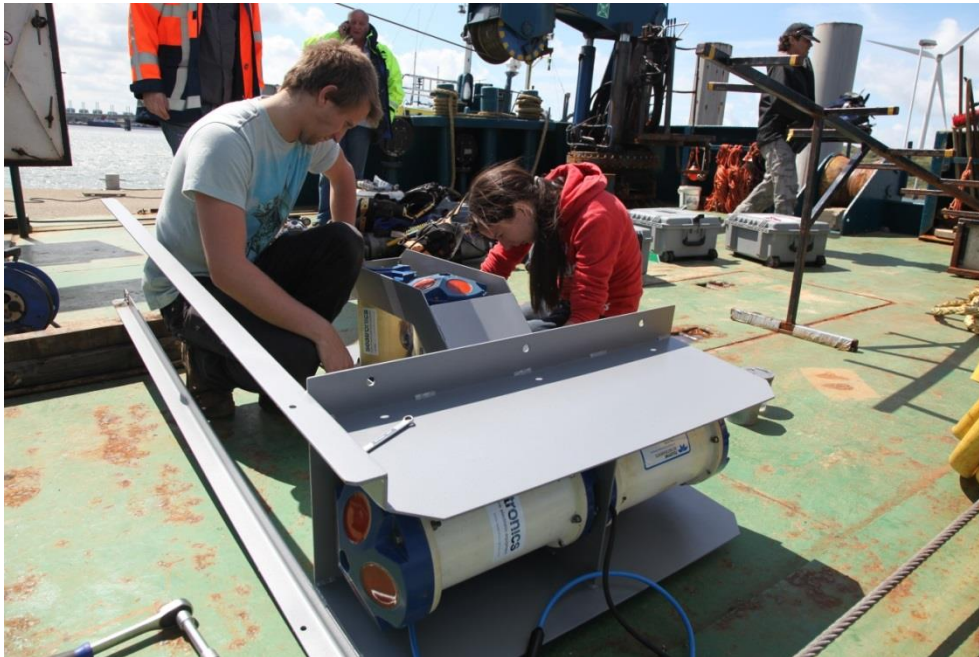


Figure A.1 bracket of vertical ADCP

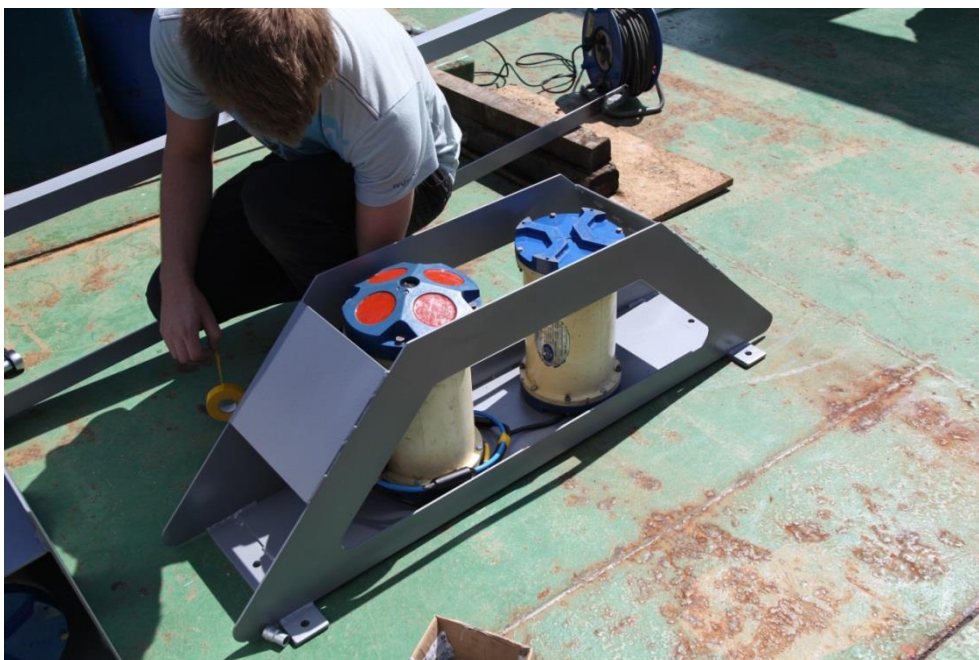


Figure A.2 bracket of horizontal ADCP



## B Quality checks on ADCP measurements without turbine deployment

### B.1 Quality checks performed by Partrac

Partrac passed both the horizontal and vertical ADCP data through an extensive quality control analysis in order to ensure that the uncertainties in the data are reduced to the minimum (Partrac, ref [2]). The QA algorithm removed data in bins that corresponded to layers above the water level (in-air measurements) and data that failed to meet accuracy standards (e.g. correlation magnitude tests, percent good tests, etc.). For a detailed description of the applied quality control algorithms one is referred to the ADCP analysis report of Partrac (ref [2]).

### B.2 Quality checks performed by Deltares

#### *Correction of the bin location of the vertical ADCP*

In the provided ADCP data files, the lowest bin for the vertical ADCP was given as -9.915 m NAP. Given the fact that the ADCP front was located at the same height as the sill beam (-9.5 m NAP), this could not be correct. The vertical locations of the vertical ADCP bins have therefore been increased with 1.105 m (lowest bin at -9.5 m NAP + blanking distance of 0.44 m + bin size of 0.25 m).

#### *Determination of the time zone of the ADCP data*

The time zone of the ADCP was not explicitly mentioned in the accompanying reports. The time zone of the ADCP data was determined by comparing the average measured velocities with the expected velocities based on the head difference over the barrier. The head difference over the barrier was calculated by subtracting the measured water level at Roompot Binnen (located on the Eastern Scheldt side of the barrier) from the measured water level at Roompot Buiten (located on the North Sea side of the barrier), see Figure 3.1 for the locations. The measured water level at these two locations was extracted from the online Waterbase database that is provided by Rijkswaterstaat. The water level data is provided in the GMT + 1h timezone. The expected average velocity through the gate was calculated using the following formula:

$$v_{avg} = \mu \sqrt{2g\Delta h}$$

In which,  $v_{avg}$  is the average velocity through the gate,  $\mu$  the discharge coefficient (according to RWS this coefficient should be about 1),  $g$  the gravitational acceleration constant and  $\Delta h$  the head difference over the barrier. shows the expected average velocity through the gate (blue line). The red and black dots together represent the average velocity in the ADCP data, which are matching the expected average velocity very well if a time zone of GMT + 2h is assumed.

#### *Removal of data*

In addition to the data already removed by Partrac, the following data of the vertical ADCP were removed as well (see upper plot of):

- Data in the period 15-08-2011 12:00 – 15-08-2011 13:00, which corresponds to the installation period of the vertical ADCP also shows that during this period the measurements do not match the expected behaviour.

- Data in the period 16-08-2011 09:00 – 16-08-2011 13:00, which corresponds to the installation period of the horizontal ADCP for which the gate was closed.
- Subsequently the ADCP data was removed when the difference between the observed average velocity and the expected average velocity was larger than 3 m/s. This occurred during some peak flood flows, which could have different reasons (e.g. vibrations of the ADCP device due to the high velocities, etc.).

For the horizontal ADCP no additional data was removed.

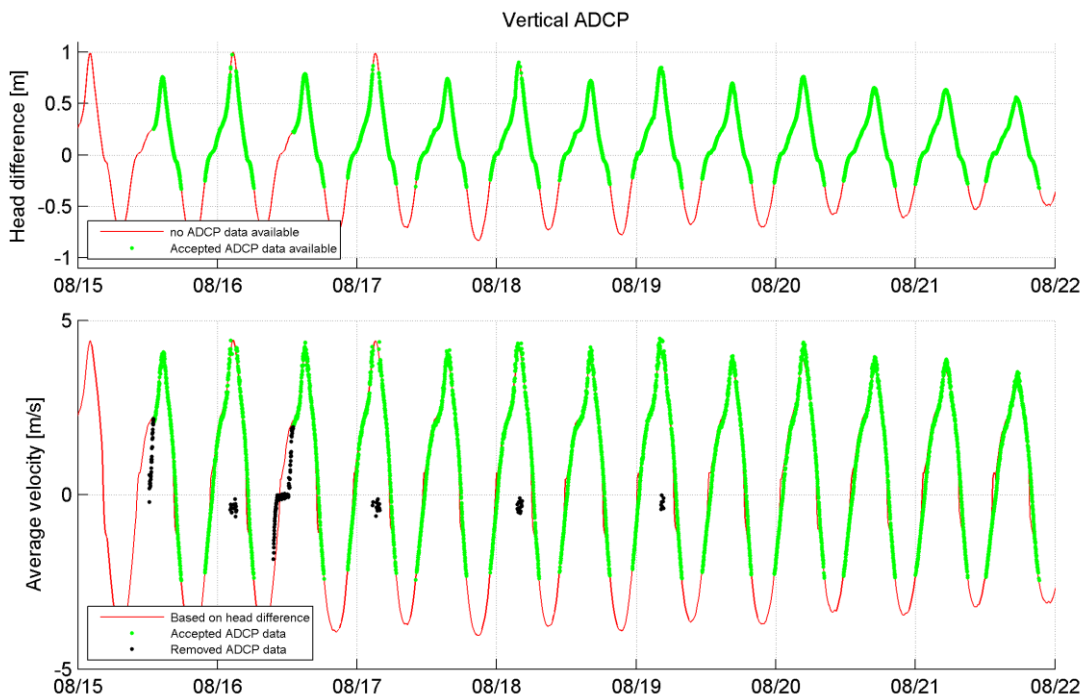


Figure B.1 Timeseries of the expected average velocity through the gate based on the measured head difference over the barrier (red line), the average velocity of the accepted vertical ADCP data (green dots) and the average velocity of the rejected vertical ADCP data (black dots). Vertical ADCP

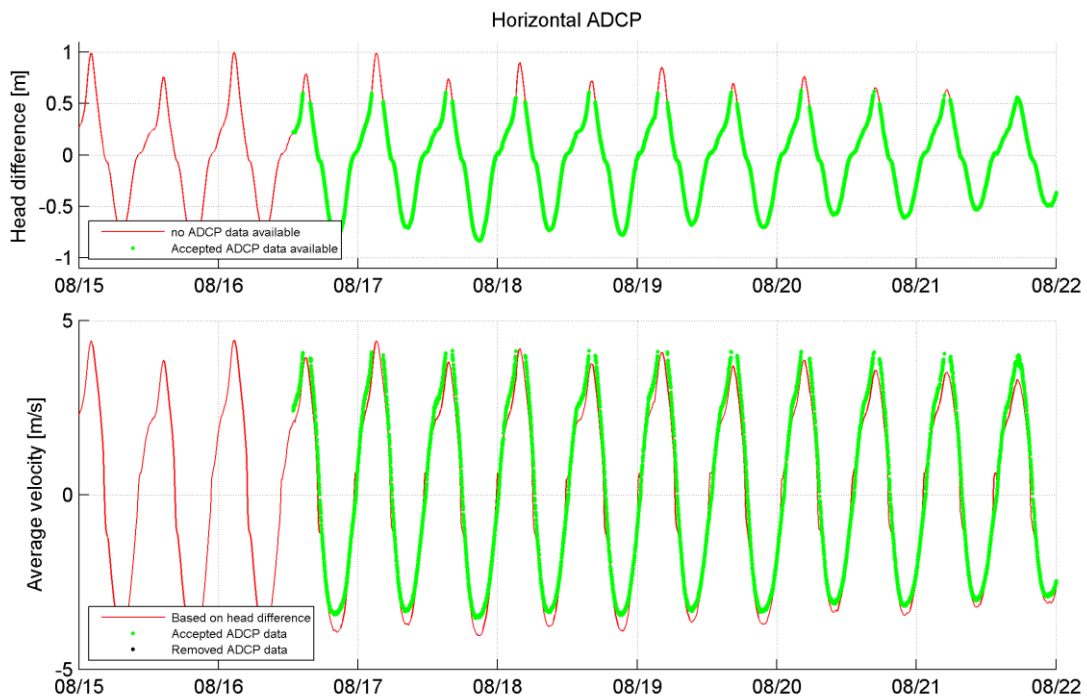


Figure B.2 Timeseries of the expected average velocity through the gate based on the measured head difference over the barrier (red line), the average velocity of the accepted vertical ADCP data (green dots) and the average velocity of the rejected vertical ADCP data (black dots). Horizontal ADCP

### B.3 Brief overview of quality checked data

Figure B.1 shows that the vertical ADCP was able to measure the current velocities almost continuously during flood (with a few exceptions during peak flood flow). During ebb, however, no vertical ADCP measurements met the Partrac QA criteria for average ebb velocities higher than -2.5 m/s (which corresponds to head differences lower than about -0.3 m).

Figure B.2 shows that the horizontal ADCP data contains reliable data during the entire ebb phase, but lacks velocity data during a head difference of more than +0.6 m.

## C Velocity profiles without turbine deployment

### C.1 Case 1 (head difference = -0.2 m)

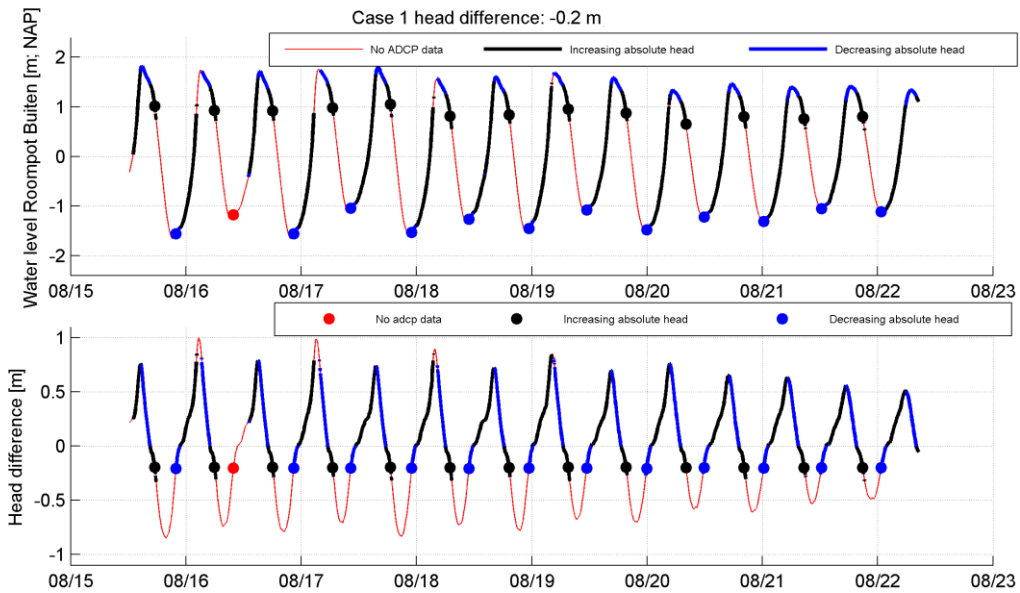


Figure C.1 Periods corresponding to a head difference of -0.2 m (Case 1) for the vertical ADCP. Upper plot: Timeseries of the water level at Roompot Buiten. The colours represent periods without quality checked ADCP data (red), quality checked ADCP data during increasing head (black) and during decreasing head (blue). Lower plot: Timeseries of the head difference over the barrier.

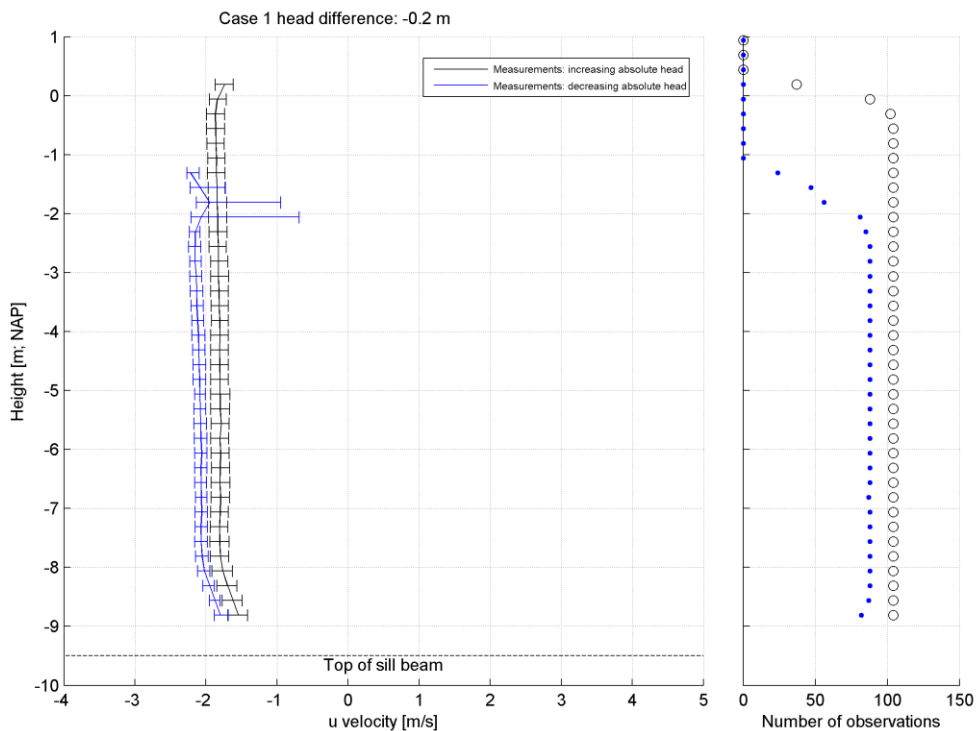


Figure C.2 Left: Velocity profile for Case 1 (head difference of -0.2 m) as measured by the vertical ADCP. Distinction is made between periods of increasing and decreasing absolute head. Right: Number of observations used per bin.

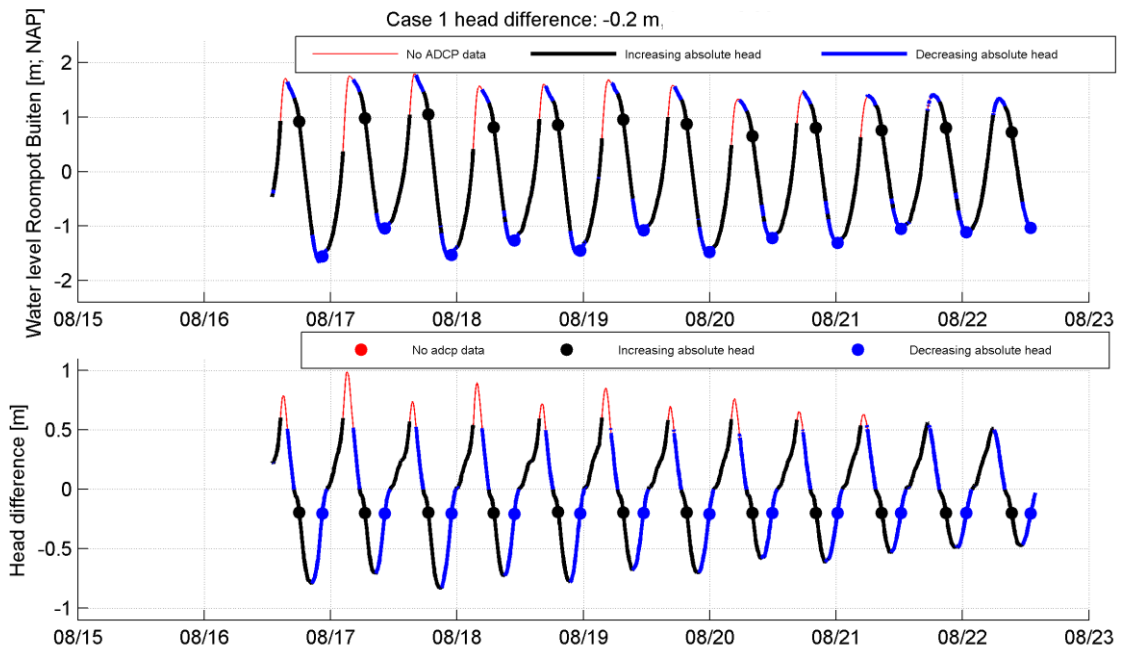


Figure C.3 Periods corresponding to a head difference of  $-0.2$  m (Case 2) for the horizontal ADCP. Upper plot: Timeseries of the water level at Roompot Buiten. The colours represent periods without quality checked ADCP data (red), quality checked ADCP data during increasing head (black) and during decreasing head (blue). The dots show the periods corresponding to a head difference of  $-0.2$  m. Lower plot: Timeseries of the head difference over the barrier.

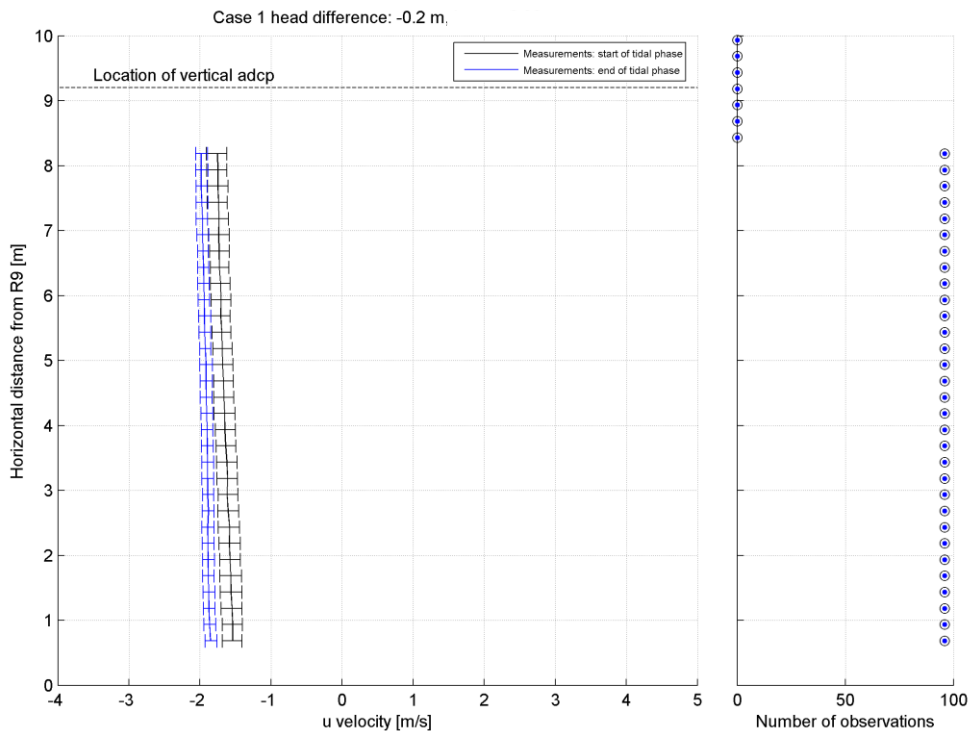


Figure C.4 Left: Velocity profile for Case 1 (head difference of  $-0.2$  m) as measured by the horizontal ADCP. Distinction is made between periods of increasing and decreasing absolute head. Right: Number of observations used per bin.

**C.2 Case 2 (head difference = -0.32 m)**

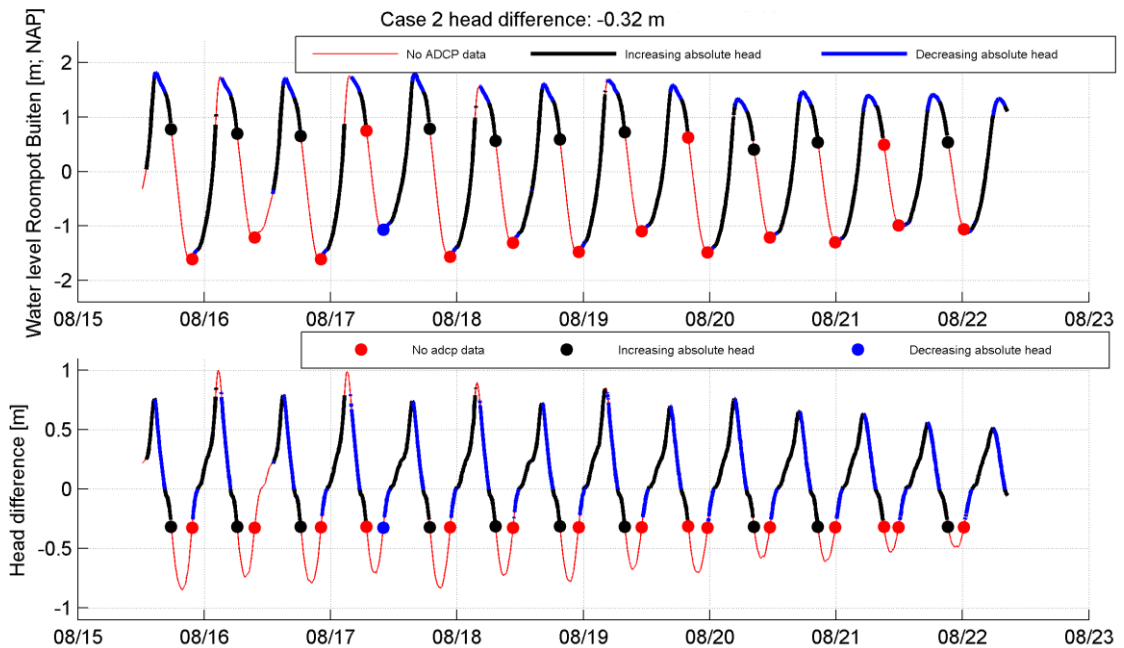


Figure C.5 Periods corresponding to a head difference of -0.32 m (Case 2) for the vertical ADCP. Upper plot: Timeseries of the water level at Roompot Buiten. The colours represent periods without quality checked ADCP data (red), quality checked ADCP data during increasing head (black) and during decreasing head (blue). Lower plot: Timeseries of the head difference over the barrier.

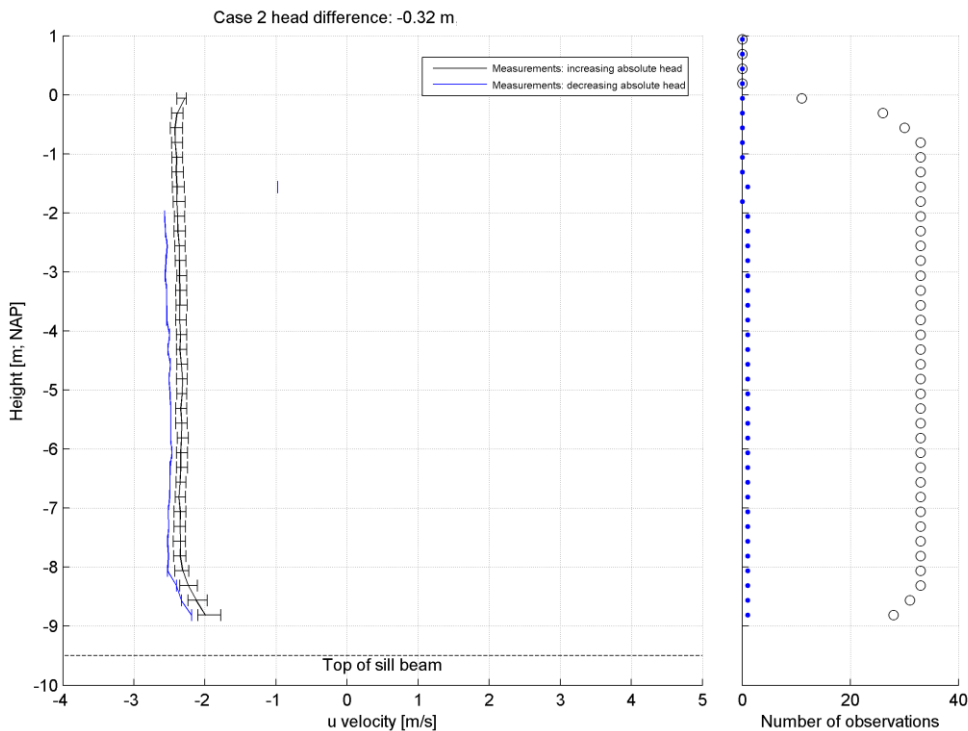


Figure C.6 Left: Velocity profile for Case 2 (head difference of -0.32 m) as measured by the vertical ADCP. Distinction is made between periods of increasing and decreasing absolute head. Right: Number of observations used per bin.

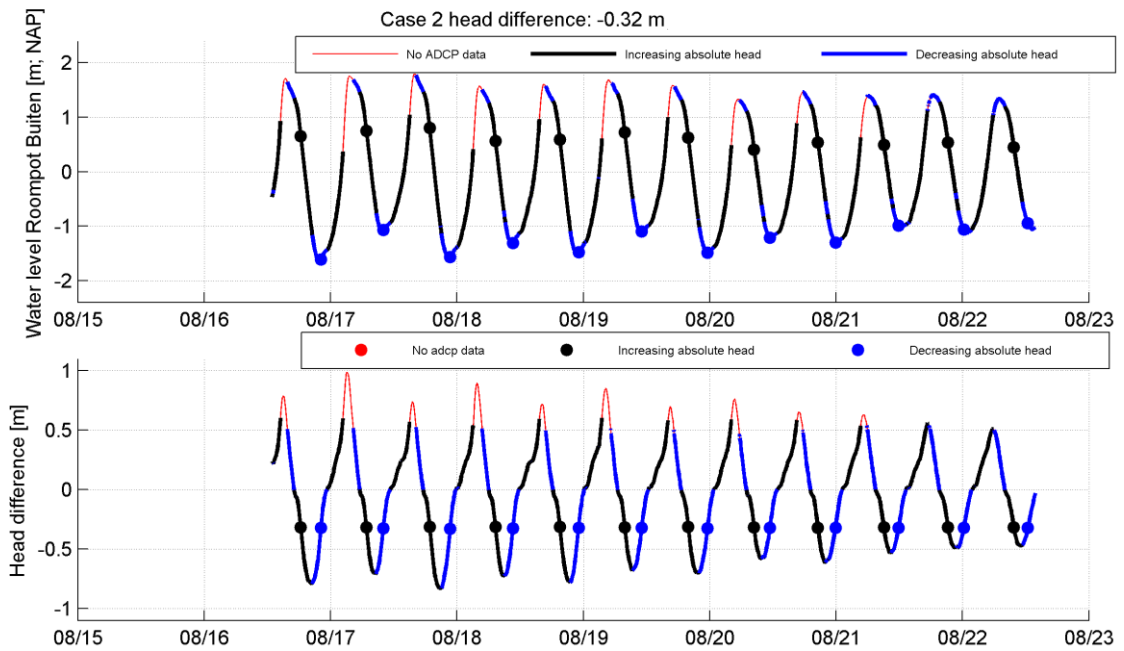


Figure C.7 Periods corresponding to a head difference of  $-0.32$  m (Case 2) for the horizontal ADCP. Upper plot: Timeseries of the water level at Roompot Buiten. The colours represent periods without quality checked ADCP data (red), quality checked ADCP data during increasing head (black) and during decreasing head (blue). The dots show the periods corresponding to a head difference of  $-0.32$  m. Lower plot: Timeseries of the head difference over the barrier.

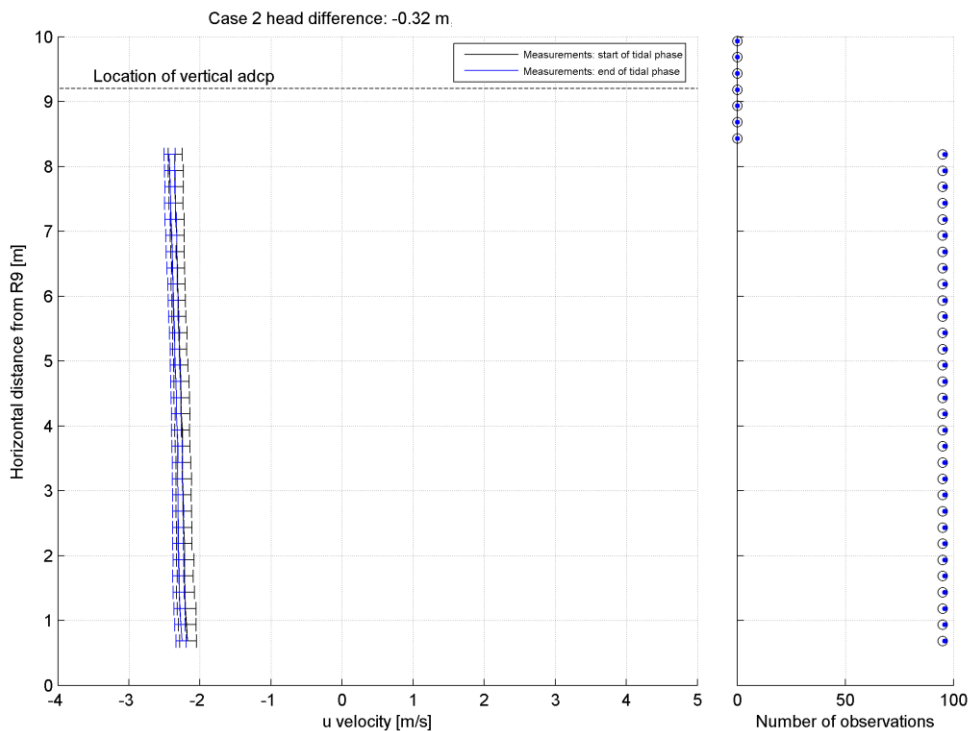


Figure C.8 Left: Velocity profile for Case 2 (head difference of  $-0.32$  m) as measured by the horizontal ADCP. Distinction is made between periods of increasing and decreasing absolute head. Right: Number of observations used per bin.



**C.3 Case 3 (head difference = +0.2 m)**

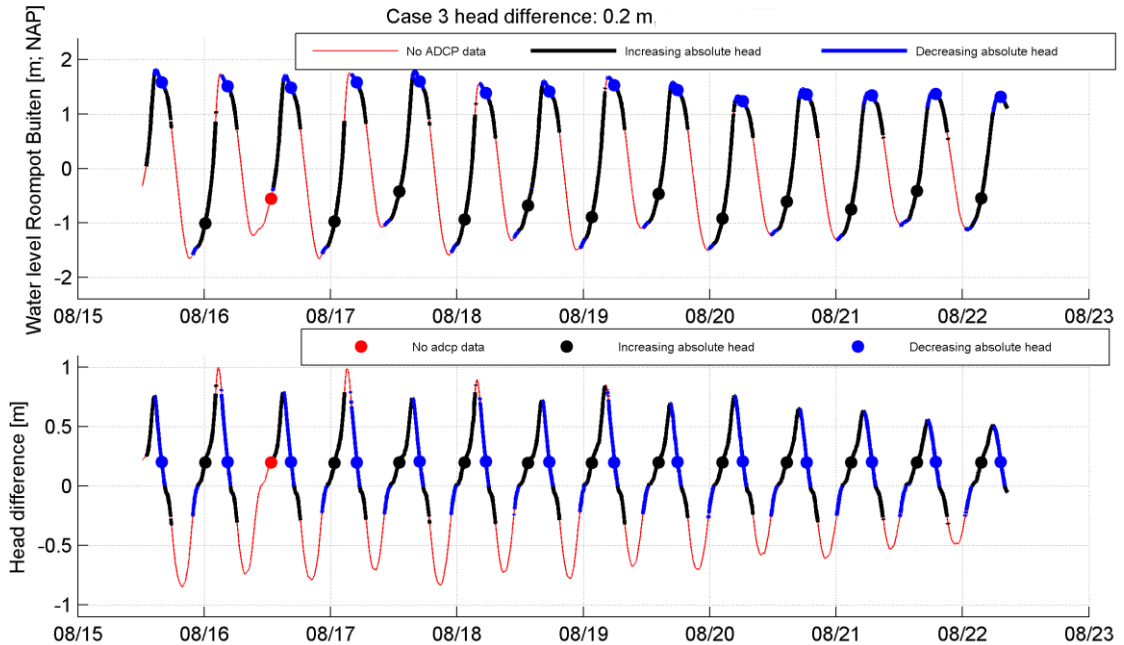


Figure C.9 Periods corresponding to a head difference of +0.2 m (Case 3) for the vertical ADCP. Upper plot: Timeseries of the water level at Roompot Buiten. The colours represent periods without quality checked ADCP data (red), quality checked ADCP data during increasing head (black) and during decreasing head (blue). The dots show the periods corresponding to a head difference of +0.2 m. Lower plot: Timeseries of the head difference over the barrier.

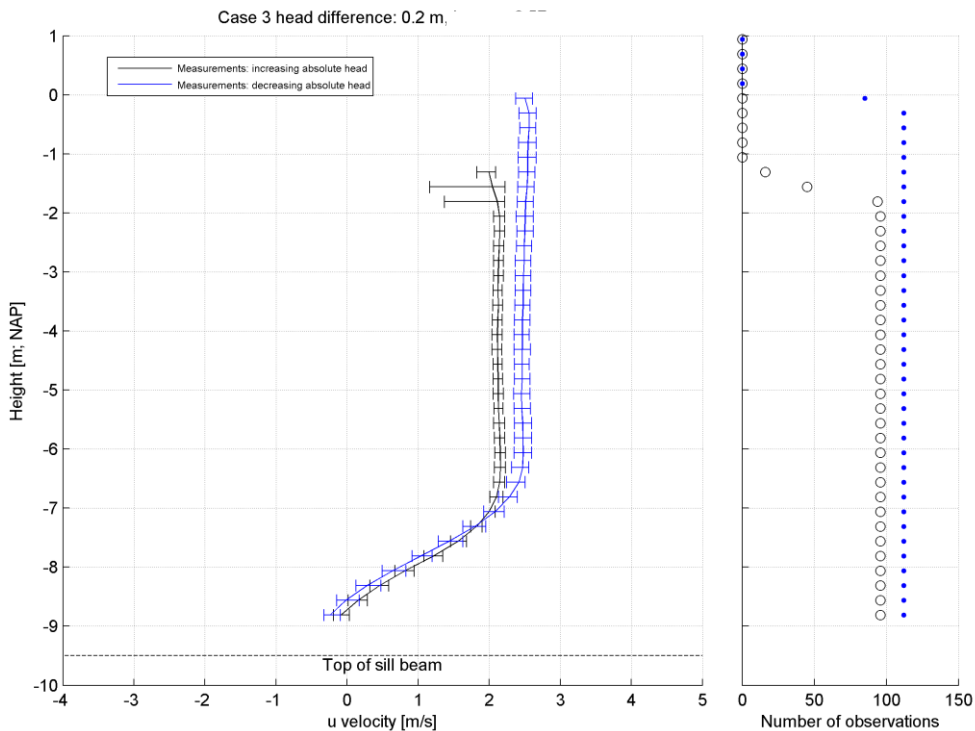


Figure C.10 Left: Velocity profile for Case 3 (head difference of +0.2 m) as measured by the vertical ADCP. Distinction is made between periods of increasing and decreasing absolute head. Right: Number of observations used per bin.

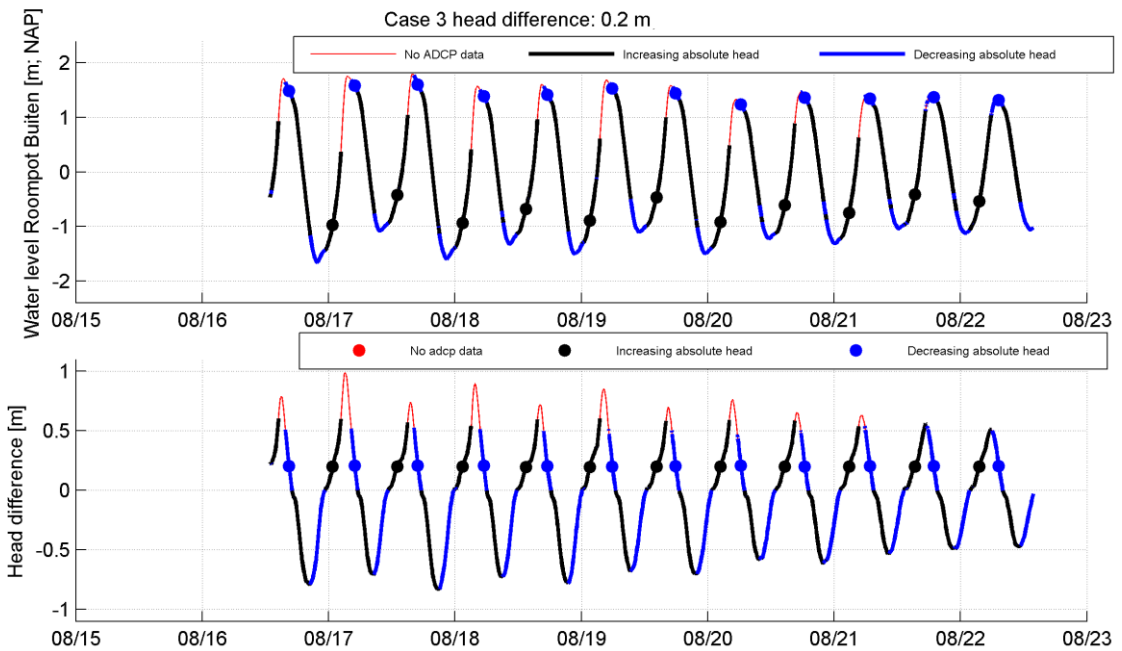


Figure C.11 Periods corresponding to a head difference of +0.2 m (Case 3) for the horizontal ADCP. Upper plot: Timeseries of the water level at Roompot Buiten. The colours represent periods without quality checked ADCP data (red), quality checked ADCP data during increasing head (black) and during decreasing head (blue). The dots show the periods corresponding to a head difference of +0.2 m. Lower plot: Timeseries of the head difference over the barrier.

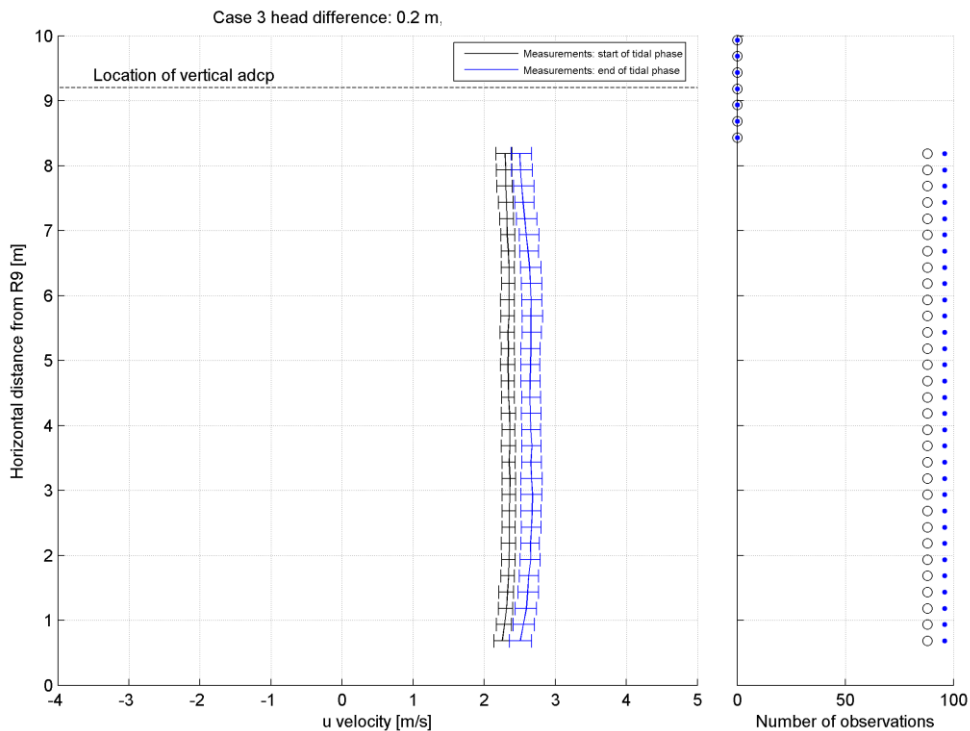


Figure C.12 Left: Velocity profile for Case 3 (head difference of +0.2 m) as measured by the horizontal ADCP. Distinction is made between periods of increasing and decreasing absolute head. Right: Number of observations used per bin.

**C.4 Case 4 (head difference = +0.55 m)**

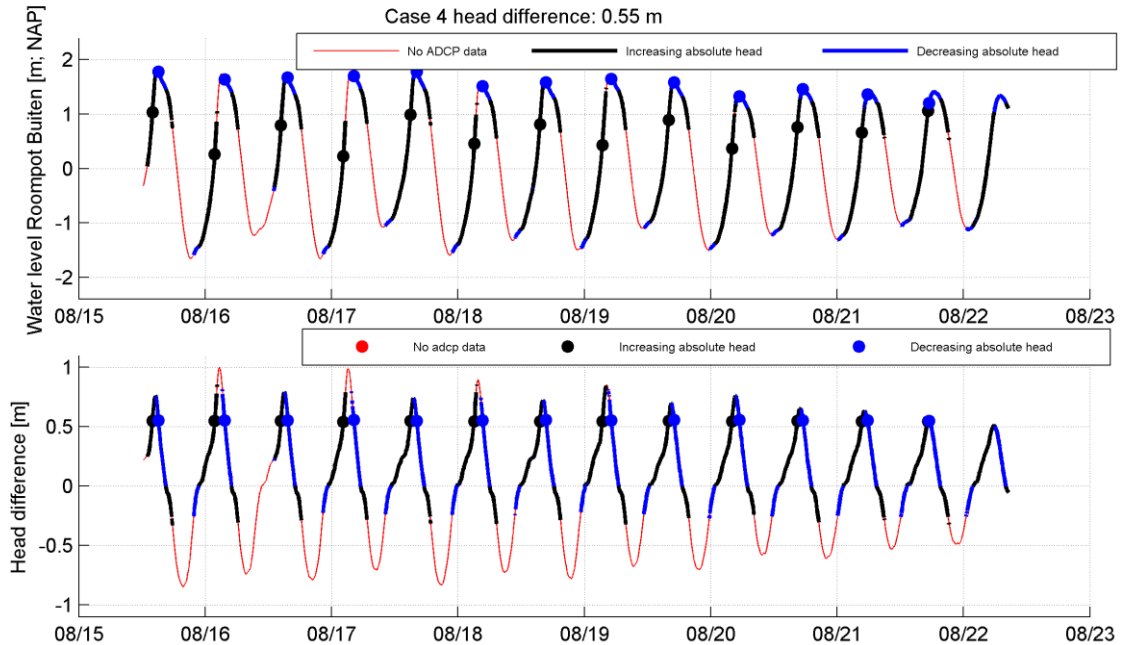


Figure C.13 Periods corresponding to a head difference of +0.55 m (Case 4) for the vertical ADCP. Upper plot: Timeseries of the water level at Roompot Buiten. The colours represent periods without quality checked ADCP data (red), quality checked ADCP data during increasing head (black) and during decreasing head (blue). The dots show the periods corresponding to a head difference of +0.55 m. Lower plot: Timeseries of the head difference over the barrier.

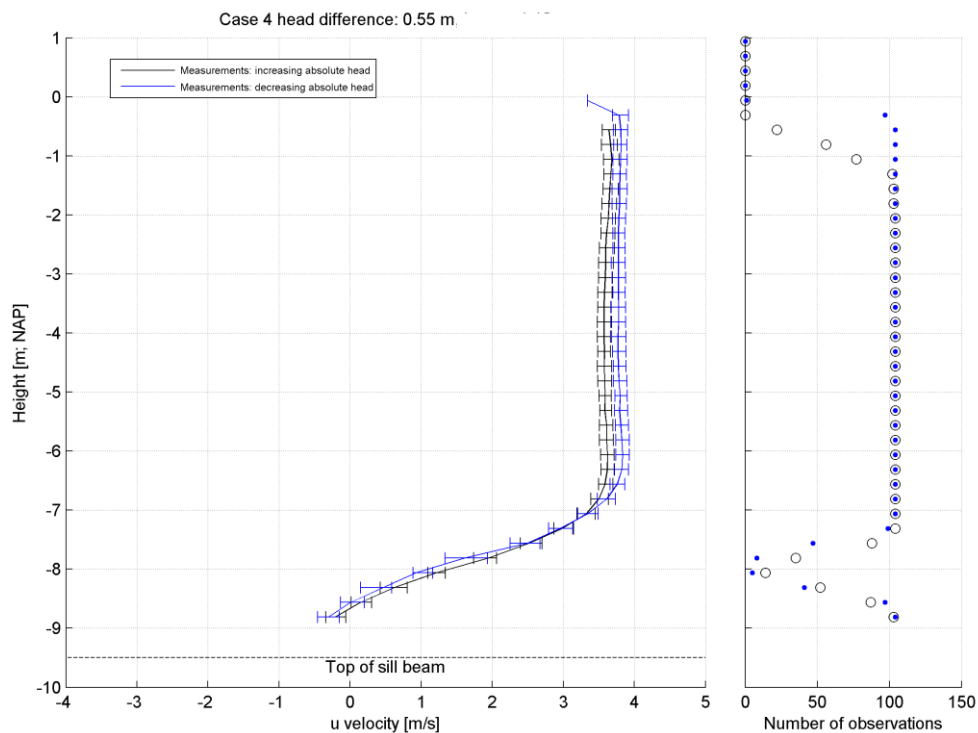


Figure C.14 Left: Velocity profile for Case 4 (head difference of +0.55 m) as measured by the vertical ADCP. Distinction is made between periods of increasing and decreasing absolute head. Right: Number of observations used per bin.

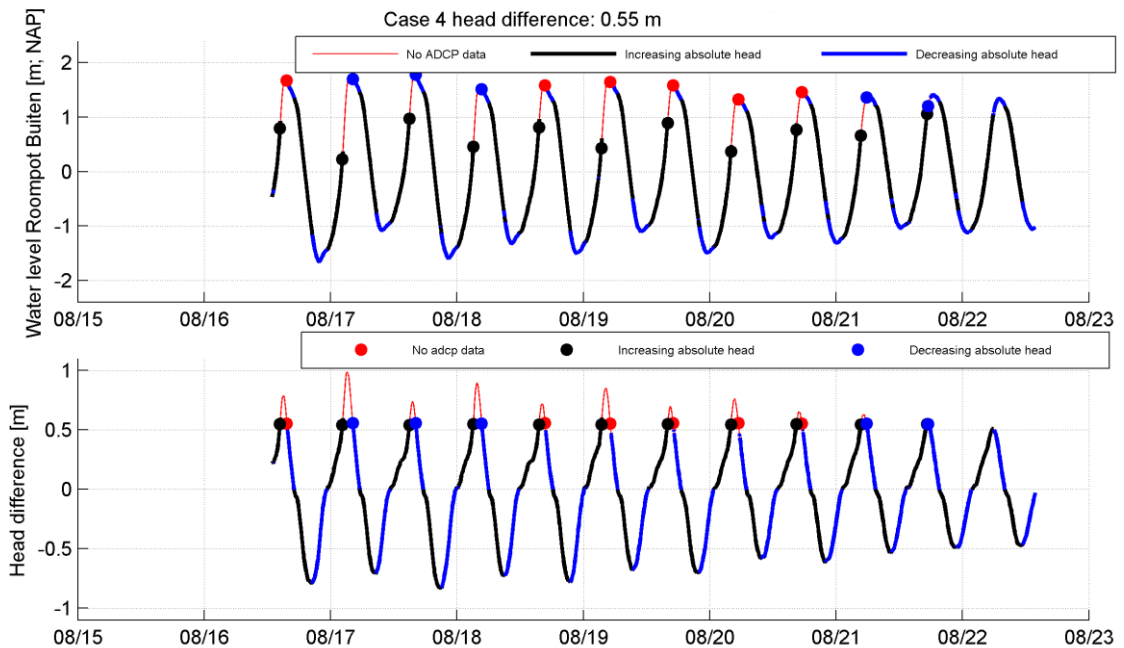


Figure C.15 Periods corresponding to a head difference of +0.55 m (Case 4) for the horizontal ADCP. Upper plot: Timeseries of the water level at Roompot Buiten. The colours represent periods without quality checked ADCP data (red), quality checked ADCP data during increasing head (black) and during decreasing head (blue). The dots show the periods corresponding to a head difference of +0.55 m. Lower plot: Timeseries of the head difference over the barrier.

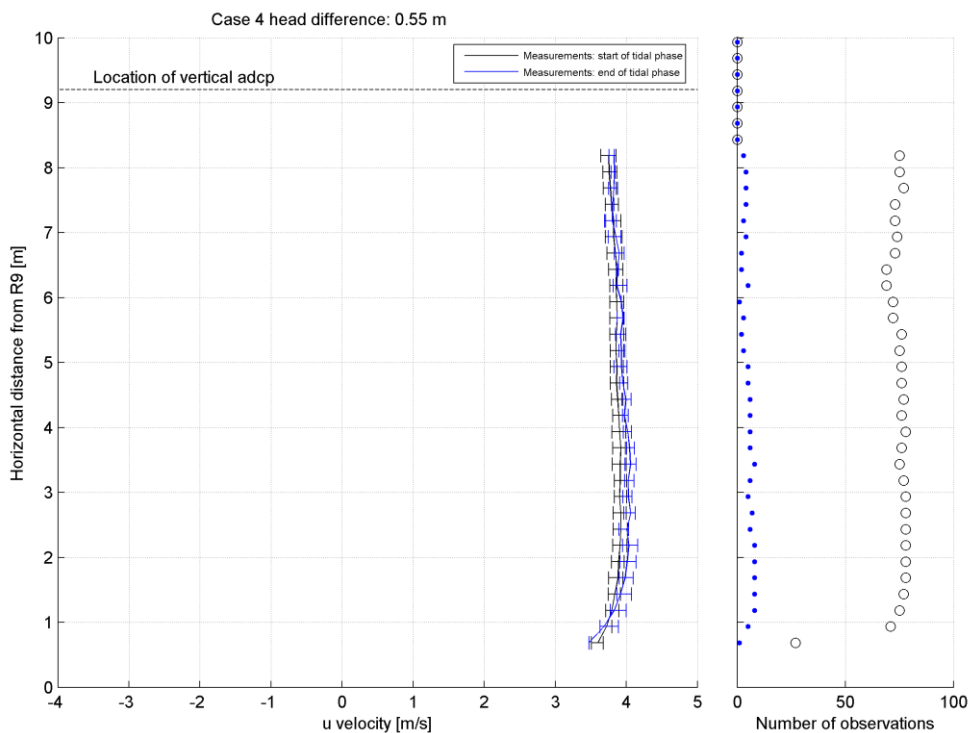


Figure C.16 Left: Velocity profile for Case 4 (head difference of +0.55 m) as measured by the horizontal ADCP. Distinction is made between periods of increasing and decreasing absolute head. Right: Number of observations used per bin.

## D Quality checks for ADCP data during turbine deployment

### D.1 Quality checks on ADCP data during normal turbine operation

The provided 15-minute ad2cp binary files contained the raw ADCP measurements. These binary files were read by means of MATLAB. The steps to arrive at reliable quality checked data are described below. In this section some of the steps will be illustrated for the forward-looking ADCP of the middle turbine (ADCP 341).

#### *Step 1: Removing data based on the quality of the ADCP signal*

The following quality checks were carried out:

- Removing data exceeding the following criteria limits for the forward-looking ADCP's:
  - Velocity > 0.8 m/s off the 1-minute median velocity
  - Correlation of the signal < 50%
  - Amplitude of the signal < 40%
  - $\frac{\Delta u}{\bar{u}} > 0.2$ , in which  $\Delta u$  is the difference in velocity between two successive bins and  $\bar{u}$  is the 1-minute median velocity. Only applied in case the  $u$  is larger
  - Bins > 41. The recorded velocity in these bins seemed very unstable
- Removing data exceeding the following criteria limits for the backward-looking ADCP's:
  - Correlation of the signal < 70%
  - Amplitude of the signal < 30%

#### *Step 2: Performing a 1-minute averaging*

To be able to process the extensive amount of the data, a 1-minute averaging was performed on the data resulting from step 1. The standard deviation of the data within each minute was also stored, which was also used in the analysis of the velocity profiles as discussed in the next sections.

#### *Step 3: Removing all data when turbines are parked*

Subsequently all data were removed when the turbines were “parked” (i.e. lifted out of the water). This is done by analysing the pitch and roll timeseries of the ADCP's.

#### *Step 4: Removing data when the RPM is outside expected range*

During the deployment, the turbines are regularly lifted out of the water (since it is not allowed for the turbines to be operational during large head differences) or put in stall mode (i.e. rotating with low RPM). During these operational changes, the ADCP may still register velocities. Since these registered velocities are not corresponding to the “normal” operation of the turbines they will need to be removed from the dataset.

For every turbine, the relation between the registered RPM and head difference over the barrier is analysed. The head difference over the barrier was calculated by subtracting the measured water level at Roompot Binnen (located on the Eastern Scheldt side of the barrier) from the measured water level at Roompot Buiten (located on the North Sea side of the barrier), see Figure 3.1 for the locations. The measured water level at these two locations was extracted from the online Waterbase database that is provided by Rijkswaterstaat. The water level data is provided in the GMT + 1h timezone. The analysis is illustrated for the middle turbine in Figure D.1. In this figure the effect of inertia is again clearly visible, see Section 3.2.2 for a detailed explanation. For the both increasing and decreasing head, the median RPM value is determined for the whole range of head differences. Subsequently an acceptable range around the median RPM values was assumed of 10% of the gradient of the

curves (black patch for increasing head and blue patch for decreasing head). All data records outside of these accepted ranges were removed from the dataset (red dots)

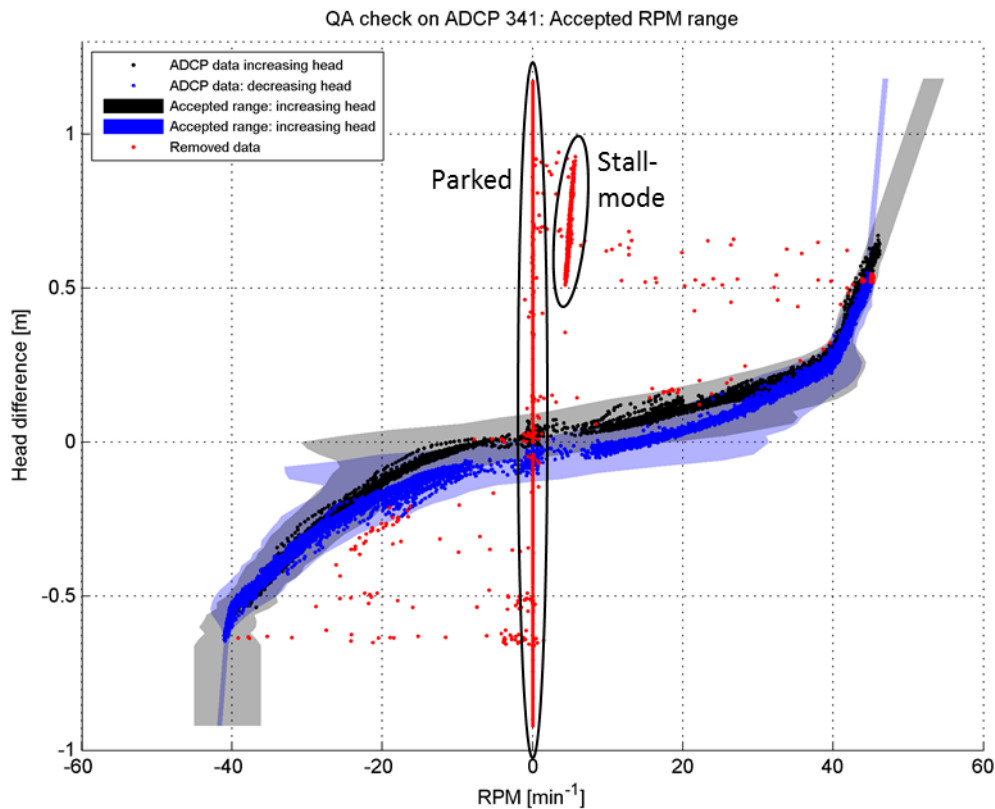


Figure D.1 Relation between registered RPM and head difference for the middle turbine for the ADCP data period. All observations within the blue and black patches are assumed to be carried out in “normal” operational conditions.

#### Step 5: Removing data when the current velocity at the sill beam is more than 1 m/s off the theoretically expected average current velocity

After the previous 4 steps most of the low-quality data was removed, but still contained some outliers. Therefore, as a last step, a comparison was made between the observed velocity at the sill beam and the theoretical velocity based on the head difference over the barrier ( $v_{avg} = \mu\sqrt{2g\Delta h}$ ). Due to inertia, the velocity in the gate lags behind the water level variation. For ADCP 341, a time lag of 15 minutes was determined. The resulting theoretical velocity curve can be seen in Figure D.2 (black line in the middle plot). This figure shows that generally the observed velocity is in a very good agreement with the shifted theoretical curve. In case the difference between the observed and theoretical velocity is larger than 1 m/s, the observation was removed from the dataset (see red dots in the lower plot of Figure D.2).

#### Overview of quality checked data

shows the quality checked data for ADCP 341 after performing the previous 5 steps. The upper plot shows the head difference over the barrier during the ADCP data period. The green lines correspond to periods containing quality checked data. During most of the period, quality checked velocity data has been obtained between a head difference of about -0.6 m and +0.8 m. The orange lines show periods when the Turbine was parked (lifted out of the water). The red lines show periods when the ADCP data was removed in the quality checks as described above. The middle plot shows in green the quality checked observed velocity in

bin 16 (at the sill beam) for ADCP 341. The blue dots represent the measurements that have been removed in step 4. These removed measurements can also visually be categorized as outliers. The purple dots represent the measurements that have been removed in step 5, by comparing the observed velocity to the shifted theoretical velocity based on the head difference (black line). The lower plot shows the registered RPM of the turbine. The colours are consistent with the upper plot.

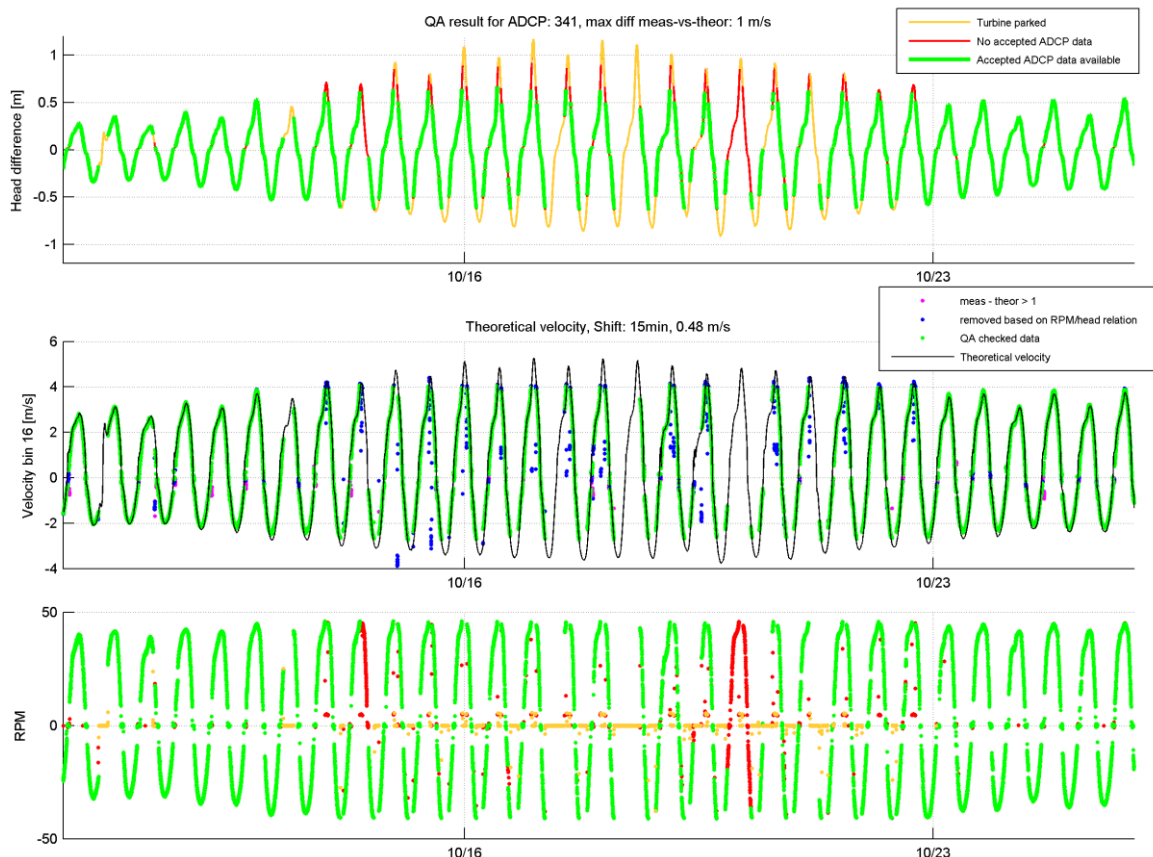


Figure D.2 Upper: Timeseries of the head difference over the barrier. Periods with quality checked data are visualised in green. Middle: Velocity data at bin 16 (above the sill beam), with the quality checked data in green, theoretical velocity based on the head difference in black, removed data due to large difference between measured and theoretical velocity (red) and removed data due to unrealistic RPM values. ADCP\_341 (middle turbine, forward-looking). Lower: Timeseries of the registered RPM of the turbine. Colours are consistent with the upper plot.

## D.2 Quality checks on ADCP data during stall mode turbine operation

The quality checks on the data recorded during stall mode are very similar to the checks as described in Section D.1 with a few small changes. These changes were related to the lower rotation speed of the rotor blade during stall mode. The rotor blocks the ADCP beams for a longer period of time, which is why the following quality criteria were added:

- Correlation of the signal < 1-minute median correlation – 5%
- Amplitude of the signal < 1-minute median amplitude – 5%

During stall mode, the RPM and Power of the turbine is lower than during normal operation. The quality check as described in the previous section based on RPM is therefore also



different for stall mode data. The ADCP data was only considered in periods when the RPM was in the range of -5 to 5.

During the stall mode measurements, the blades of the northern turbine were not in place. Due to the lower resistance at this location, the velocities in the northern part of the gate were lower than in the southern part of the gate, see Figure D.3. This non-uniformity along the gate needs to be included in the interpretation of the results. In the remainder of this report, the ADCP results of the northern turbine are not shown.

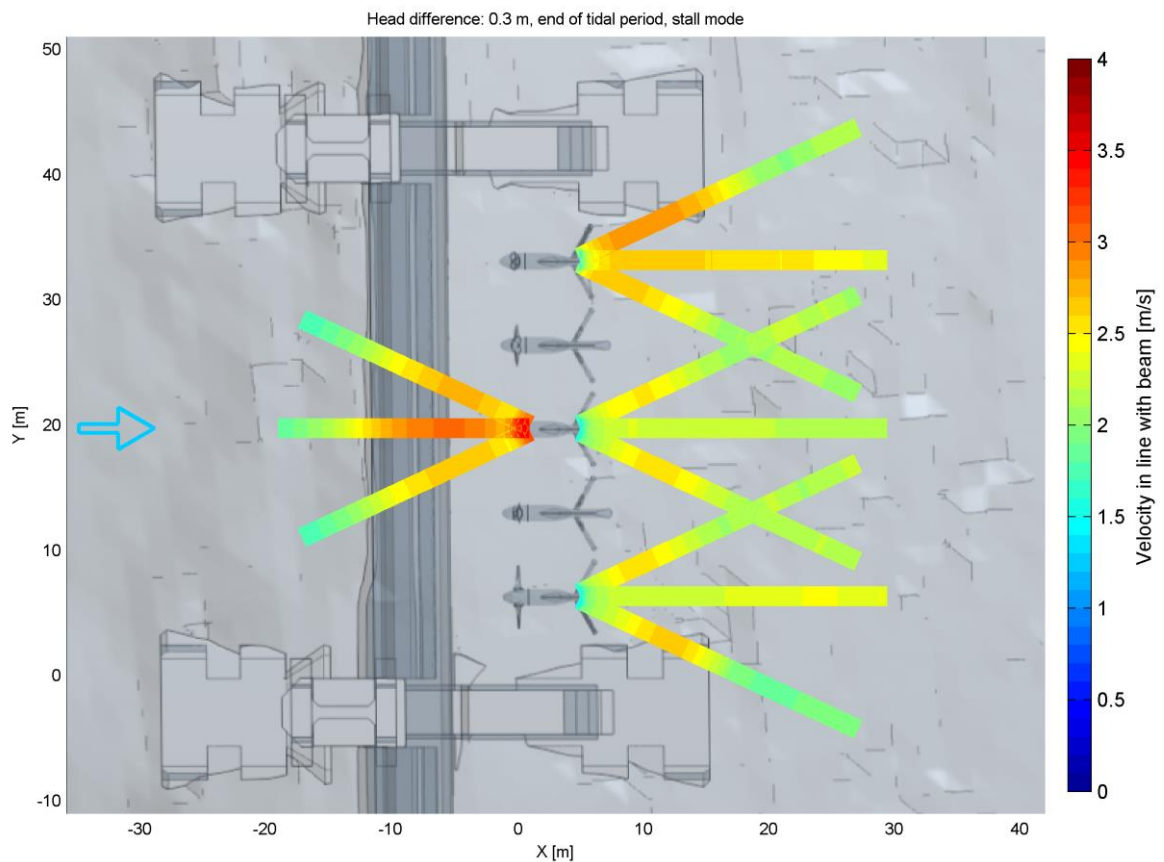


Figure D.3Left: Velocity profile for a head difference of +0.3 m as measured in the horizontal plane by the forward-looking and backward-looking ADCP devices during stall mode operation.

### D.3 Results of quality checks for the 1-beam measurements (normal turbine operation)

For each turbine a figure is included showing the relation between the registered RPM of the turbine and the observed head difference over the barrier. For the both increasing and decreasing head, the median RPM value is determined for the whole range of head differences. Since the median RPM value, for example, for a head difference of +0.8 m doesn't correspond to normal operation, the median RPM outliers have been removed by assuming that the RPM needs to increase (become more positive) for increasing head difference. Subsequently an acceptable range around the median RPM values was assumed of 10% of the gradient of the curves (black patch for increasing head and blue patch for decreasing head). All data records outside of these accepted ranges were removed from the dataset (red dots).

Subsequently, for each ADCP a figure is included showing the resulting quality checked data after performing the quality checks as described in Section D.1. The upper plot shows the head difference over the barrier during the ADCP data period. The green lines correspond to periods containing quality checked data. During most of the period, quality checked velocity data has been obtained between a head difference of about -0.6 m and +0.8 m. The orange lines show periods when the turbine was parked (lifted out of the water). The red lines show periods when the ADCP data was removed in the quality checks as described above. The middle plot shows in green the quality checked observed velocity in bin 16 (at the sill beam) for the forward-looking ADCP's and at bin 11 (10 m east of the rotor) for the backward-looking ADCP's. The blue dots represent the measurements that have been removed based on the relation between the registered RPM and the head difference as visualised in the first figure. For the forward-looking ADCP's also purple dots are shown, which represent the measurements that have been removed by comparing the observed velocity to the shifted theoretical velocity based on the head difference (black line). The lower plot shows the registered RPM of the turbine. The colours are consistent with the upper plot.

### D.3.1 Southern turbine

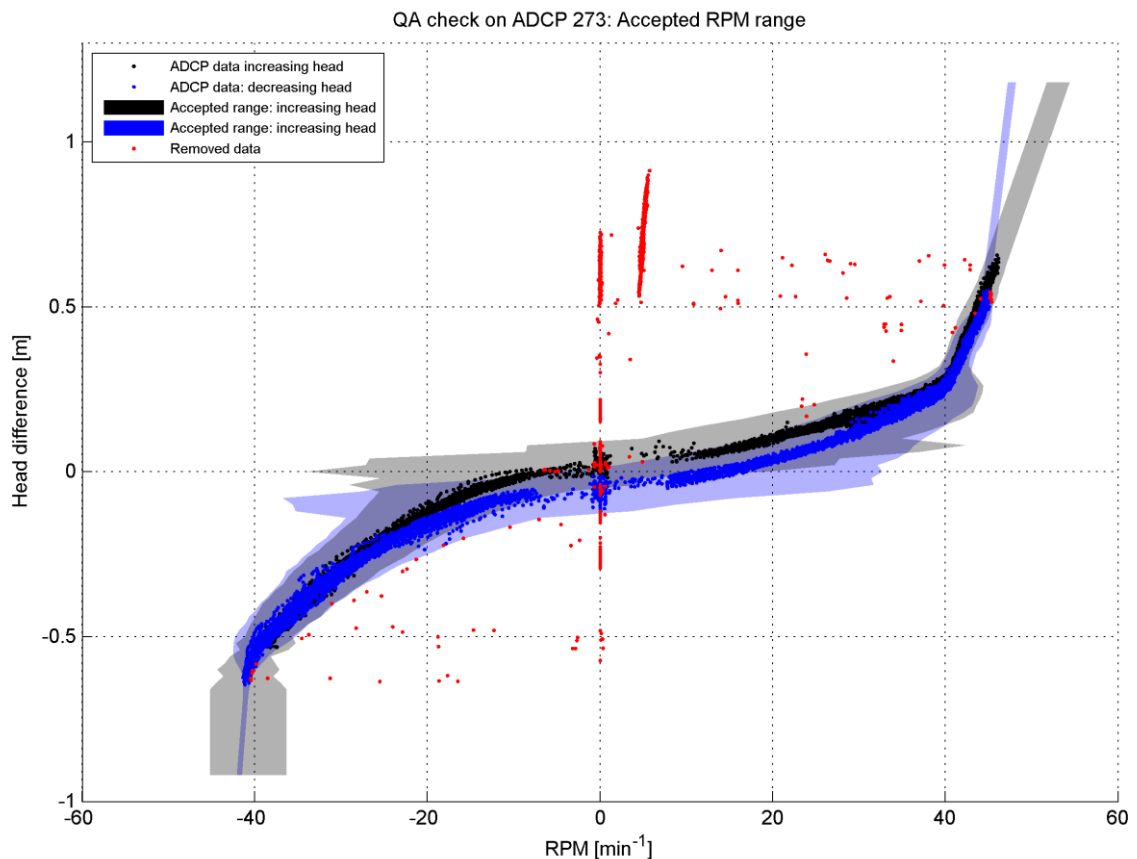


Figure D.4 Relation between registered RPM and head difference for the southern turbine for the ADCP data period. All observations within the blue and black patches are assumed to be carried out in "normal" operational conditions.

## D.3.1.1 ADCP 273, backward-looking

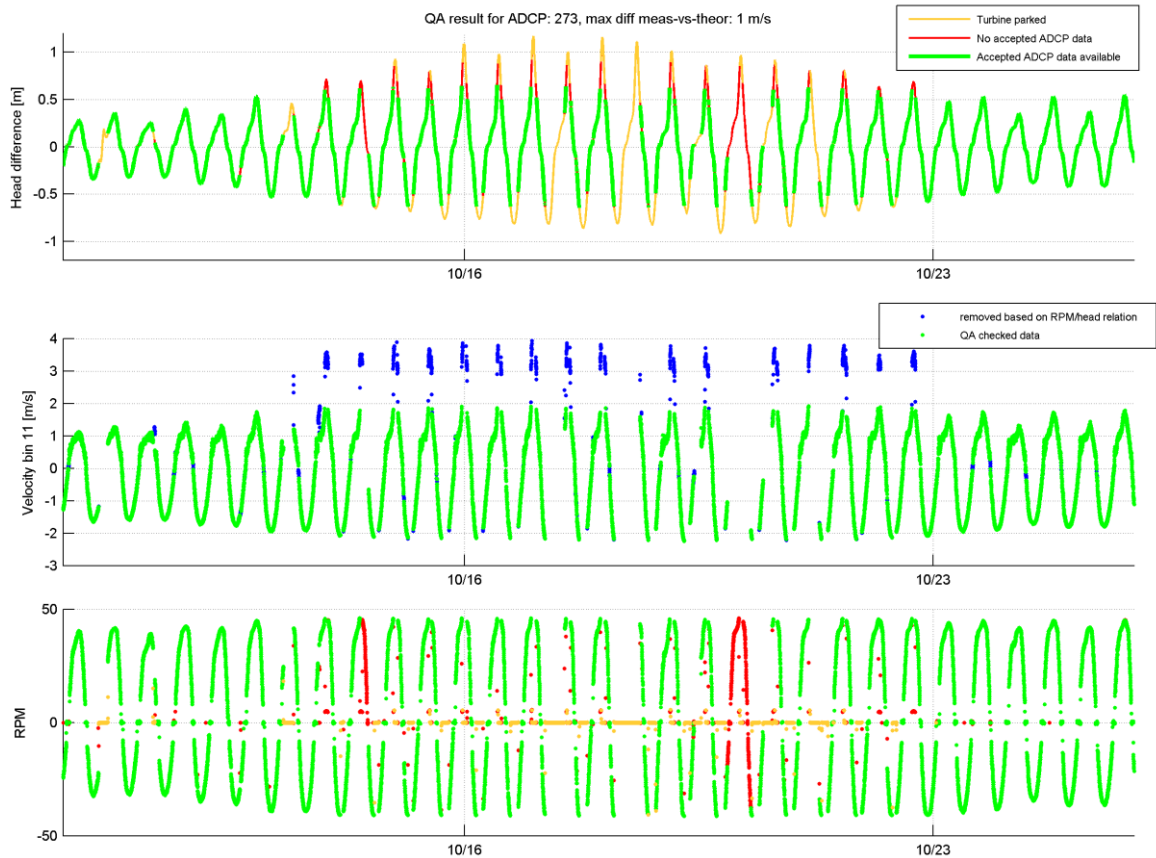


Figure D.5 Upper: Timeseries of the head difference over the barrier. Periods with quality checked data are visualised in green. Middle: Velocity data at bin 16 (above the sill beam), with the quality checked data in green, theoretical velocity based on the head difference in black, removed data due to large difference between measured and theoretical velocity (red) and removed data due to unrealistic RPM values. Lower: Timeseries of the registered RPM of the turbine. Colours are consistent with the upper plot. ADCP\_273 (southern turbine, backward-looking).

## D.3.2 Middle turbine

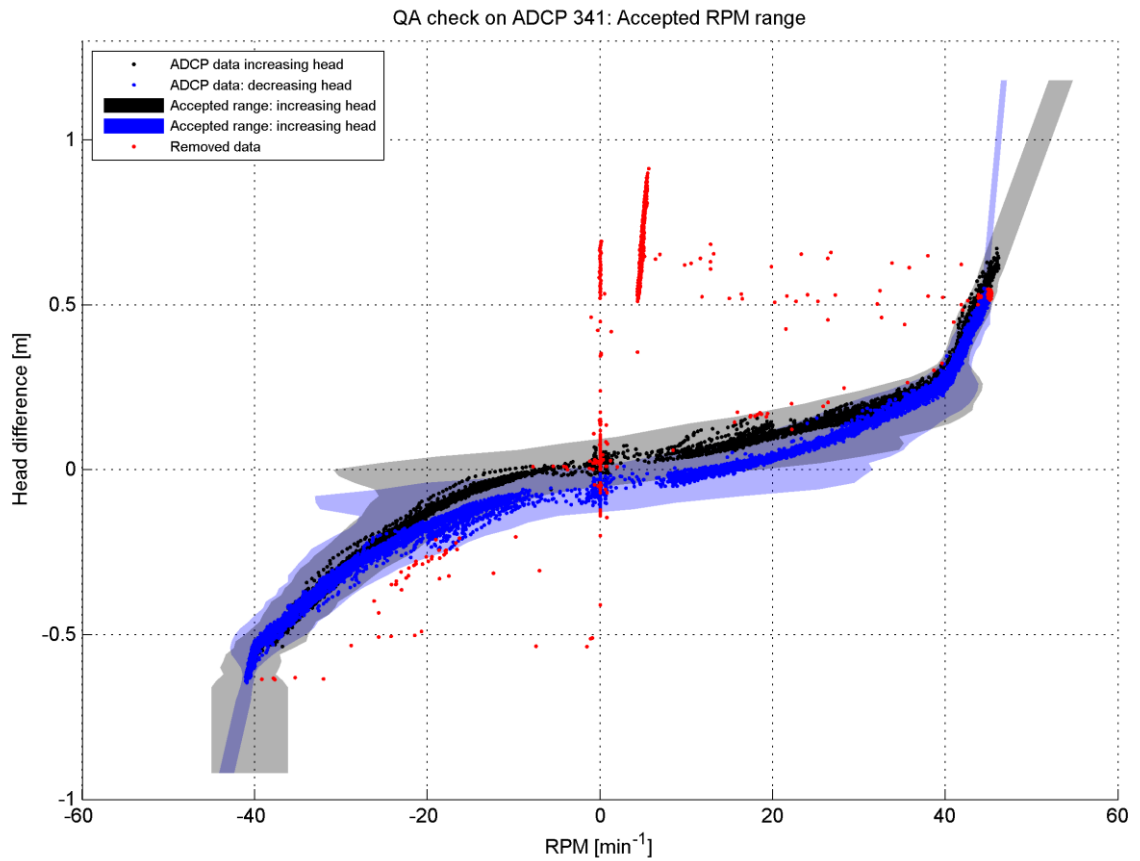


Figure D.6 Relation between registered RPM and head difference for the middle turbine for the ADCP data period. All observations within the blue and black patches are assumed to be carried out in "normal" operational conditions.

## D.3.2.1 ADCP 341, forward-looking

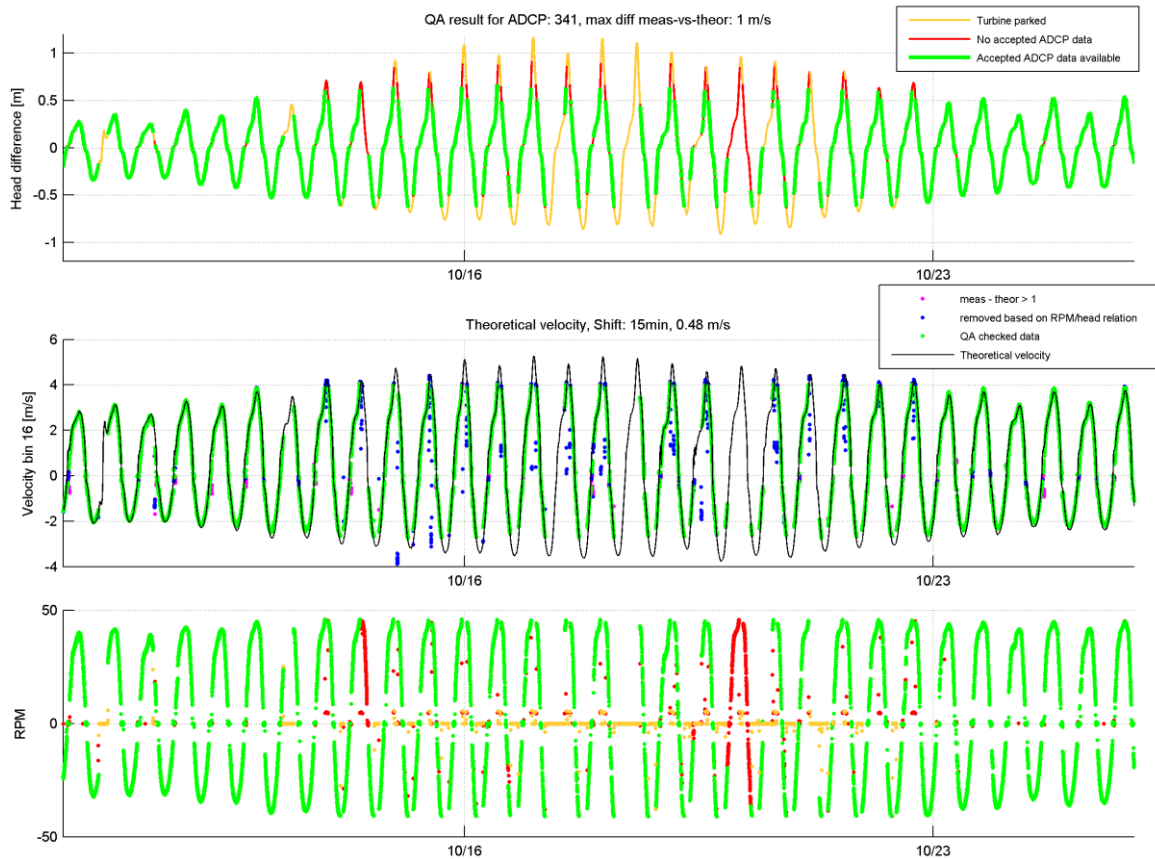


Figure D.7 Upper: Timeseries of the head difference over the barrier. Periods with quality checked data are visualised in green. Middle: Velocity data at bin 16 (above the sill beam), with the quality checked data in green, theoretical velocity based on the head difference in black, removed data due to large difference between measured and theoretical velocity (red) and removed data due to unrealistic RPM values. Lower: Timeseries of the registered RPM of the turbine. Colours are consistent with the upper plot. ADCP\_341 (middle turbine, forward-looking).

## D.3.2.2 ADCP 253, backward-looking

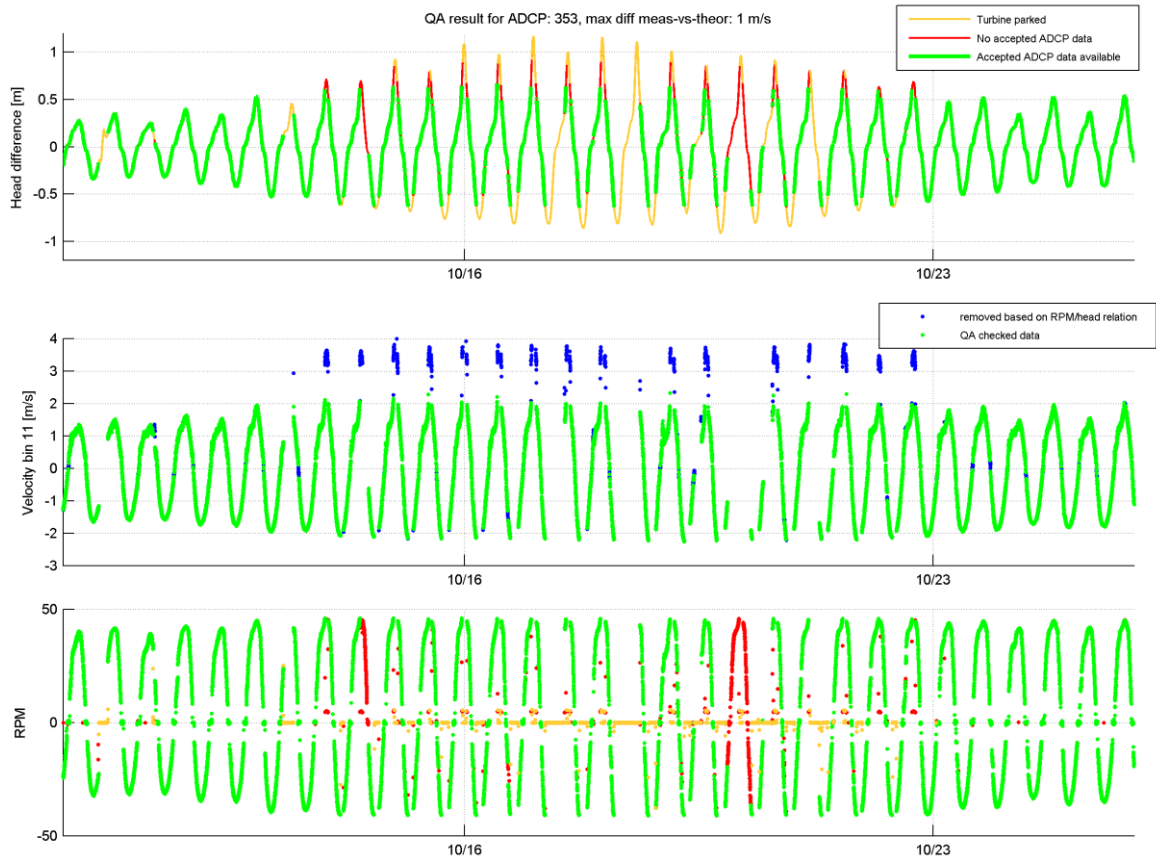


Figure D.8 Upper: Timeseries of the head difference over the barrier. Periods with quality checked data are visualised in green. Middle: Velocity data at bin 16 (above the sill beam), with the quality checked data in green, theoretical velocity based on the head difference in black, removed data due to large difference between measured and theoretical velocity (red) and removed data due to unrealistic RPM values. Lower: Timeseries of the registered RPM of the turbine. Colours are consistent with the upper plot. ADCP\_253 (middle turbine, backward-looking).

## D.3.3 Northern turbine

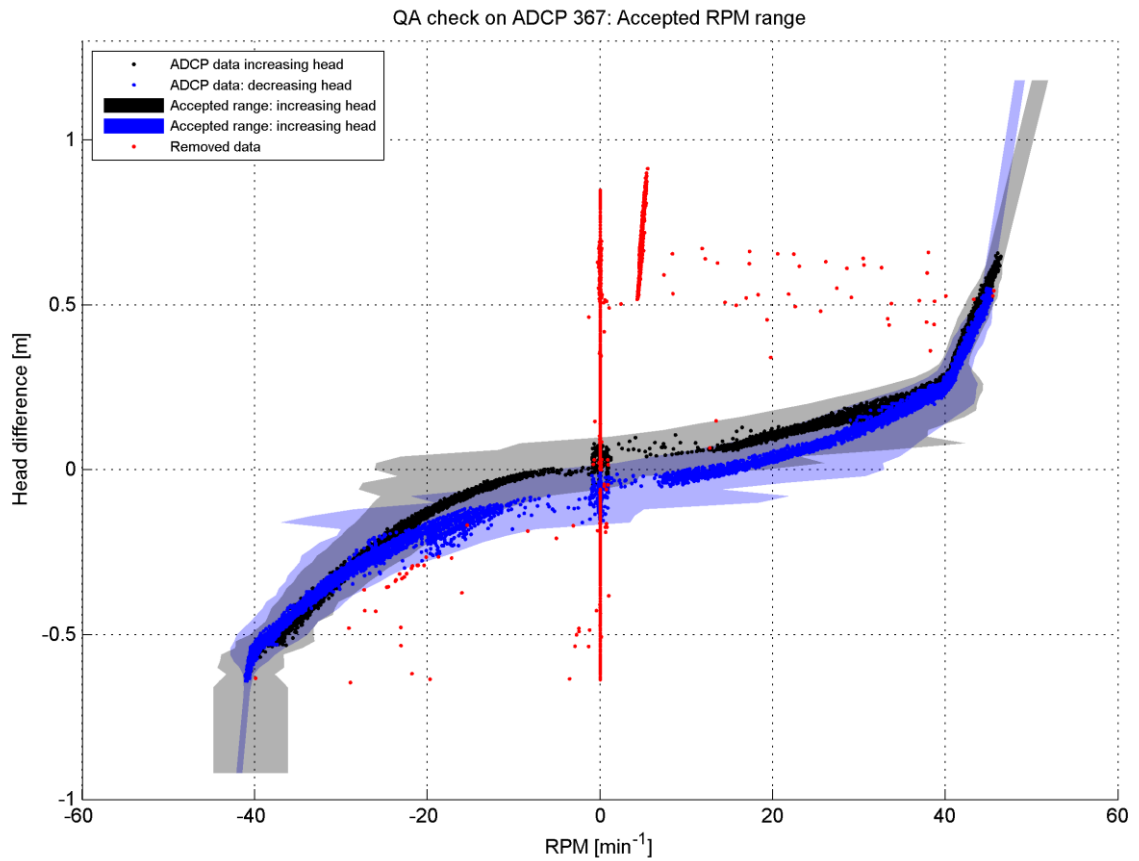


Figure D.9 Relation between registered RPM and head difference for the northern turbine for the ADCP data period. All observations within the blue and black patches are assumed to be carried out in "normal" operational conditions.



## D.3.3.1 ADCP 367, forward-looking

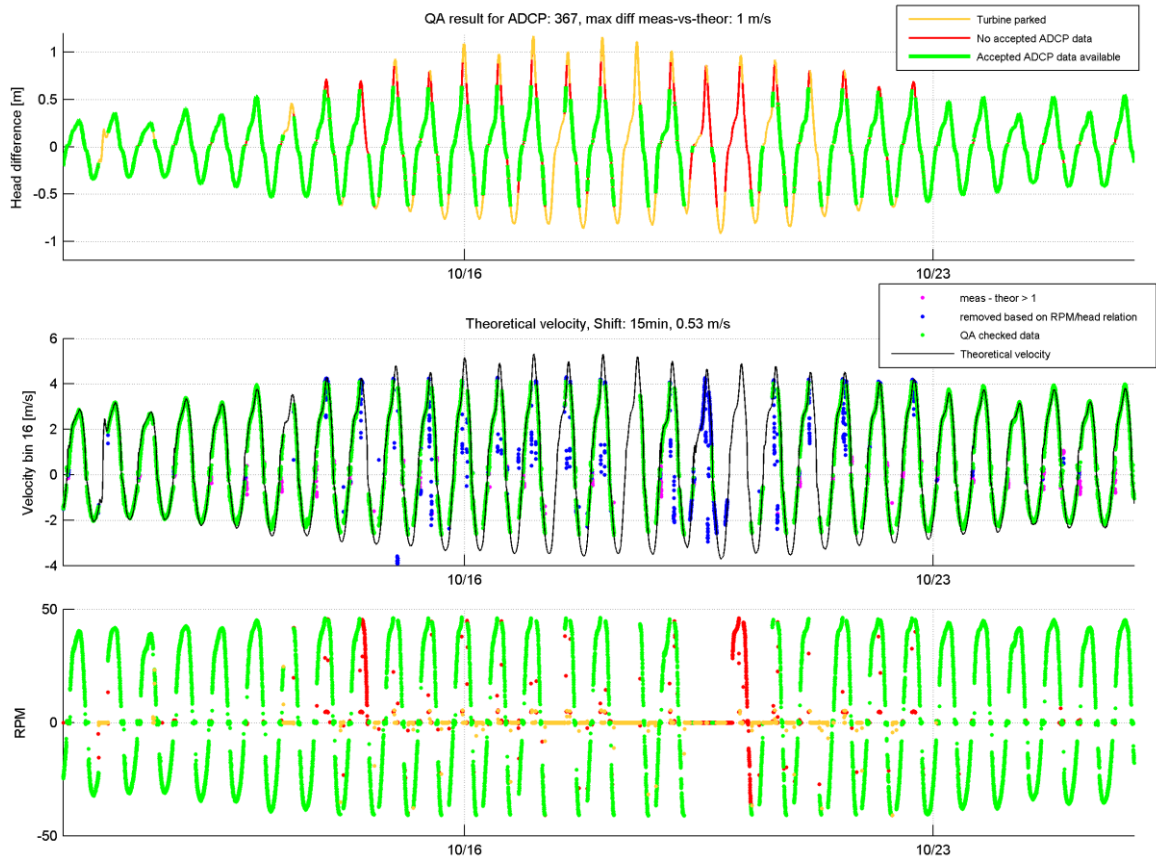


Figure D.10 Upper: Timeseries of the head difference over the barrier. Periods with quality checked data are visualised in green. Middle: Velocity data at bin 16 (above the sill beam), with the quality checked data in green, theoretical velocity based on the head difference in black, removed data due to large difference between measured and theoretical velocity (red) and removed data due to unrealistic RPM values. Lower: Timeseries of the registered RPM of the turbine. Colours are consistent with the upper plot. ADCP\_367 (northern turbine, forward-looking).

## D.3.3.2 ADCP 368, backward-looking

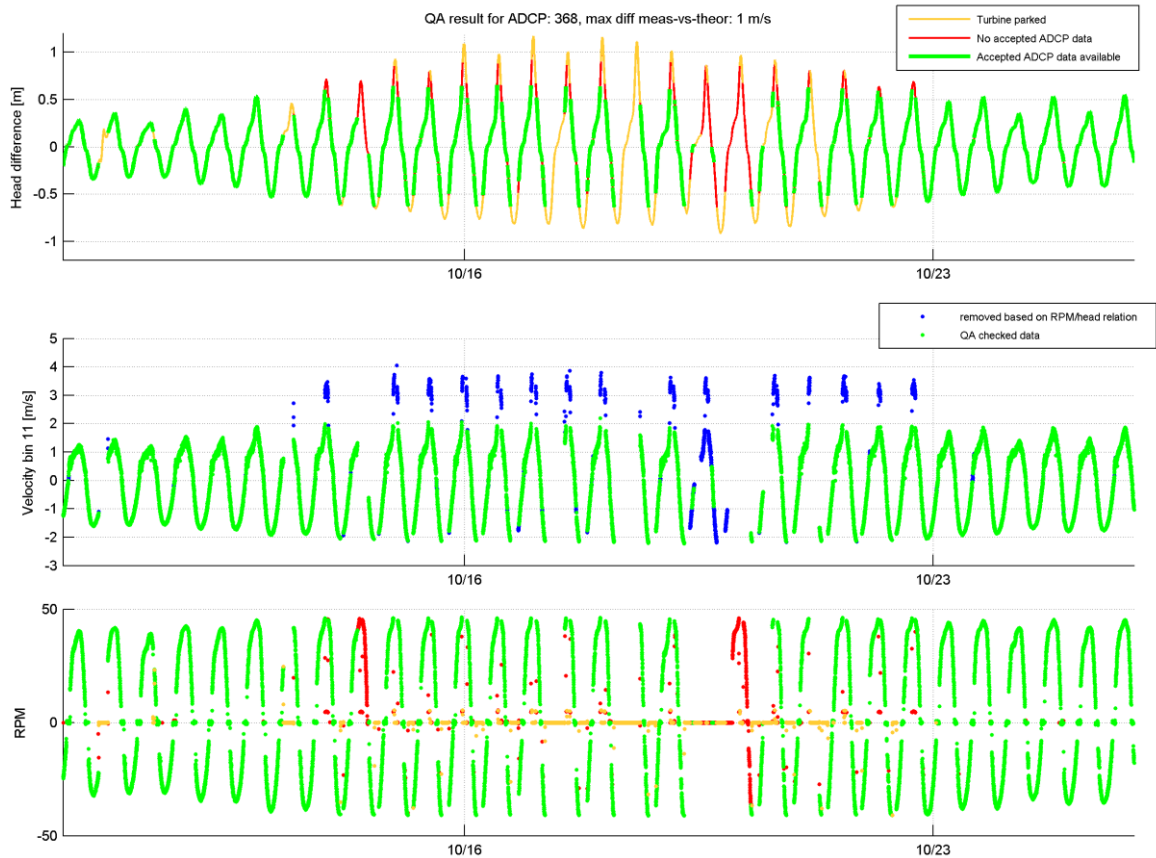


Figure D.11 Upper: Timeseries of the head difference over the barrier. Periods with quality checked data are visualised in green. Middle: Velocity data at bin 16 (above the sill beam), with the quality checked data in green, theoretical velocity based on the head difference in black, removed data due to large difference between measured and theoretical velocity (red) and removed data due to unrealistic RPM values. Lower: Timeseries of the registered RPM of the turbine. Colours are consistent with the upper plot. ADCP\_368 (southern turbine, backward-looking).

## E Velocity profiles during turbine deployment

For each case the results for all three turbines which are equipped with ADCP devices are included. The cable forward-looking ADCP of the southern turbine was not connected, which is why only the backward-looking ADCP results are visualised for this turbine.

### E.1 Case 1 (head difference = -0.2 m)

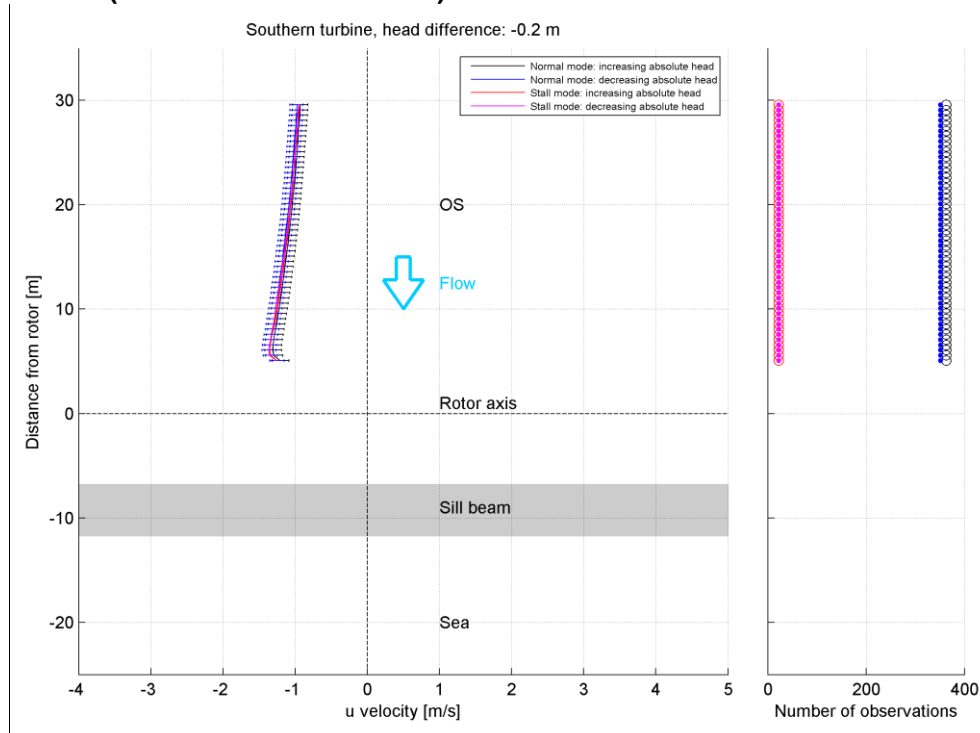


Figure E.1 Left: Velocity profile for Case 1 (head difference of -0.2 m) as measured by the forward-looking and backward-looking ADCP devices on the southern turbine. Distinction is made between periods of increasing and decreasing absolute head. Right: Number of observations used per bin.

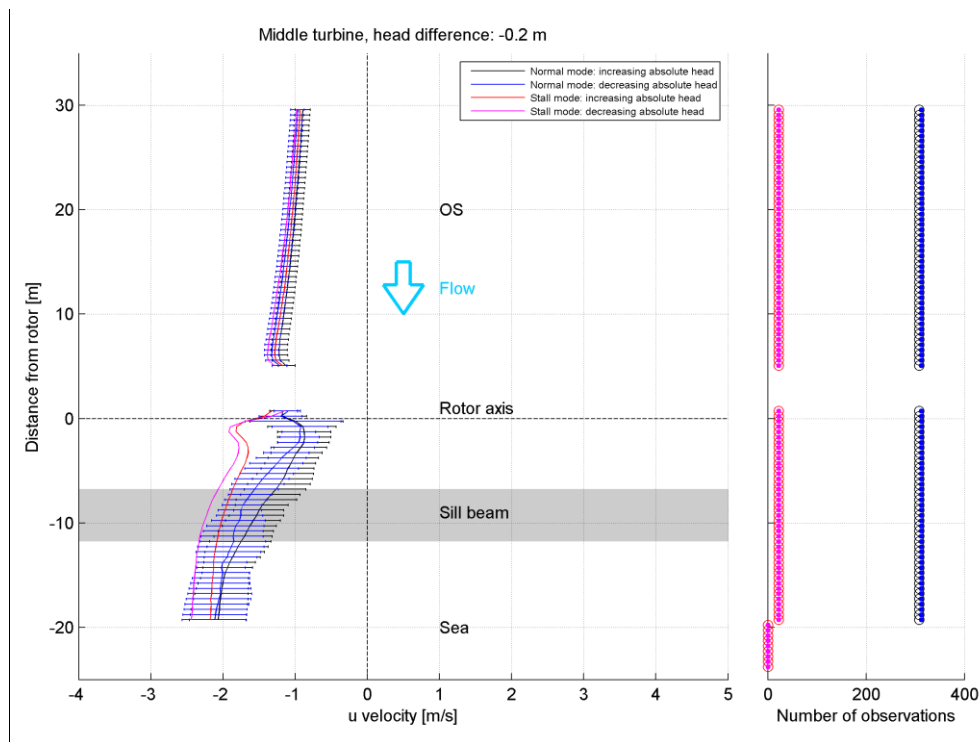


Figure E.2 Left: Velocity profile for Case 1 (head difference of -0.2 m) as measured by the forward-looking and backward-looking ADCP devices on the middle turbine. Distinction is made between periods of increasing and decreasing absolute head. Right: Number of observations used per bin.

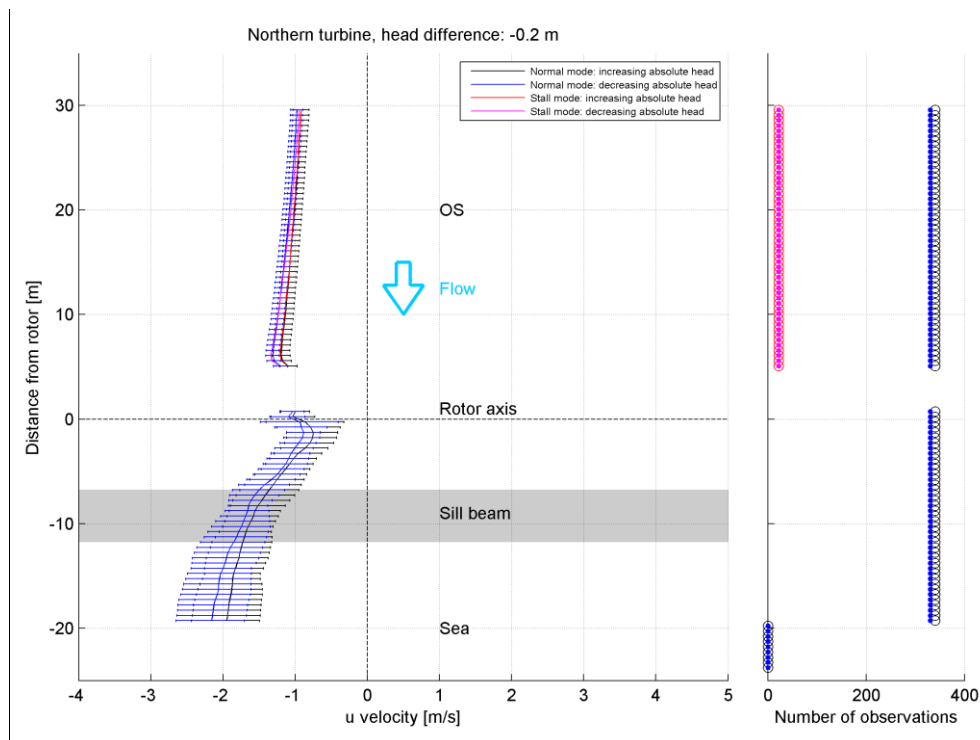


Figure E.3 Left: Velocity profile for Case 1 (head difference of -0.2 m) as measured by the forward-looking and backward-looking ADCP devices on the northern turbine. Distinction is made between periods of increasing and decreasing absolute head. Right: Number of observations used per bin.

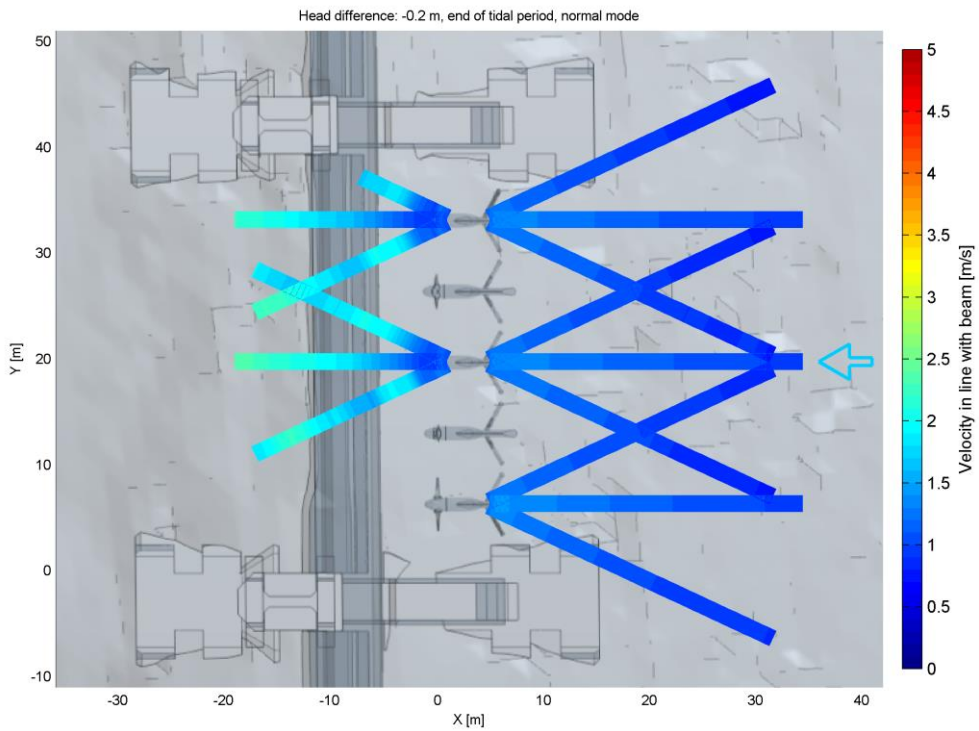


Figure E.4 Velocity profile for Case 1 (head difference of -0.2 m) as measured in the horizontal plane by the forward-looking and backward-looking ADCP devices during normal mode operation.

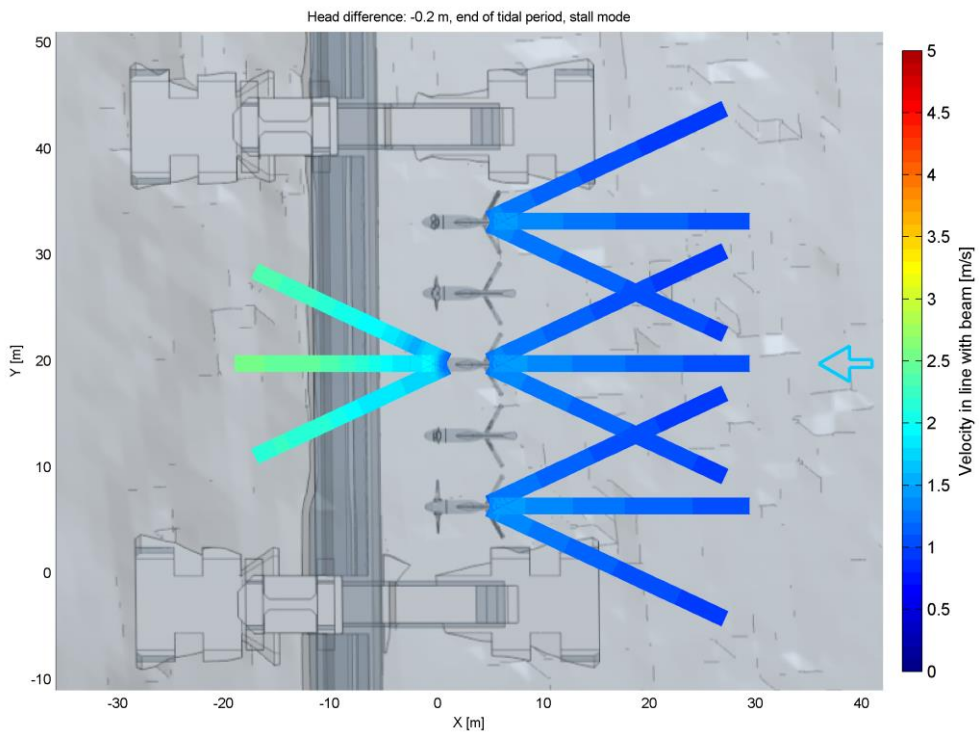


Figure E.5 Velocity profile for Case 1 (head difference of -0.2 m) as measured in the horizontal plane by the forward-looking and backward-looking ADCP devices during stall mode operation.

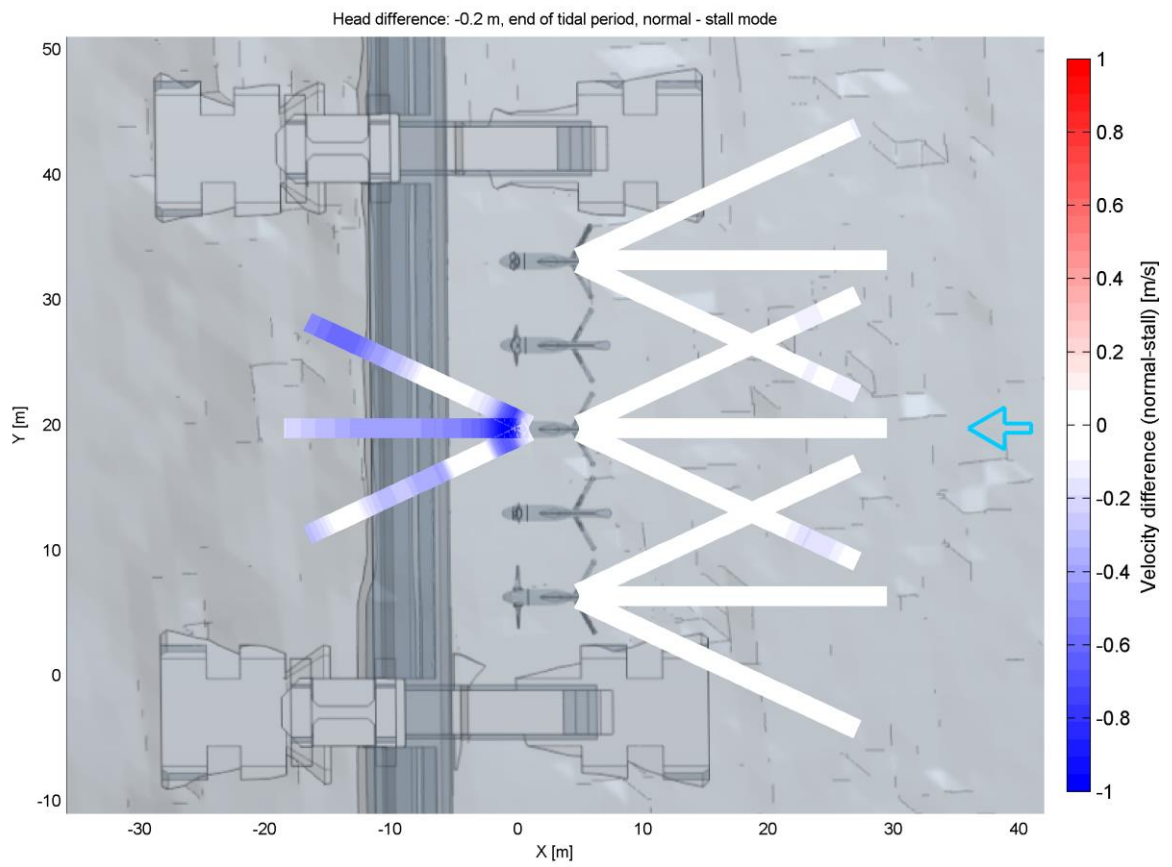


Figure E.6 Comparison of the measured velocities along 5-beams during normal operation against stall mode operation. Case 1 (head difference of -0.2 m).

**E.2 Case 2 (head difference = -0.32 m)**

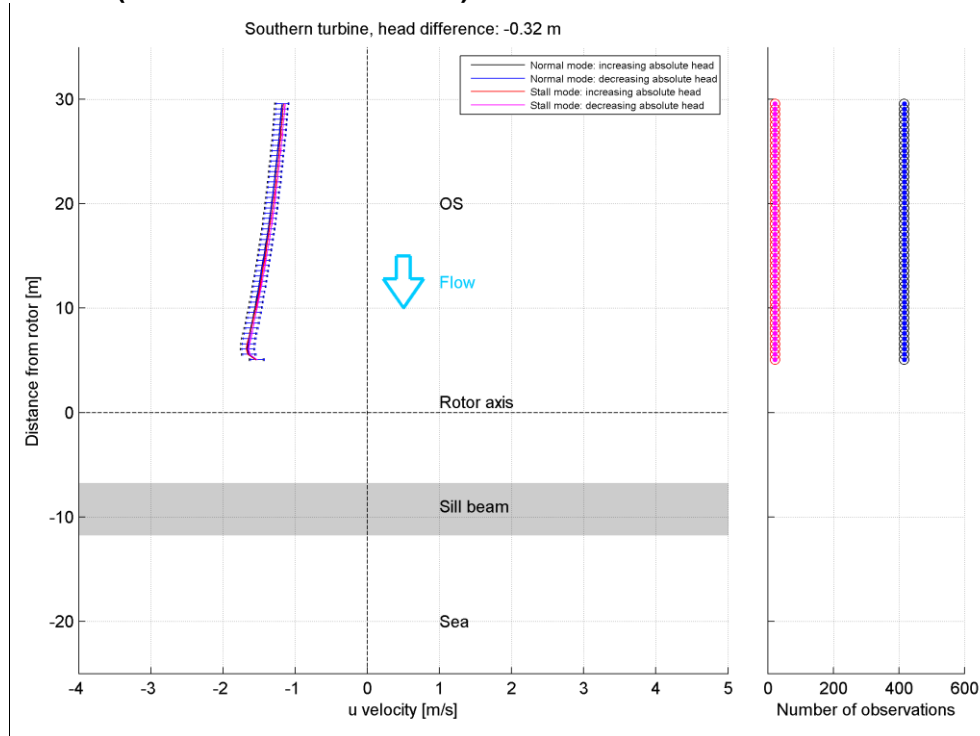


Figure E.7 Left: Velocity profile for Case 2 (head difference of -0.32 m) as measured by the forward-looking and backward-looking ADCP devices on the southern turbine. Distinction is made between periods of increasing and decreasing absolute head. Right: Number of observations used per bin.

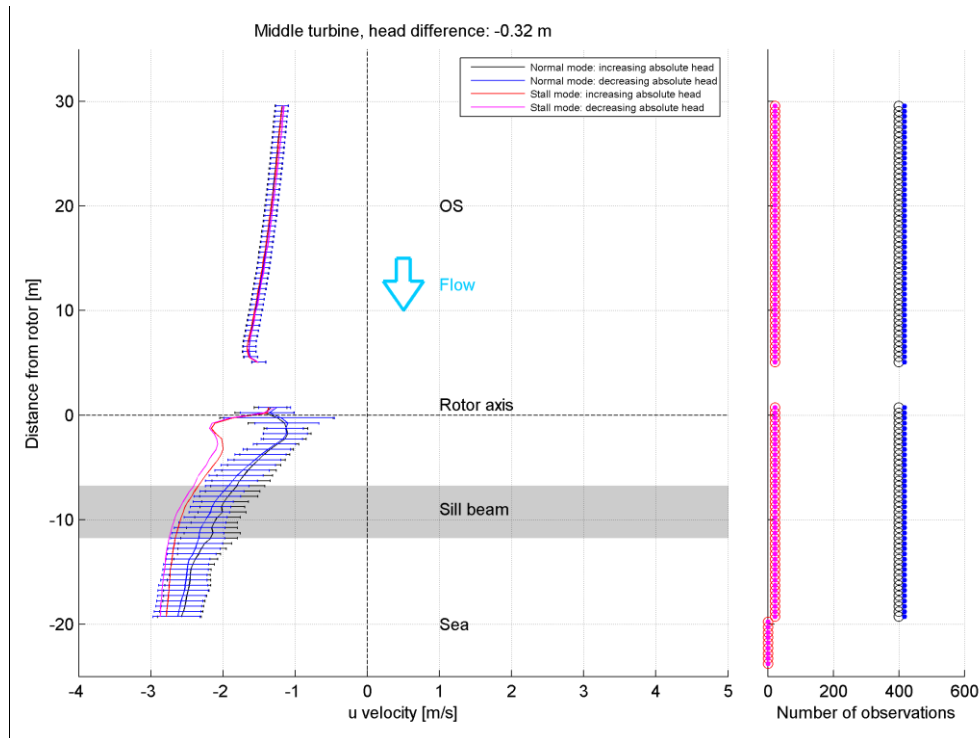


Figure E.8 Velocity profile for Case 2 (head difference of -0.32 m) as measured by the forward-looking and backward-looking ADCP devices on the middle turbine. Distinction is made between periods of increasing and decreasing absolute head. Right: Number of observations used per bin.



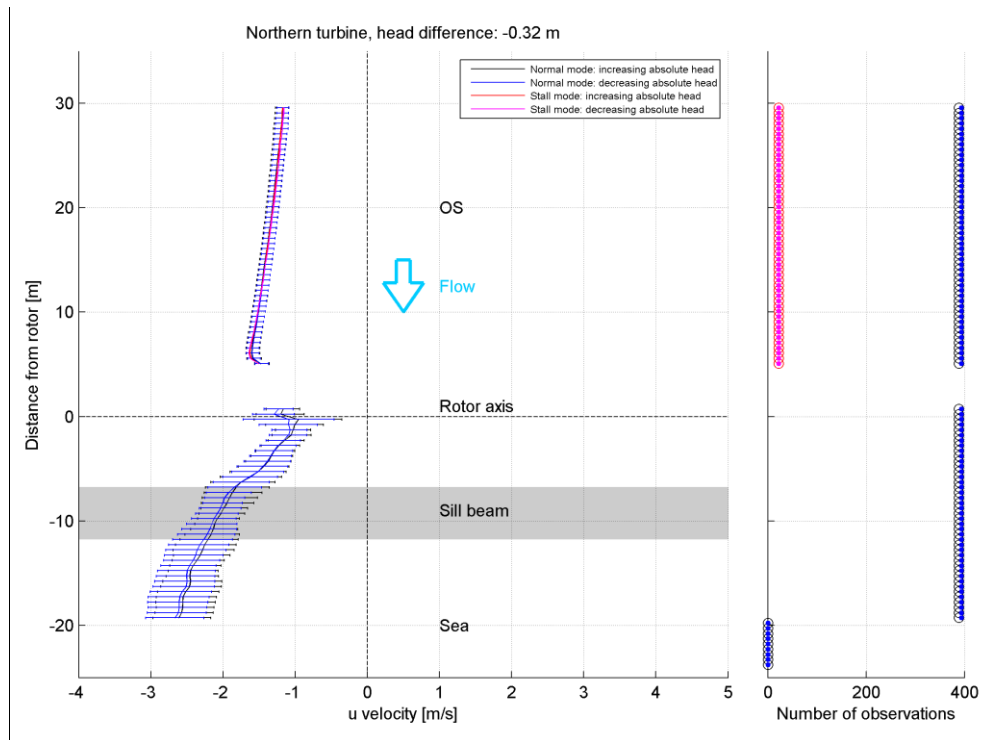


Figure E.9 Velocity profile for Case 2 (head difference of -0.32 m) as measured by the forward-looking and backward-looking ADCP devices on the northern turbine. Distinction is made between periods of increasing and decreasing absolute head. Right: Number of observations used per bin.

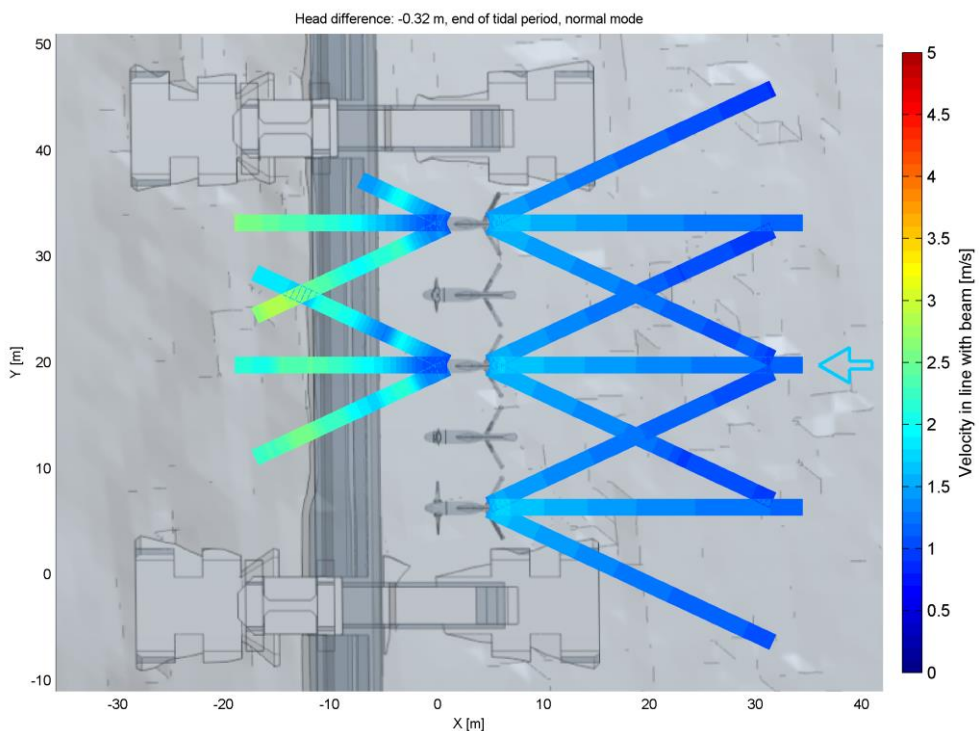


Figure E.10 Velocity profile for Case 2 (head difference of -0.32 m) as measured in the horizontal plane by the forward-looking and backward-looking ADCP devices during normal mode operation.

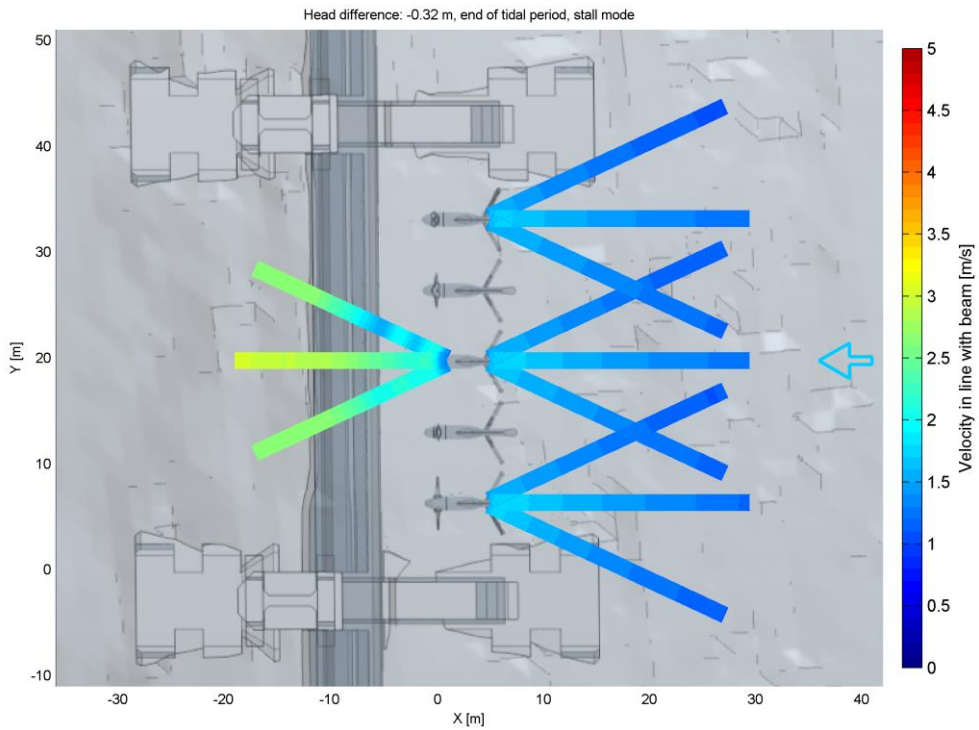


Figure E.11 Left: Velocity profile for Case 2 (head difference of -0.32 m) as measured in the horizontal plane by the forward-looking and backward-looking ADCP devices during stall mode operation.

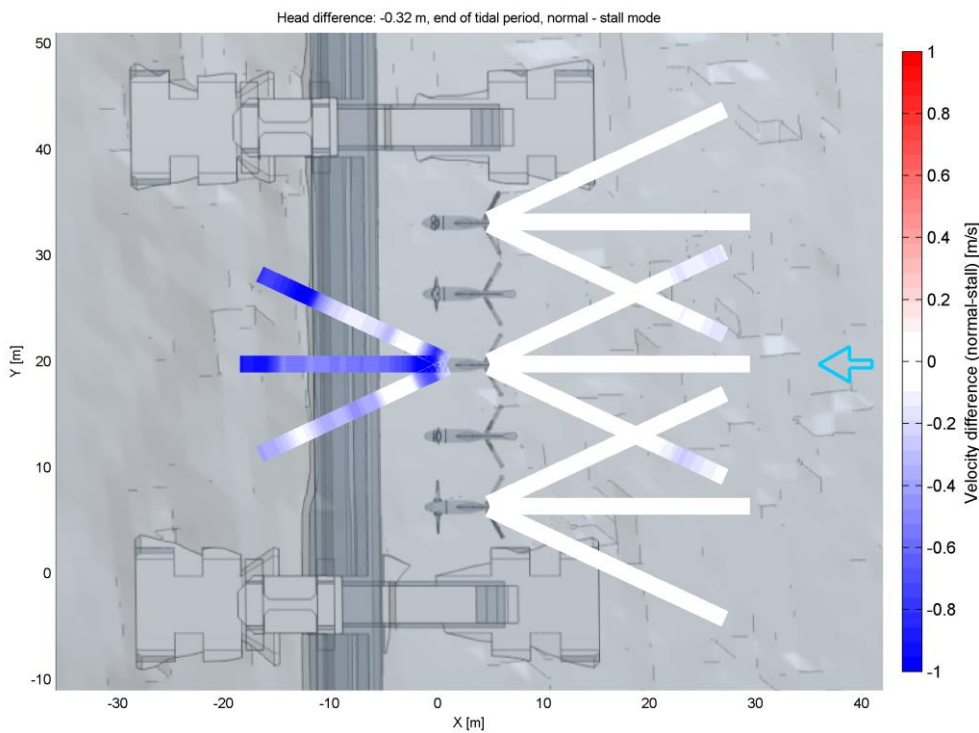


Figure E.12 Left: Comparison of the measured velocities along 5-beams during normal operation against stall mode operation. Case 2 (head difference of -0.32 m).

**E.3 Case 3 (head difference = +0.2 m)**

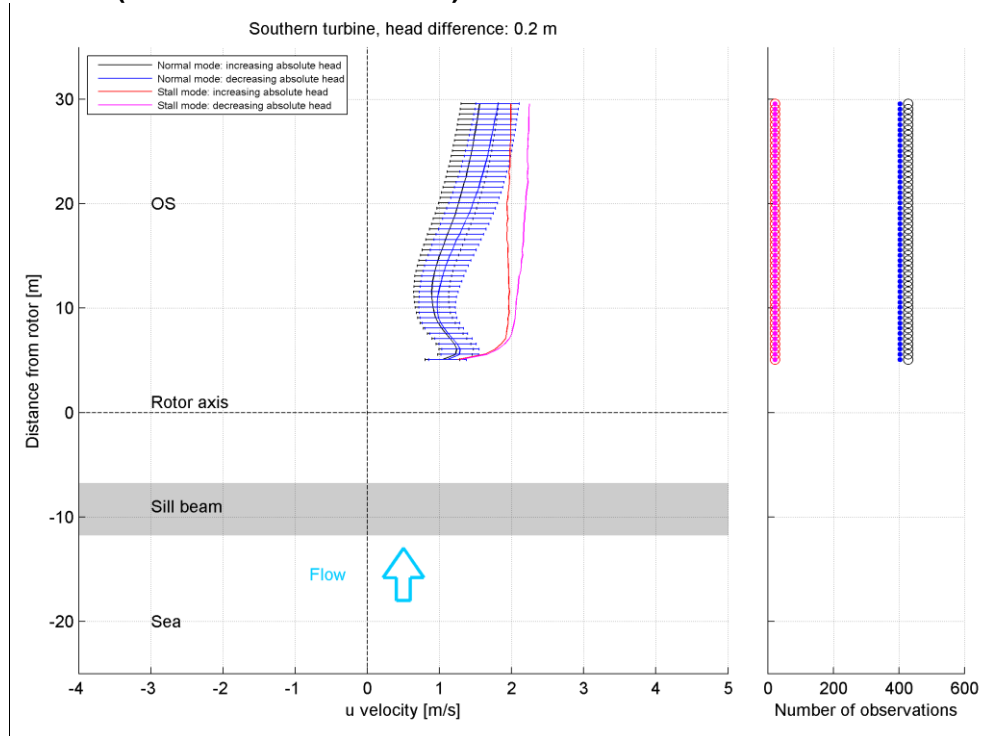


Figure E.13 Left: Velocity profile for Case 3 (head difference of +0.2 m) as measured by the forward-looking and backward-looking ADCP devices on the southern turbine. Distinction is made between periods of increasing and decreasing absolute head. Right: Number of observations used per bin.

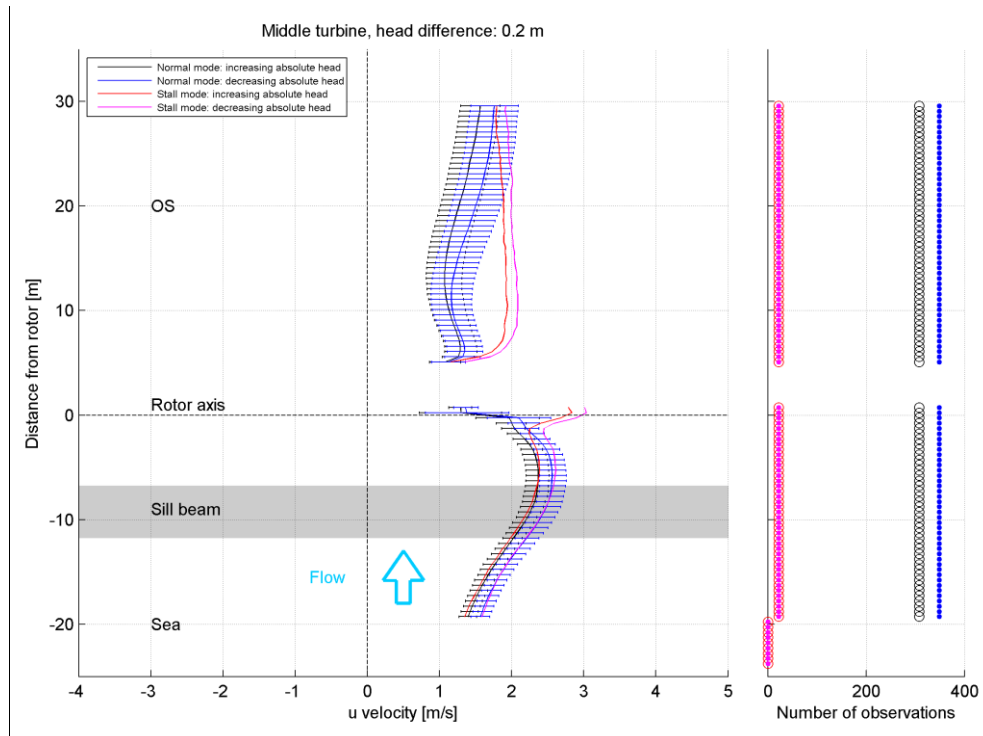


Figure E.14 Left: Velocity profile for Case 3 (head difference of +0.2 m) as measured by the forward-looking and backward-looking ADCP devices on the middle turbine. Distinction is made between periods of increasing and decreasing absolute head. Right: Number of observations used per bin.

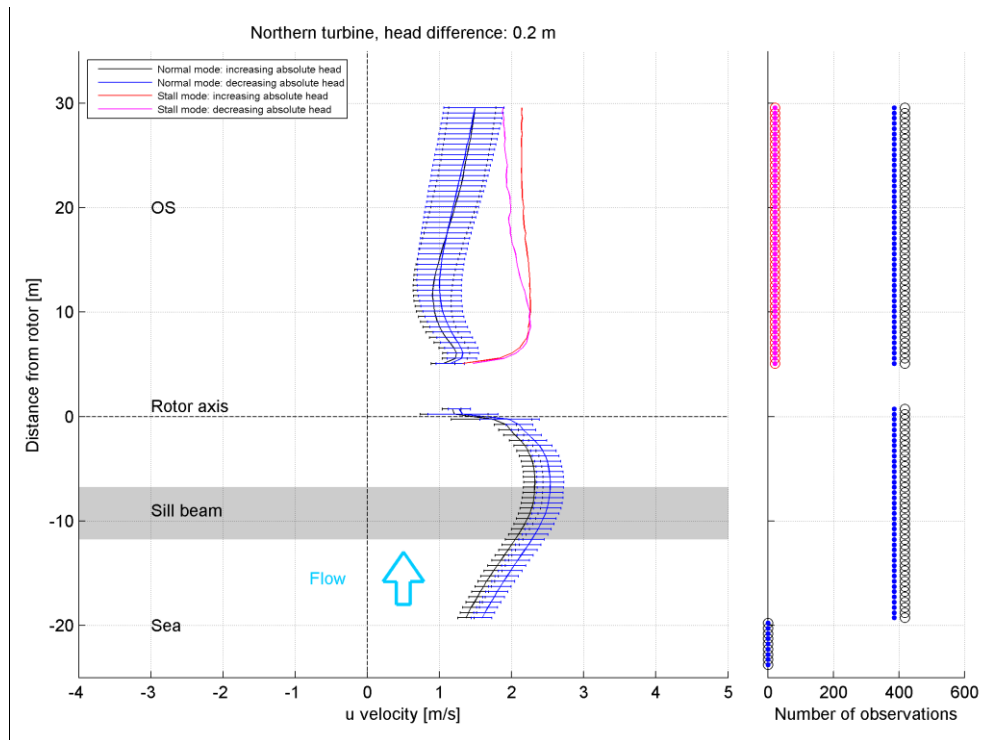


Figure E.15 Left: Velocity profile for Case 3 (head difference of +0.2 m) as measured by the forward-looking and backward-looking ADCP devices on the northern turbine. Distinction is made between periods of increasing and decreasing absolute head. Right: Number of observations used per bin.

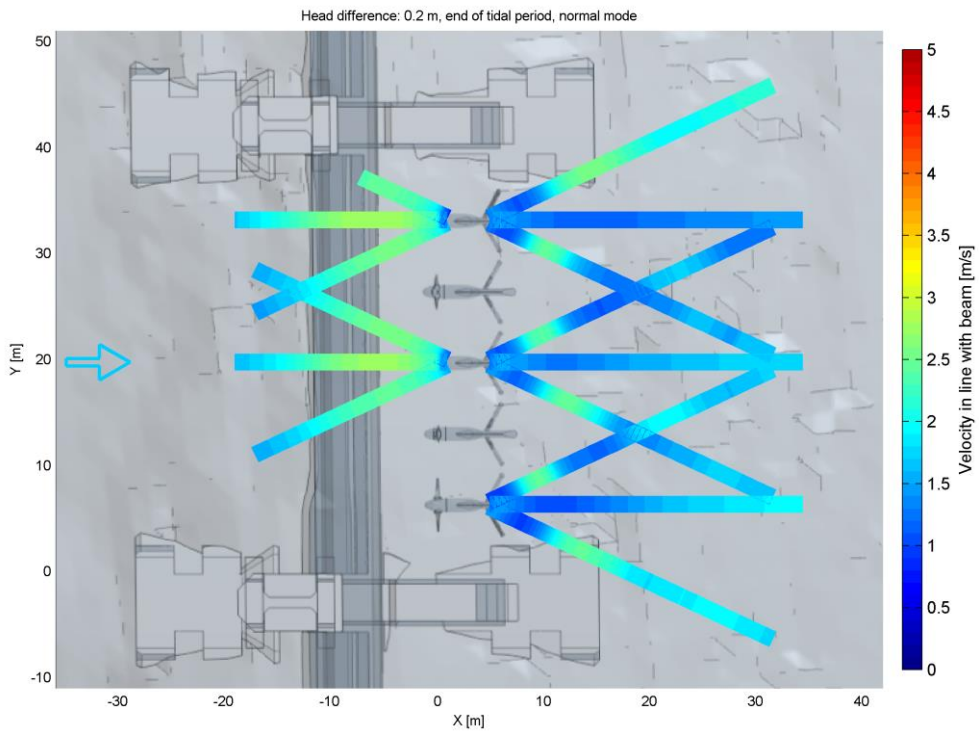


Figure E.16 Velocity profile for Case 3 (head difference of +0.2 m) as measured in the horizontal plane by the forward-looking and backward-looking ADCP devices during normal mode operation.

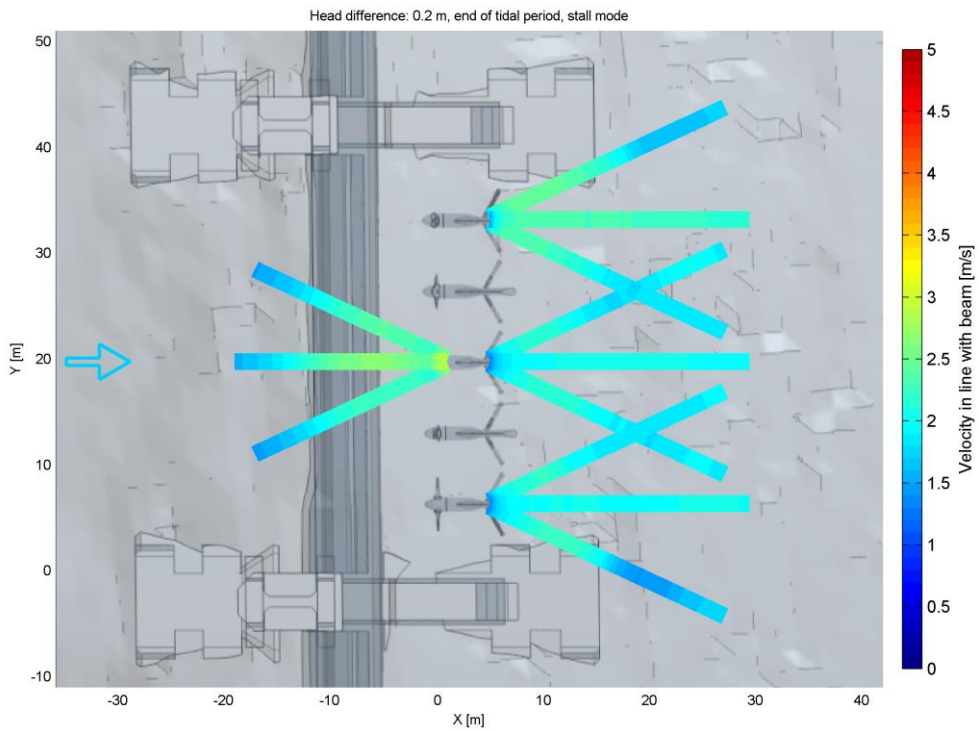


Figure E.17 Velocity profile for Case 3 (head difference of +0.2 m) as measured in the horizontal plane by the forward-looking and backward-looking ADCP devices during stall mode operation.

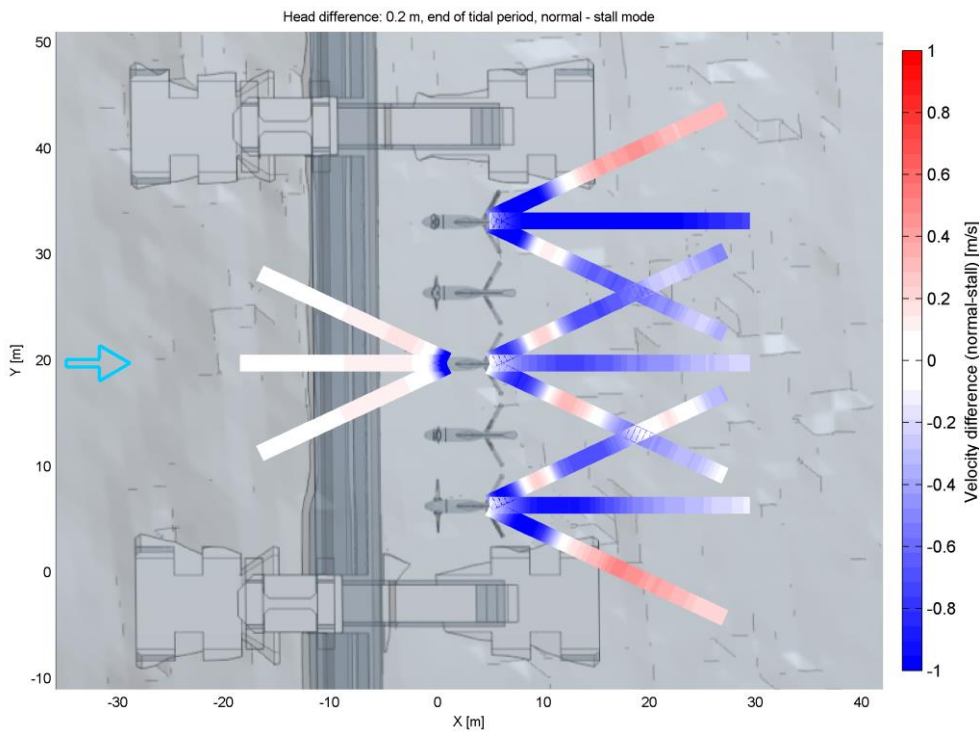


Figure E.18 Comparison of the measured velocities along 5-beams during normal operation against stall mode operation. Case 3 (head difference of +0.2 m).



**E.4 Case 4 (head difference = +0.55 m)**

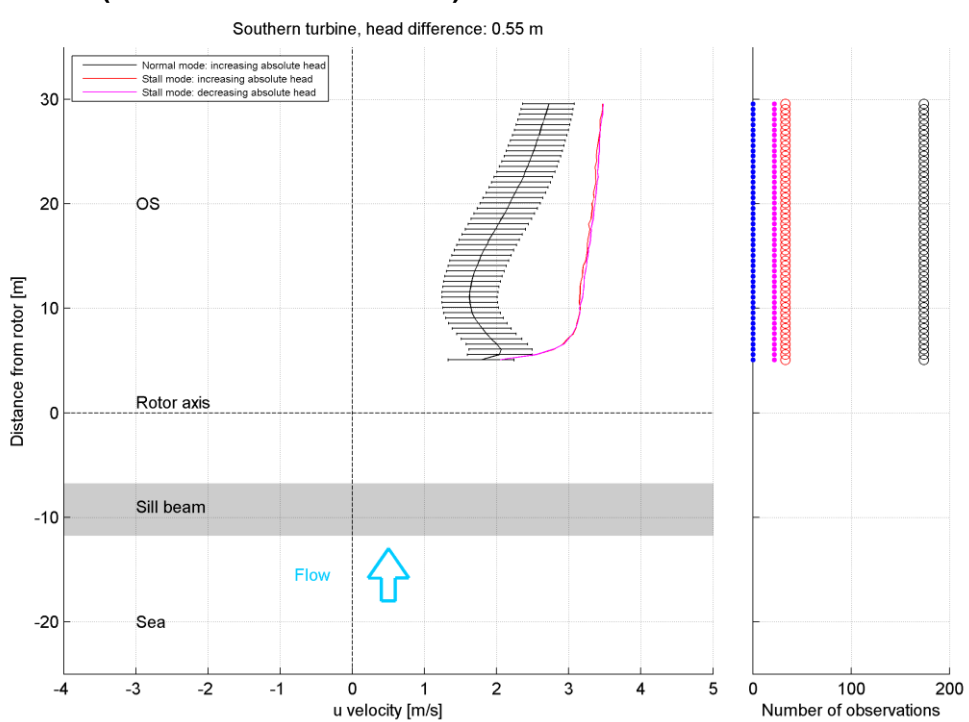


Figure E.19 Left: Velocity profile for Case 4 (head difference of +0.55 m) as measured by the forward-looking and backward-looking ADCP devices on the southern turbine. Distinction is made between periods of increasing and decreasing absolute head. Right: Number of observations used per bin.

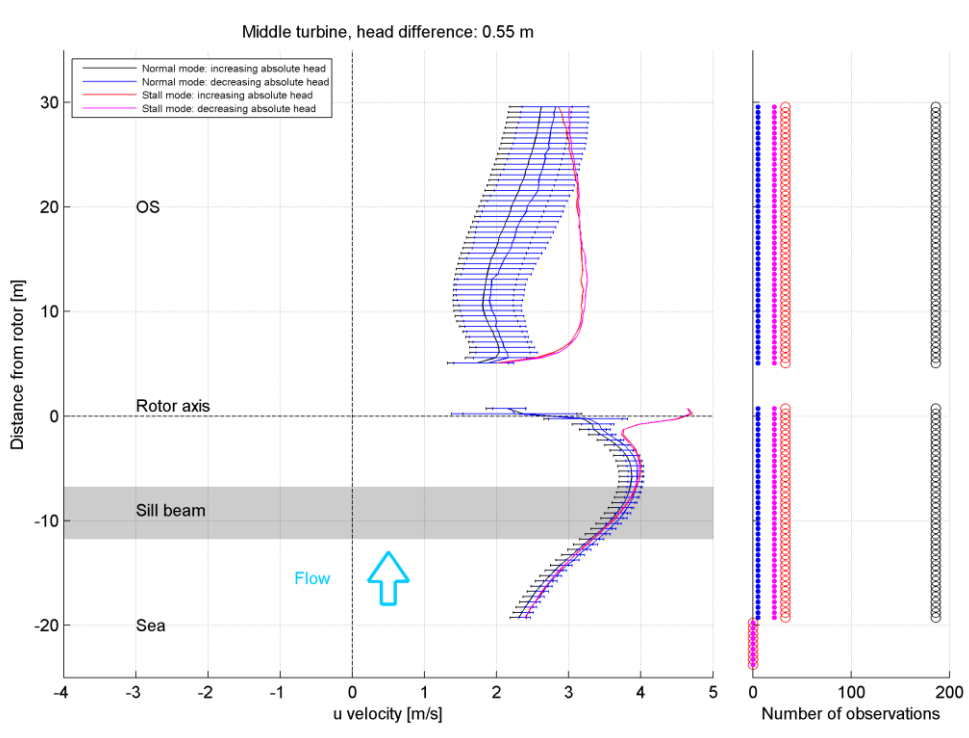


Figure E.20 Left: Velocity profile for Case 4 (head difference of +0.55 m) as measured by the forward-looking and backward-looking ADCP devices on the middle turbine. Distinction is made between periods of increasing and decreasing absolute head. Right: Number of observations used per bin.

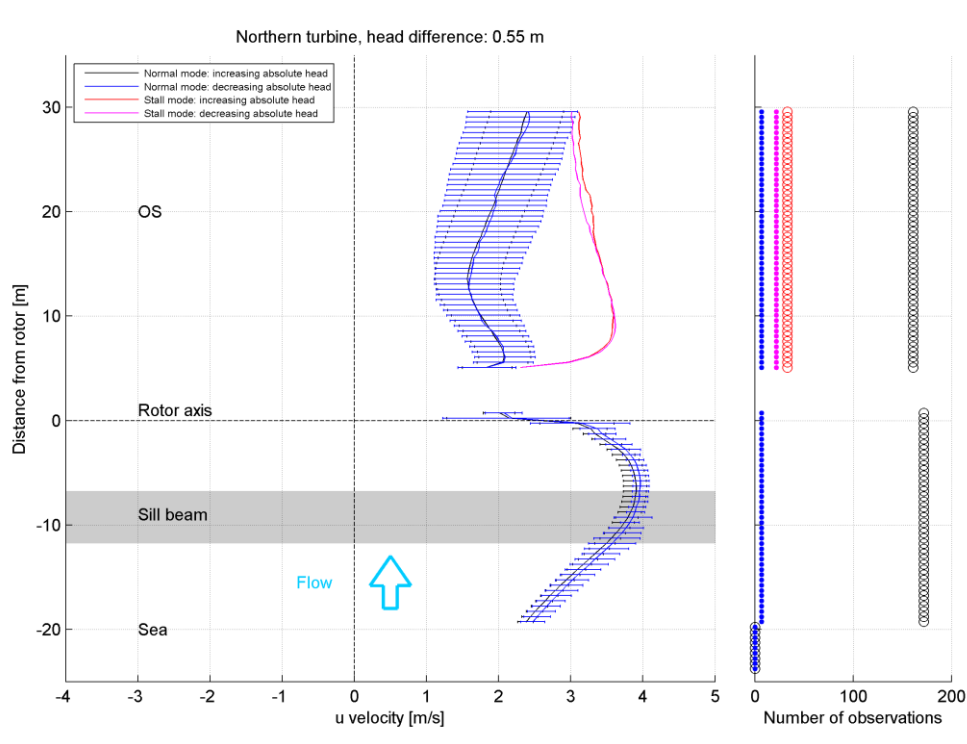


Figure E.21 Left: Velocity profile for Case 4 (head difference of +0.55 m) as measured by the forward-looking and backward-looking ADCP devices on the northern turbine. Distinction is made between periods of increasing and decreasing absolute head. Right: Number of observations used per bin.

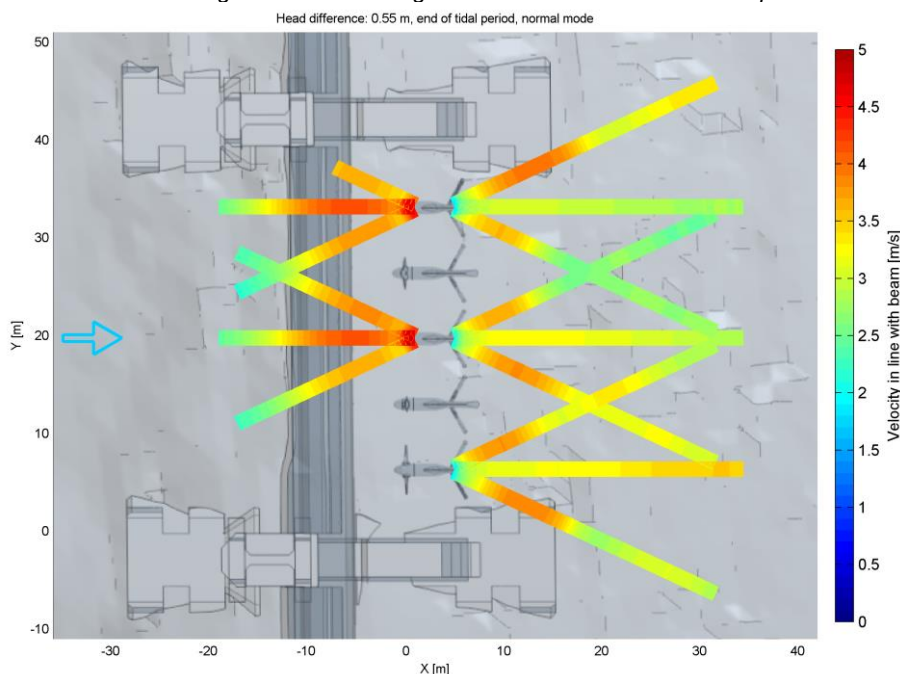


Figure E.22 Velocity profile for Case 4 (head difference of +0.55 m) as measured in the horizontal plane by the forward-looking and backward-looking ADCP devices during normal mode operation.

The stall mode dataset unfortunately didn't contain reliable measurements during a head difference of +0.55m. A comparison to normal operation can therefore not be made for Case 4.



## F Relation between RPM, Power, thrust and head difference

Tocardo provided in addition to the ADCP data also records of the RPM and Power per turbine and the thrust for two turbines (T0011 and T0009). Figure F.1 shows the names of the different turbines. This appendix shows the RPM, Power and thrust in relation to the head difference for all the turbines.

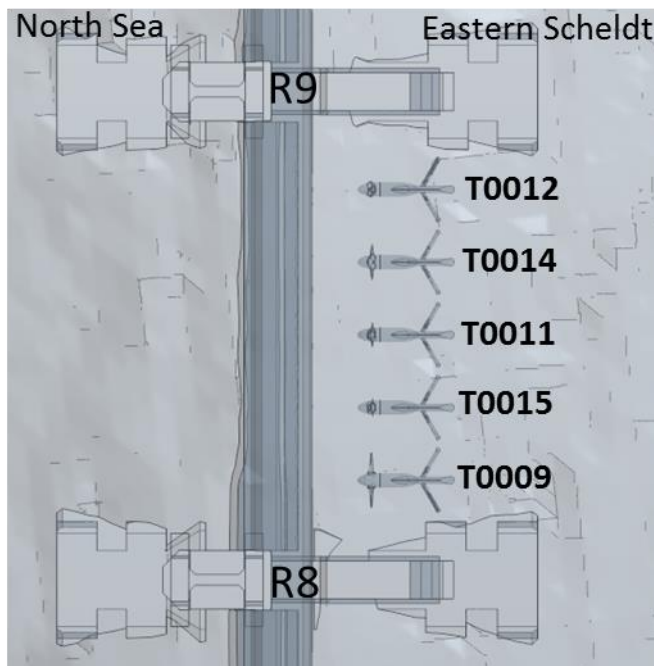


Figure F.1 Overview of the 5 turbines

**F.1 Turbine T0012**

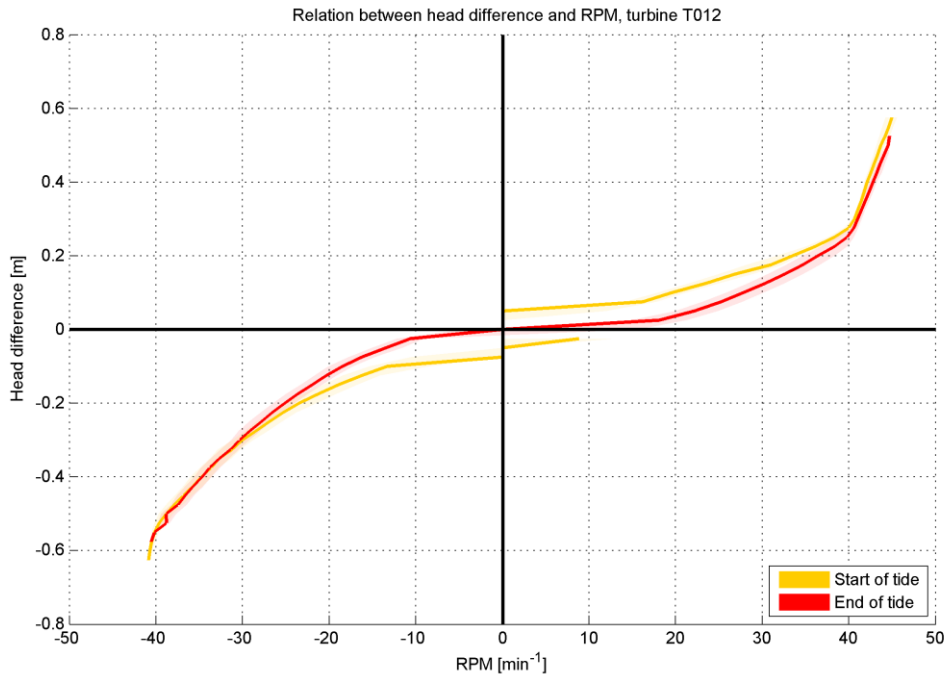


Figure F.2 Relation between registered RPM and head difference for turbine T0012 for the ADCP data period.

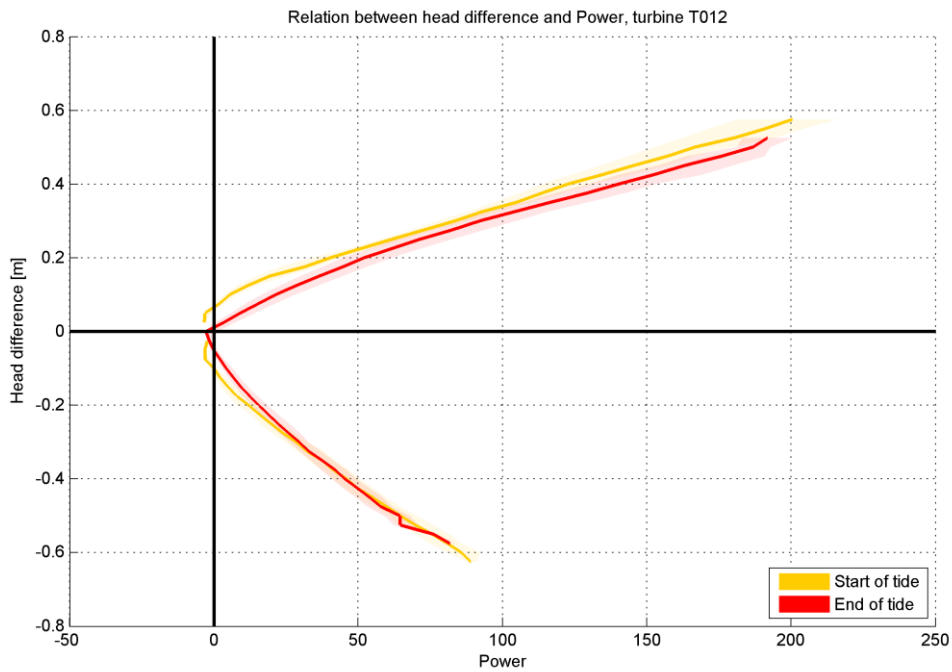


Figure F.3 Relation between registered Power and head difference for turbine T0012 for the ADCP data period.

## F.2 Turbine T0014

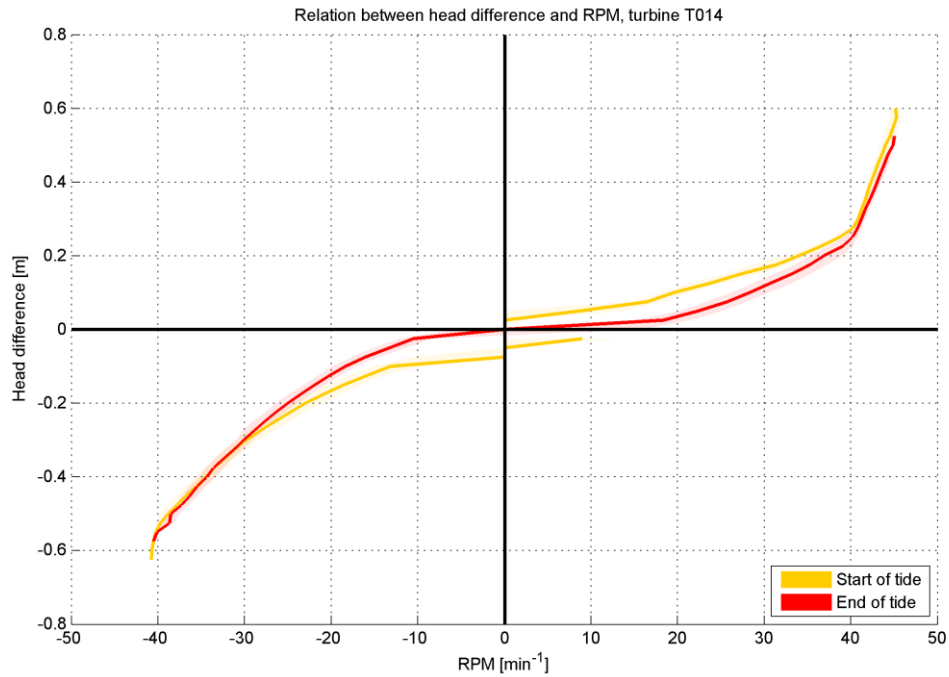


Figure F.4 Relation between registered RPM and head difference for turbine T0014 for the ADCP data period.

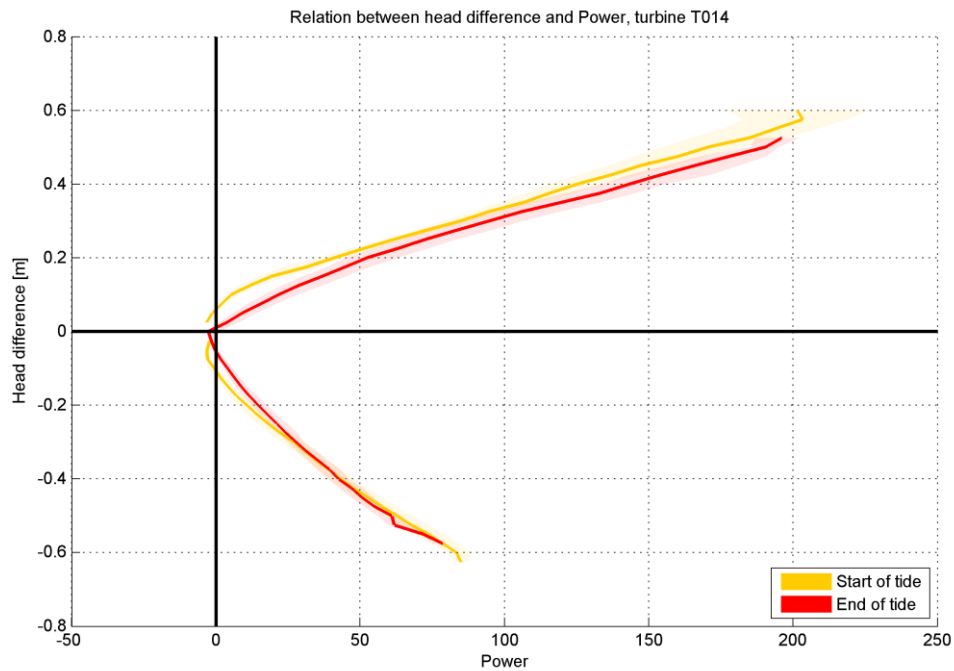


Figure F.5 Relation between registered Power and head difference for turbine T0014 for the ADCP data period.

### F.3 Turbine T0011

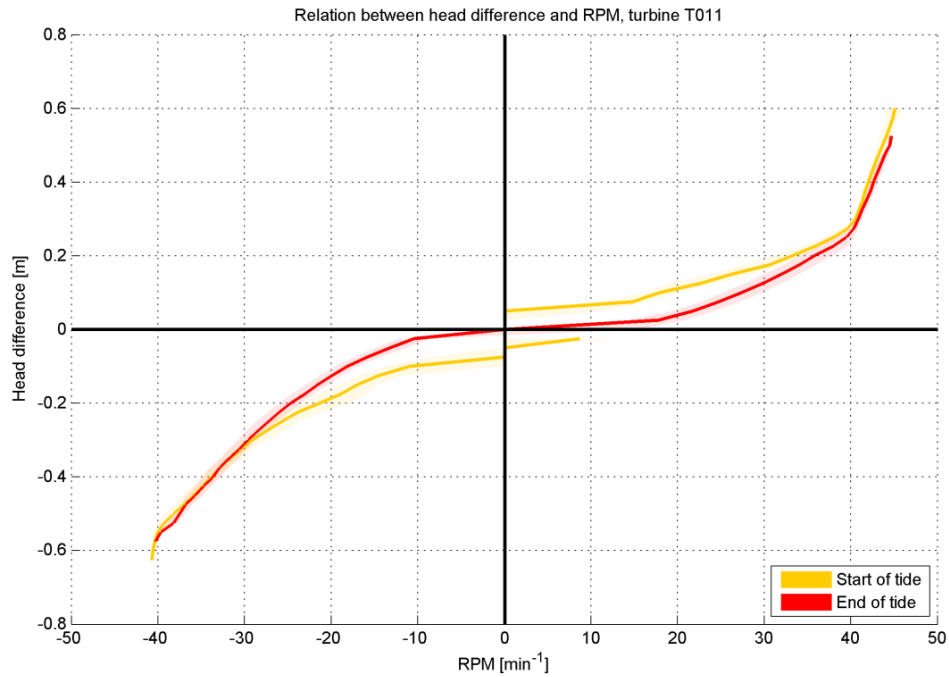


Figure F.6 Relation between registered RPM and head difference for turbine T0011 for the ADCP data period.

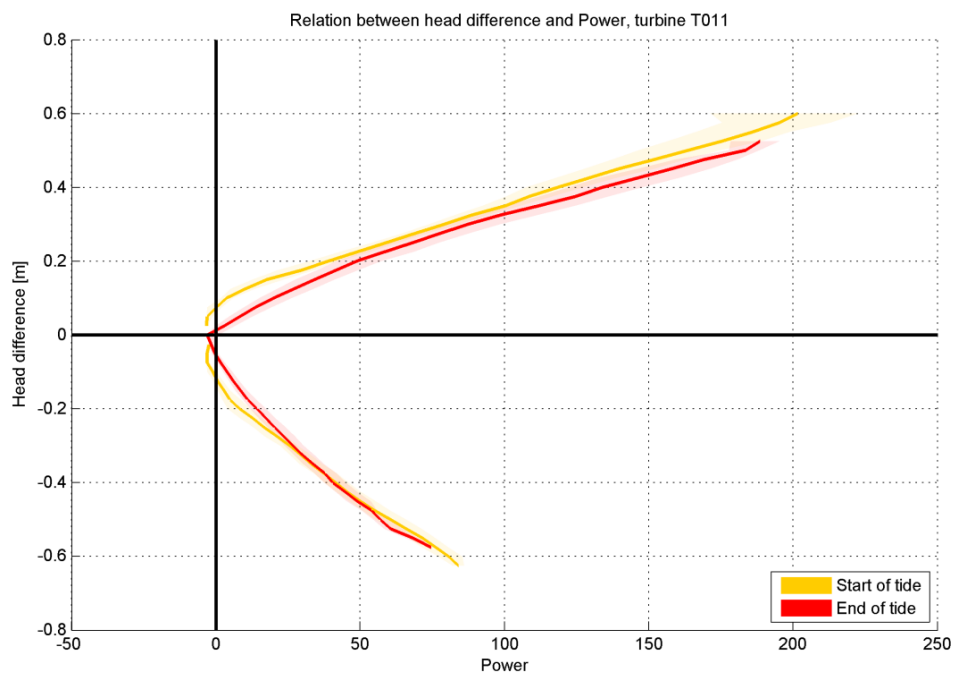


Figure F.7 Relation between registered Power and head difference for turbine T0011 for the ADCP data period.

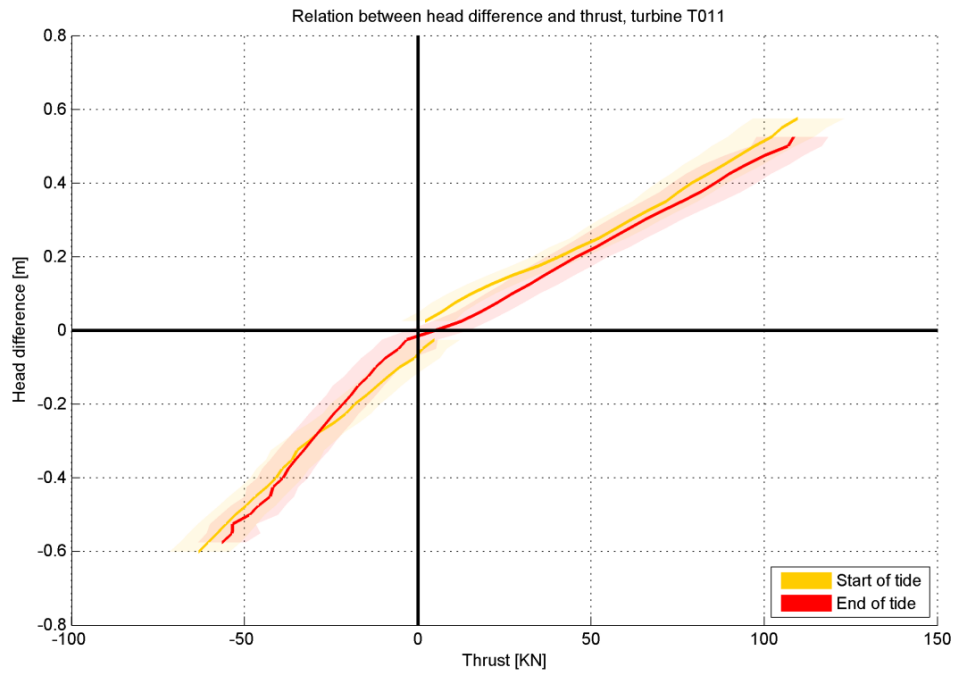


Figure F.8 Relation between registered thrust and head difference for turbine T0011 for the ADCP data period.

### F.4 Turbine T0015

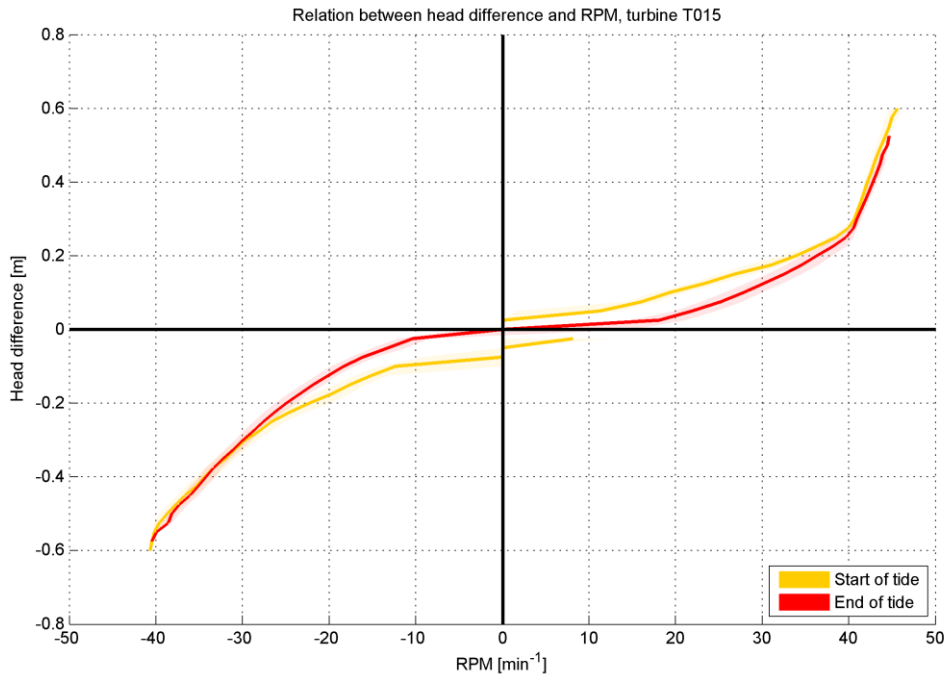


Figure F.9 Relation between registered RPM and head difference for turbine T0015 for the ADCP data period.

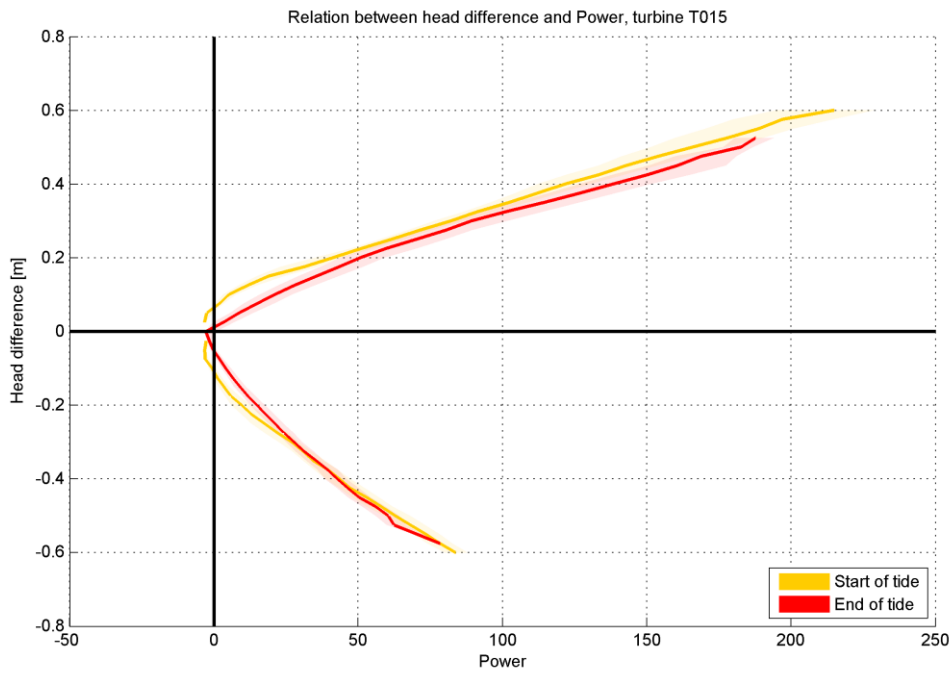


Figure F.10 Relation between registered Power and head difference for turbine T0015 for the ADCP data period.

**F.5 Turbine T0009**

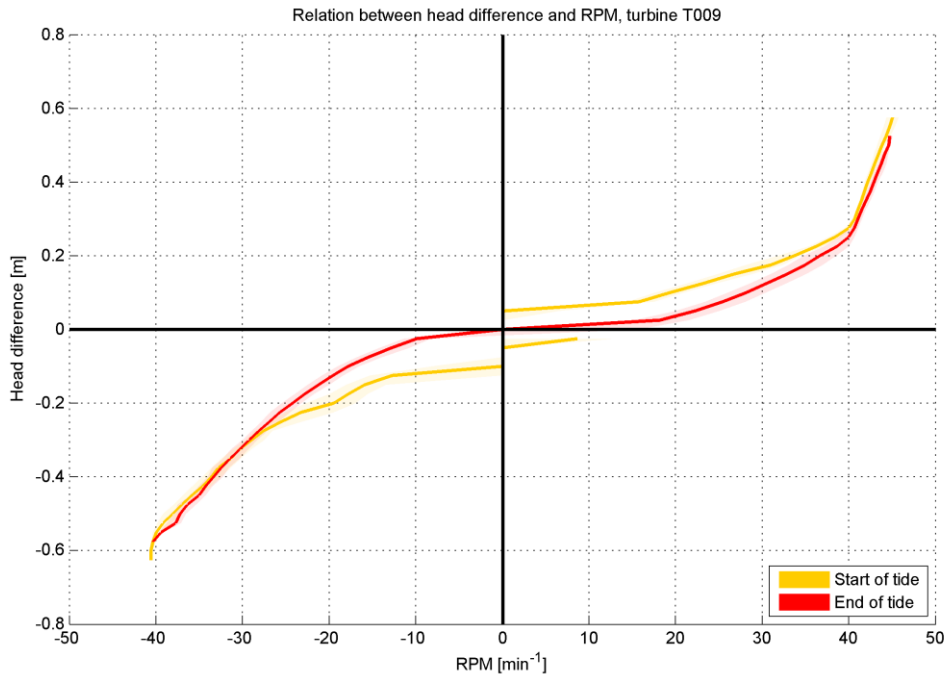


Figure F.11 Relation between registered RPM and head difference for turbine T0009 for the ADCP data period.

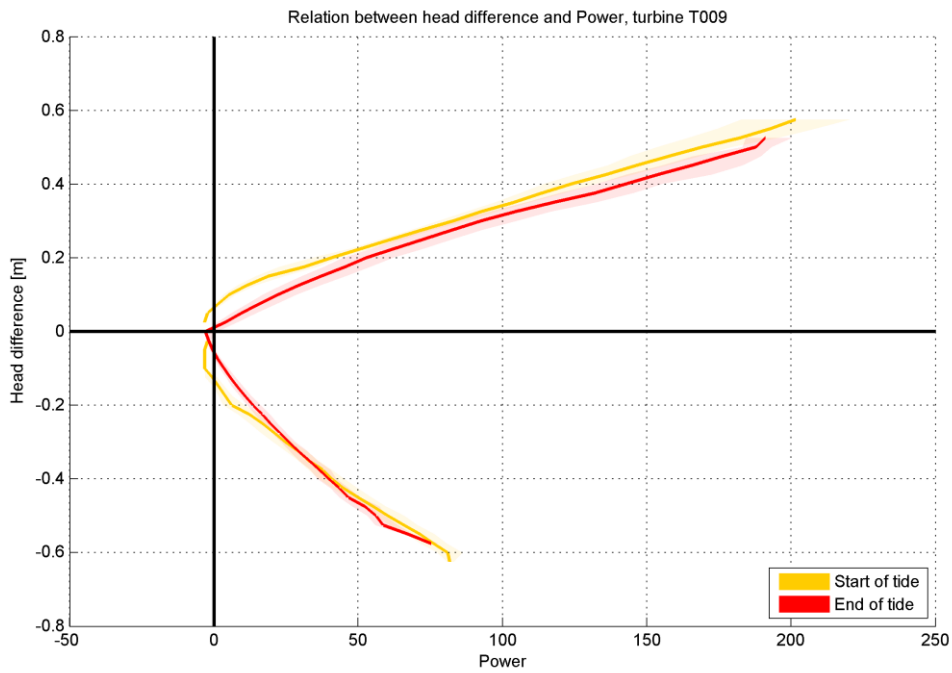


Figure F.12 Relation between registered Power and head difference for turbine T0009 for the ADCP data period.



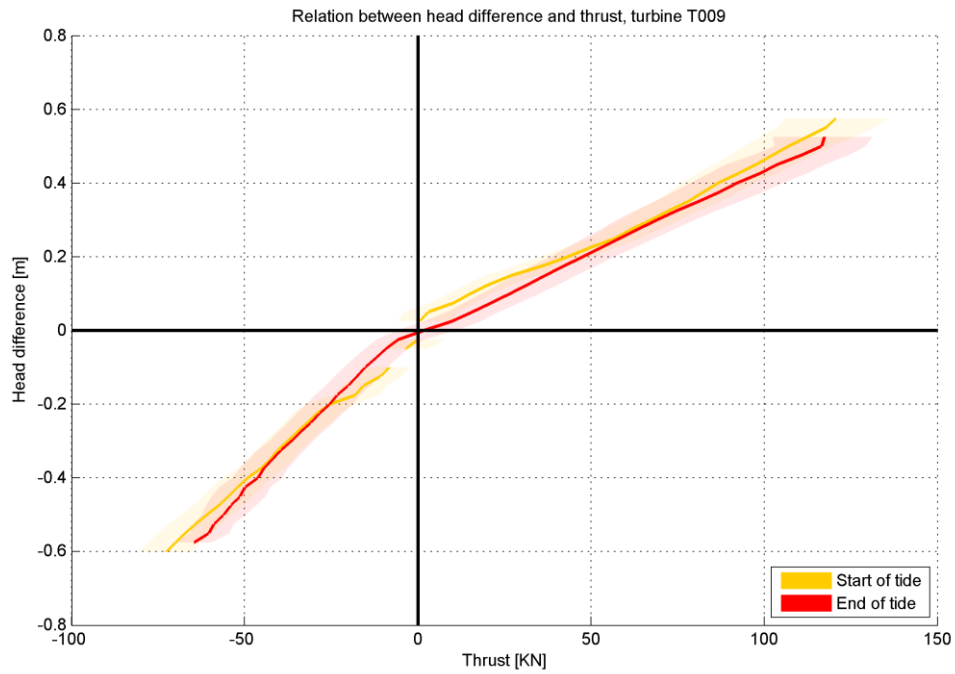


Figure F.13 Relation between registered Thrust and head difference for turbine T0009 for the ADCP data period.

